

ABSTRACT

Title of Document:

**SURVEILLANCE OF THE PERFORMANCE
OF ELASTOMERIC BEARINGS ON
MARYLANDS CONCRETE BRIDGES**

Charles J. Angelilli, Masters of Science, Civil
Engineering, 2007

Directed By:

Chung C. Fu, Research Professor, Department of
Civil Engineering

This thesis presents an investigation of the performance of elastomeric bearings in concrete girder bridges. Varying design practices create unpredictable performance in the field. The goal of the research is to correlate the AASHTO design parameters to a bearings performance in the field and further to make recommendations to improve as well as reduce the variability of the design for elastomeric bearings.

A field study was performed to collect data on the condition of bearings in over 80 bridges. Each bearing was given a PONTIS condition rating in order to quantify the level of degradation and to perform analysis. Exploratory analysis was performed using spreadsheet software to determine possibly significant design parameters. The results from the spreadsheet analysis were either confirmed or rejected using a logistic regression analysis of the field data. Finite element analysis was used to verify preliminary recommendations from the field study and logistic regression.

This study can conclude that limitations should be applied to the combined compression and rotation, the shape factor and the shear strains in elastomeric bearings.

SURVEILLANCE OF THE PERFORMANCE OF ELASTOMERIC BEARINGS
ON MARYLANDS CONCRETE BRIDGES

By

Charles J. Angelilli

Thesis submitted to the Faculty of the Graduate School of the
University of Maryland, College Park, in partial fulfillment
of the requirements for the degree of
Master of Science
2007

Advisory Committee:
Professor Chung C. Fu, Chair/Advisor
Professor Donald W. Vannoy
Professor Amde M. Amde

© Copyright by
Charles J. Angelilli
2007

Acknowledgements

I would like to express my sincere thanks to many people who contributed, aided, and supported me throughout my research: Dr. C.C. Fu for his constant guidance, dedication, and expertise throughout this entire process. The University of Maryland Civil Engineering Department, Chi Epsilon, and ASCE which offered extensive academic and financial support.

I also thank Mehul Dave, for crawling under dozens and dozens of bridges with me during my field study and provided incredible insight; Kunal Suthar, whose knowledge of finite element modeling was invaluable; Dr G.L. Chang and his graduate staff who aided with logistic regression; Pat Johnson for endlessly editing my many drafts; Bryce Lehman, Jarod Broadwater, and Erin Mahoney, my colleagues who know firsthand the rigors of graduate research, from the many successes and all-too-many failures.

I would also like to express my sincere appreciation to my family and friends, who gave me the encouragement, support, and semblance of sanity I needed to persevere: My parents, for always pushing me to push myself; My late grandfather, Charles C. Deel, for instilling the values of hard work and confidence; My Uncle Cliff Deel, for his profound wisdom and for being the model of success in both Civil Engineering and character; My brothers, Matt and Bryan, and sister, Kaitlynn, whose comic relief got me through the most difficult times; and last but not least, Angie, Ben, Nehemias, Hiruy, and Rony, my friends who provided endless moral support.

Table of Contents

ABSTRACT	II
ACKNOWLEDGEMENTS	II
TABLE OF CONTENTS	III
LIST OF FIGURES	VII
LIST OF TABLES	VIII
CHAPTER 1	1
INTRODUCTION AND LITERATURE REVIEW	1
1.0 INTRODUCTION	1
1.1 Problem Statement	2
1.2 Approach to Problem Solving	2
1.2.1 Background Data Collection	3
1.2.2 Field Study	4
1.2.3 Analysis	4
1.3 Literature Review	5
1.3.1 Previous Studies	5
1.3.2 Thermal Effects	6
1.3.3 Elastomers	7
CHAPTER 2	9
FIELD STUDY	9
2.0 FIELD STUDY	9
2.1 Bridge Selection and State Highway Administration Criteria	9
2.1.1 Bearings Failure Modes	9
2.1.1.1 Pad Deterioration	10
2.1.1.2 Pad Slip	10
2.1.1.3 Creep and Bulging	11
2.1.1.4 Aging	12
2.1.1.5 Delamination	12
2.1.1.6 Poor Quality	12
2.1.1.7 Crushing	13
2.1.1.8 Rupture of Reinforcement	13
2.1.2 Inspection Items	14

CHAPTER 3 **16**

FIELD STUDY RESULTS AND FINDINGS	16
3.0 FIELD STUDY FINDINGS	16
3.1 Failing Bearings by Mode	16
3.1.1 Pad Deterioration	16
3.1.2 Pad Slip	17
3.1.3 Creep	19
3.1.4 Bulging	21
3.1.5 Aging	22
3.1.6 Delamination	23
3.1.7 Poor Quality	24
3.1.8 Crushing	24
3.1.9 Rupture of Reinforcement	25
3.2 Group and Ranking of Failing Bearings	26

CHAPTER 4 **28**

OVERVIEW AND PROGRESSION OF AASHTO CODES AND DESIGN METHODS	28
4.0 EVOLUTION OF AASHTO CODES AND INDUSTRY PRACTICES	28
4.1 Approach	28
4.2 Data Collection	29
4.2.1 Bridge Background	30
4.2.2 Field Study	30
4.2.3 SHA File Search	31
4.2.4 Load Generation	31
4.2.5 File Organization	31
4.2.6 Evolution of AASHTO Codes	32
4.2.7 10 th Edition	33
4.2.7.1 Design Criteria	34
4.2.8 12 th Edition	35
4.2.8.1 Design Criteria	36
4.2.9 14 th Edition	37
4.2.9.1 Design Criteria	40
4.2.10 15 th Edition	45
4.2.10.1 Design Criteria	45
4.2.11 4 th Edition LRFD	50
4.2.11.1 Method B	51
4.2.12 Comparisons of Different Editions of Standard Specifications for Highway Bridges	55
4.2.12.1 Plan Area vs. Total Load	55
4.2.12.2 Elastomer Layer Thickness vs. Total Load	56
4.2.12.3 Plan Area vs. Total Load by Shape Factor	57
4.2.12.4 Layer Thickness vs. Total Load by Shape Factor	59

CHAPTER 5 **61**

MULTI-VARIABLE REGRESSION ANALYSIS	61
5.0 INTRODUCTION	61
5.1 Logistic Regression Process	61

5.2	Studied Variables	62
5.2.1	Exploratory Investigation	62
5.2.2	X1 – Shape Factor, S	64
5.2.3	X2 – Elastomer Thickness, h_{rt}	65
5.2.4	X3 – Plan Area, A	65
5.2.5	X4 – Shear Area	66
5.2.6	X5 – Bulge Area	66
5.2.7	X6 – Shear Strain, ϵ_s	67
5.2.8	X7 – Compressive Stress, σ_s	67
5.2.9	X8 – Combined Compression and Rotation, $\frac{\sigma_s}{GS}$	67
5.2.10	X9 – Compressive Stress divided by Bulge Area, $\frac{\sigma_s}{2h_{rt}(L+W)}$	68
5.3	Logistic Regression Results	68
CHAPTER 6		70
FINITE ELEMENT MODELING		70
6.0	OVERVIEW OF FINITE ELEMENT MODELING	70
6.1	Models	70
6.1.1	As Built Bearing for Bridge 1097	71
6.1.1.1	Performance of Finite Element Model for As Built Situation	72
6.1.2	Suggested Bearing for Bridge 1097	74
6.1.2.1	Design	75
6.1.2.2	Performance of Finite Element Model for Suggested Bearing	78
6.2	Results (Graphs)	80
CHAPTER 7		83
OVERVIEW AND RECOMMENDATION		83
7.0	OVERVIEW OF STATISTICAL ANALYSIS SUMMARY	83
7.1	Overview	83
7.2	Results and Discussion	83
7.2.1	Shape Factor	83
7.2.2	Shear Strain	86
7.2.3	Compressive Stress, σ_s	89
7.2.4	Combined Compression and Rotation σ_s/GS	92
7.3	Recommendations	93
7.3.1	Shape Factor	93
7.3.2	Shear Strain	93
7.3.3	Combined Compression and Rotation	94
CHAPTER 8		96
CONCLUSIONS AND FUTURE RESEARCH		96

APPENDIX A – GOOGLE SCREENSHOTS	98
PLANNED TRIPS	98
ACTUAL INSPECTIONS	103
APPENDIX B - DATA SETS	108
BASIC BRIDGE INFORMATION	108
BEARING DETAILS	111
APPENDIX C – FIELD STUDY TRIPS	115
C.1 Bridge Location	115
C.1.1 Mapping in the Bridge Inventory Book	115
C.1.2 Mapping on Google Earth	115
C.2 BRIDGE GROUPINGS	117
C.2.1 Trip Planning	123
C.2.2 Schedule	123
C.3 Actual Trip Schedule	125
REFERENCES	130

List of Figures

FIGURE 3.1 - PAD DETERIORATION IN BRIDGE #1169	17
FIGURE 3.2 - BEARING SLIP IN BRIDGE #9015	18
FIGURE 3.3 - BEARING SLIP IN BRIDGE #2006	19
FIGURE 3.4 - CREEP AT A PIER IN A GIRDER BRIDGE	19
FIGURE 3.5 - CREEP AT AN ABUTMENT IN A GIRDER BRIDGE	20
FIGURE 3.6 - BEGINNING STAGES OF CREEP	21
FIGURE 3.7 - BULGING IN A LAMINATED BEARING	22
FIGURE 3.8 - DELAMINATION OF AN ELASTOMERIC PAD	23
FIGURE 3.9 - DETERIORATION DUE TO POOR QUALITY	24
FIGURE 3.10 - CRUSHING IN A SLAB BRIDGE	25
FIGURE 4.1 – COMBINED COMPRESSION AND ROTATION LIMITS	54
FIGURE 4.2 – PLAN AREA VS. TOTAL LOAD BY AASHTO EDITIONS	56
FIGURE 4.3 – LAYER THICKNESS VS. TOTAL LOAD BY AASHTO EDITIONS	57
FIGURE 4.4 – PLAN AREA VS. LOAD BY SHAPE FACTORS (METHOD A)	58
FIGURE 4.5 – PLAN AREA VS. LOAD BY SHAPE FACTORS (METHOD B)	59
FIGURE 4.6 - LAYER THICKNESS VS. LOAD BY SHAPE FACTOR (METHOD A)	60
FIGURE 4.7 – LAYER THICKNESS VS. LOAD BY SHAPE FACTOR (METHOD B)	60
FIGURE 5.2 – EXAMPLE OF A USABLE EXPLORATORY COMPARISON	63
FIGURE 5.2 – EXAMPLE OF AN UNUSABLE EXPLORATORY COMPARISON	64
FIGURE 5.3 - DEFORMED BEARING DUE TO TEMPERATURE LOADING	66
TABLE 5.1 – LOGISTIC REGRESSION SUMMARY OF MEANINGFUL VARIABLES	69
FIGURE 6.1 – BEARING CREEP IN BRIDGE 1097	72
FIGURE 6.2 – UNDEFORMED MODEL (3-D VIEW)	73
FIGURE 6.3 – UNDEFORMED MODEL (SIDE VIEW)	73
FIGURE 6.4 – STRESS CONTOURS FOR THERMAL LOADING	73
FIGURE 6.5 – STRESS CONTOURS FOR COMPRESSIVE LOADING	74
FIGURE 6.6 – STRESS CONTOURS FROM THERMAL AND COMPRESSIVE LOADING	74
FIGURE 6.7 – STRESS CONTOURS FROM THERMAL AND COMPRESSIVE LOADING (3D)	74
FIGURE 6.8 – UNDEFORMED MODEL (3-D VIEW)	78
FIGURE 6.9 – UNDEFORMED MODEL (SIDE VIEW)	79
FIGURE 6.10 – STRESS CONTOURS FOR THERMAL LOADING	79
FIGURE 6.11 – STRESS CONTOURS FOR COMPRESSIVE LOADING	79
FIGURE 6.12 – STRESS CONTOURS FROM THERMAL AND COMPRESSIVE LOADING	79
FIGURE 6.13 – STRESS CONTOURS FROM THERMAL AND COMPRESSIVE LOADING (3D)	80
FIGURE 6.14 – STEEL STRESS FROM THERMAL AND COMPRESSIVE LOADING (3D)	80
FIGURE 6.15 – STRESS VS SHAPE FACTOR FOR 16X26X1 5/8” LAMINATED BEARING	82
FIGURE 7.1 – BEARING CONDITION BY SHAPE FACTOR	84
FIGURE 7.2 – TOTAL COMPRESSIVE STRESS VS. SHAPE FACTOR	85
FIGURE 7.3 – BEARING CONDITION BY SHEAR STRAINS	87
FIGURE 7.4 – SHEAR STRAIN VS. ELASTOMER THICKNESS FOR ALL SAMPLE BRIDGES	88
FIGURE 7.5 – SHEAR STRAIN VS. ELASTOMER THICKNESS FOR GIRDER BRIDGES	88
FIGURE 7.6 – BEARING CONDITION BY COMPRESSIVE STRESS	89
FIGURE 7.7 – COMPRESSIVE STRESS VS. ELASTOMER THICKNESS FOR ALL SAMPLE BRIDGES	91
FIGURE 7.8 – COMPRESSIVE STRESS VS. ELASTOMER THICKNESS FOR GIRDER BRIDGES	91
FIGURE 7.9 – COMBINED COMPRESSION AND ROTATION LIMITS OF ELASTOMERIC BEARINGS	92
FIGURE 7.10 – COMBINED COMPRESSION AND ROTATION LIMITS OF ELASTOMERIC BEARINGS	95

List of Tables

TABLE 2.1 - INSPECTION ITEMS FOR ELASTOMERIC BEARINGS	15
TABLE 4.1 - PERCENTAGE OF BEARINGS BY PONTIS RATING AND AASHTO DESIGN EDITION	32
TABLE 4.2 - ALLOWABLE SHEAR MODULUS AND CREEP DEFLECTION PER AASHTO	41
TABLE 4.3 – BEARING SUITABILITY	51
TABLE 6.1 – RESULTS OF FINITE ELEMENT ANALYSIS	81

Chapter 1

Introduction and Literature Review

1.0 Introduction

Elastomeric bearings have been used frequently in the design of concrete bridge structures in Maryland for the past 50 years. The function of a bridge bearing is to transfer compression/tension, shear and rotational forces in the superstructure to the substructure while still allowing free movement of the superstructure. Elastomeric bearings provide the same function as other commonly used bearings such as roller bearings or rocker bearings but are easier to install, require less maintenance and are easier to install. Elastomers bearings do not freeze, corrode, or deteriorate, giving it distinct advantages over typical metal bearings. Advances in elastomers have allowed for the manufacturing and use of fully synthetic elastomers, such as neoprene, instead of natural rubbers. The quality of the elastomers being produced is continually being improved.

Elastomeric bearings can be either single elastomeric pads or multiple pads laminated with steel shims. Prestressed concrete slab bridges tend to have many plain pads along the width of the bridge and concrete girder bridges tend to have larger, laminated bearings. The laminated bearing can withstand higher compressive, shear forces and movement than thinner plain pads. Plain pads are weaker and more flexible than laminated bearings which make them more susceptible to the effects of shear forces.

1.1 Problem Statement

Elastomeric bearings which are designed and installed properly have a life expectancy of over three to four decades. For the last 50 years, Maryland has used elastomeric bearings for concrete bridge structures. For bridges with the same characteristics (size, type) and the same loading conditions, many different sizes of elastomeric bearings can be designed. The state of Maryland would now like to unify the design elastomeric bearings. Elastomeric bearings, like any other structural element, has a defined design procedure which has been improved (by AASHTO) through the years. Performance problems and the understanding of elastomer material have been the driving force behind these continuing revisions. Problems with elastomeric bearings could be due to poor quality, improper installation, bearing stiffening during maximum bridge contraction or a number of other reasons. The specific reasons that elastomeric bearings have had trouble are not understood and have not been investigated in Maryland.

The request of the Maryland SHA is to study the condition of bearings which are in use, determine the common physical symptoms/problems having to do with age, design or weather condition. Through these findings determine the cause of ill performing bearings.

1.2 Approach to Problem Solving

To determine this feasibility, the background of the use of elastomeric bearings in Maryland must be studied. Elastomeric bearing candidates will be selected and than studied. After bearings are selected for the study, a field study will be preformed to evaluate the in-situ condition of the bearings. Using the evaluation of the current conditions of each bearing, they will be categorized by failure mode and by PONTIS

ranking. To understand older bearings their designs will be analyzed and compared to current bearing design guidelines. Finite element models will be assembled to further investigate how well current and past AASHTO bearing designs perform.

1.2.1 Background Data Collection

To begin the analysis, background information of Maryland’s use of elastomeric bearings must be collected. There are many bridges using elastomeric bearings in Maryland. Not all of these bearings would be beneficial to the outcome of the study so a list of bridges was selected to study. The criteria used to select the candidates for study were taken from the “Guide for Completing Structure Inventory and Appraisal Input Forms”. The first criterion had to do with the structure type, item 43a and 43b. Item 43a designates the structure type. Prestressed (pretensioned) concrete and prestressed (pretensioned) continuous concrete bridges were considered. Item 43b indicates the predominate design type of the bridge. Bridges constructed using slab, girder and box beam construction schemes were considered. Once bridges were narrowed down, the bearing type (item 242a) was used to further narrow the list of candidates. The designation for elastomeric bearings is H, J or I. These criteria narrowed the Maryland bridge inventory to 81 acceptable candidates for study. Additional data (listed below) was collected to determine bridge characteristics and conditions.

Item #	Item Description	Item #	Item Description
210	Number of Spans	240	Original Spacing
211	Span 1 - Length	54a	Feature Under Bridge
212	Span 2 - Length	54b	Min. Vertical. Underclearance
213	Span 3 - Length	55a	Feature Under Bridge
214	Span 4 - Length	55b	Min. Lat. Underclearance(right)
215	Span 5 - Length	56	Min. Lat. Underclearance(left)
216	Span 6 - Length	31	Design Load

217	Span 7 - Length	70	Bridge Posting
218	Span 8 - Length	66a	Type of Loading
238	Original Number of Girders	66b	Gross Load (tons)
239	Added Girders		

All information pertaining to the design or construction of each bearing if available should be collected and studied. Data such as age, girder/slab span, structure type, location, conditions underneath the bridge, as built dimensions, and bearing properties should all be noted. Whether the bearing is plain or laminated should be noted and if it is laminated, the thickness of the steel plate should be considered. Trip plan can be found in Appendix A and all information collected can be found in Appendix B of this thesis.

To understand the in-situ state of each bearing, the failure modes of elastomeric bearings should be researched. Understanding of how elastomers behave when exposed to long term loading, and weathering is critical in diagnosing the symptoms of each bearing.

1.2.2 Field Study

Once background data is gathered and studied, the bearings must be inspected in the field. During the field study, data will be collected in relation to the conditions of the bearing. These notes will be cross-referenced with the background data to determine how each bearing has performed over its lifetime. Details of the field study are presented in chapter 2.

1.2.3 Analysis

To fully understand the problems with each bearing, the design calculations were analyzed. AASHTO's "Standard Specifications for Highway Bridges" has presented the standard design method for elastomeric bearings since the late 1950's. Changes and

improvements have been made to each edition so to eliminate problems with previous bearing designs. To determine if a bearing was under designed, each bearing which is failing will be compared to today's AASHTO bearing design standards. If a bearing does not meet a certain facet of today's design standards, the mode by which it seemed to be failing in the field will be compared to this design flaw to see if there is correlation. Details of the analysis are presented in chapter 4.

Finite element analysis will be used on bearings which have been classified as failing to determine actual stresses in the bearing. Correlations, if any, will be made between the failing bearing and their finite element models. SAP2000, a commercial FEM software, will be used to perform the analysis. Details of the analysis are presented in chapter 5.

1.3 Literature Review

Elastomeric bearings have been used in concrete bridge structures for the past 50 years. (Park 2001) Their favorable material properties in addition to being cheap have made elastomeric bearings the leading alternative to more expensive types of bearings.

Elastomeric bearings were first used in the US in 1957 on a bridge in Texas. (Potter et al. 2004)

1.3.1 Previous Studies

A forensic study was performed by the Florida DOT on the Bryant Patton Bridge located in Eastpoint, Florida. The objective of the study was to find the state of the bearing after 40 years of service. (Potter et al. 2004) The hot and humid environment of Florida exposed the bearings to harsh weathering conditions while 40 years of traffic provided sustained loading conditions.

The bearings, which were installed in 1964, were 6" x 18" x 1" plain elastomeric pads, which supported Type II AASHTO girders. Girder spans were 55' which provided an average dead load of 325 and 365 psi for exterior and interior girders, respectively.

Visual examination of the pads suggested that the bearings had experienced long term creep over their service life. Measurements confirmed that the bearings lengths and widths had increased up to 3/8" in some case while the thickness of the pads had decreased a maximum of 1/8" in areas which were loaded. Unloaded areas did not have a decrease in thickness, but did experience cracking or weathering. These cracks were attributed to exposure to ozone and weather. To determine how far these cracks had propagated, some bearings had core samples taken. The cracks that formed had not penetrated the elastomer further than 1/8". The deterioration of the bearings was minimal.

Durometer testing was also performed on the bearings to determine the changes in hardness over the service life. The estimated design durometer was 70. The average internal durometer of the pads were 74. This is an insignificant change in hardness according to current testing methods which allow a change of 15 durometer. Shear tests were also performed on samples of the bearings. Results revealed that the current shear modulus was nearly 2 times current allowable values. A shear modulus of 514 psi was calculated while the current AASHTO standard for 70 durometer pads is between 160 and 260 psi. AASHTO had no restrictions on the shear modulus at the time of the design so the shear modulus at fabrication was unknown.

1.3.2 Thermal Effects

The effects of thermal radiation on elastomeric bearings occurs both directly and indirectly. Directly in the sense that as the ambient temperature increases, so does that of the bearing. Indirectly in that as the ambient temperature increases, the bridge deck expands causing lateral deformation of the bearing.

The direct effect of temperature is that as ambient temperatures increase and decrease so do those of the bearings. Unlike steel or concrete, the stiffness changes dramatically for elastomers, becoming stiffer as temperature decreases. (Yura et al. 2001) Temperature increases don't generally affect the bearings performance as the elastomer will have a greater ability to deform without a loss of compressive strength. Rather, when the bearing decreases in temperature the elastomer begins to crystallize becoming brittle. This becomes a problem when combined with thermal contraction of the bridge deck.

As the outside temperature decreases, the bridge deck and girders will shorten. When this is coupled with the stiffening of the elastomer the worst case loading situation will occur. The further the temperature decreases, the worse the loading condition is and the greater the elastomers susceptibility is to tearing. (Park 2000)

1.3.3 Elastomers

“Elastomers are polymers capable of recovering substantially in size and shape after removal of a load.” (Mackerle et al. 1997) Rubber is classified as a naturally occurring elastomer, but elastomers may also be synthetic. The difference between natural and synthetic elastomers is the addition of sulfur and other additives to hydrocarbon polymers found in natural rubber. Different additives can produce different elastomer properties depending on the desired result. The most common synthetic elastomers are neoprene and

chloroprene. Elastomers have a good resistance to weathering and are able to sustain large deformations without experiencing material fatigue. Other advantages of elastomers include low susceptibility to freezing, corrosion and deterioration. (Park 2000) Although with temperature changes the shear modulus of elastomers change, becoming stiffer and more brittle with decreasing temperature. As the elastomer becomes brittle, the elastomers capacity for deformation decreases causing the elastomer to tear in some cases.

Elastomers are nearly incompressible, meaning that there is no (or an extremely small) change in the volume of the elastomer as it is loaded. Elastomers have the ability to change shape but do not experience volume changes. Incompressible materials are said to be hyperelastic. The accurate modeling of elastomeric bearings using finite element software has been limited in the past by insufficient hyperelastic material models. Advances in these material models have allowed accurate finite element models to determine the behavior and performance of elastomeric bearings.

Chapter 2

Field Study

2.0 Field Study

To begin to the investigation into what is causing failures in bearings, data dealing with the conditions of bearings which were currently in use was compiled. Data from bearings which were in degraded condition as well as those in good condition was collected so that comparisons could be made between the two states. Bridges had to first be selected for the study. Failure modes of bearings were identified and evaluation sheets were made to collect data. Bridge locations were confirmed using Google Earth and trips were planned based on the location of the bridges. After data was collected for each bearing, analyses were performed to quantify the results of the field study.

2.1 Bridge Selection and State Highway Administration Criteria

The bridge selection process was simple. All concrete bridges which used elastomeric bearings in the SHA database were selected as a candidate for study. A total of 81 bridges were selected. Of these there were 48 slab bridges, 26 girder bridges and 5 box beam bridges. A database was created listing all attributes for the bridges including span lengths, age and the whether spans were simple or continuous.

2.1.1 Bearings Failure Modes

The presence of rubber or neoprene in elastomeric bearings results in various failure modes. The two basic modes of failure are compressive failure and rupture of the steel laminates. Besides these two modes, there are failures associated with pad deterioration,

pad slip, creep, bulging, aging, delamination between rubber and metal, poor quality of the bearing and the effects of diagonal tension strains. A unique property of elastomeric bearings is that material properties change with the temperature as well as aging. The susceptibility to temperature and aging play an important role in bearing failure, even if bearings are sized to develop all of the stresses and strains associated with compression and shear.

2.1.1.1 Pad Deterioration

Pad deterioration in elastomeric bearings has a relatively high occurrence but rarely causes failure (Yura et al. 2001). Plain bearings being undersized causes shear strains too high for the bearing to develop properly. This results in the areas of high shear stress beginning to deteriorate due to weathered elements as well as compression. Pad deterioration generally occurs only on the outside of the bearing. The interior portions of aged elastomeric bearings have been found to have the same physical properties as they did when they were made. Deterioration is a common problem found in older bearings and undersized bearings.

2.1.1.2 Pad Slip

Pad slip can be described as the effect when bearing surfaces in contact with the sole plates move due to the compressive force or shear (Park 2000). There are a few factors which cause pad slip. Because bearings are susceptible to ozone, they will deteriorate if not properly protected. A common technique for protecting bearings is coating them with paraffin wax. This wax does help to protect the bearing from ozone degradation, but it also lubricates the edges of the bearing causing the bearing to slip or “walk” from its

original position. The presence of paraffin wax can be traced to multiple occurrences of slip in the same bearing. This has been a common problem in bearings protected with paraffin wax. Another cause of slip is when the bearing is not positively secured to the sole plate by mechanical devices. Typically bearings are secured to sole plates by a few methods. Either the bearing can be attached with an epoxy, strong enough to develop to shear force at the interaction between bearing and sole plate, or anchoring with dowels. Both of these methods are acceptable to prevent walking.

2.1.1.3 Creep and Bulging

It is well known that elastomers display the behavior of creep. Creep in elastomers is defined as the “continuing time-dependent deformation under constant load.” (Yura et al. 2001) Creep in elastomers is the function of two different factors, physical makeup and chemical makeup. The physical properties will dominate the creep process when the bearing is at ambient temperatures while, at high temperatures, the chemical makeup will dominate. The rate of physical relaxation has been found to decrease linearly with the logarithm of time. Creep is caused mostly by compressive forces and moments in the bearing, as these will cause the bearing to bulge. Bulging, to some extent, is experienced by every bearing which is undergoing compressive loading. The edges which are bulging will experience the highest shear stresses. Stress relaxation will be highest at the edges as well. The magnitude of the “bulge” in a bearing will be dependent on the temperature as well as the hardness of the bearing. The softer the bearing is at ambient temperature, the more the bearing will bulge and eventually creep. As the temperature decreases the bearing will become stiffer and bulge less (vice versa for increasing temperature).

2.1.1.4 Aging

The properties of elastomers degrade over time. The facet of this degradation which is caused by heat, UV radiation and exposure to oxygen is called aging (Yura et al. 2001). Of these factors the effects of oxygen seem to be most critical as it is always present. Oxidation causes elastomers to become hard and brittle. The constant presence of oxygen on the bearing coupled with heat and UV cause the bearings to crack on their exposed edges. These factors coupled with compressive forces can cause the outside of the bearing to develop cracks as well as tear. Applying paraffin wax to the outside of the bearing has been used as a technique to slow the aging process. The wax reduces the permeability of the elastomer, thereby slowing aging. One major problem with applying paraffin wax is that it has caused slipping in the bearings.

2.1.1.5 Delamination

Delamination between the elastomer and the steel reinforcement used in laminated bearings can be the result of a few things (Yura et al. 2001). High shear stresses can cause the bearing to split and eventually delaminate. Delamination is usually not a result of a failure of the bond between the elastomer and the shim. Rather, splitting of the elastomer due to an inconsistency in the elastomers matrix begins delamination. This crack will then propagate near the surface of the steel shim causing delamination.

Delamination is usually found in aged bearings as they are more susceptible because of their brittle edges.

2.1.1.6 Poor Quality

The manufacturing of elastomeric bearings is of key importance in terms of bearing failure. Elastomeric pads can have variations in its matrix, making one area of the pad stronger than another. When the weak areas experience high shear stresses, age cracks will begin to form causing delamination and deterioration. Poor quality in the bond between the steel shims and the elastomer can cause delamination. Poor quality in the attachment between bearings and sole plates can lead to slipping of the bearing (Park 2000).

2.1.1.7 Crushing

Crushing of an elastomeric bearing is an indication of compressive failure. A pad being undersized is the main cause of crushing. This is not a problem in newer bearings but bearings designed by the 10th-12th edition of AASHTO had a less stringent thickness requirement. Bearings designed from this era of AASHTO are mostly plain bearings resulting in less compressive strength of the bearing. More recent bearing designs are using laminated bearings which have higher compressive strength. If a bearing does crush, the forces in the superstructure become directly transferred to the substructure leading to failures in the girders as well as the abutment or pier. Crushing, more than anything else, will affect the ride quality of the road.

2.1.1.8 Rupture of Reinforcement

The rupture of steel shims in elastomeric bearings is rare. High stresses due to rotation and compression causing bulging will lead to rupture. As the ends of the bearing bulge they will rotate causing the reinforcement to rotate as well (Park 2000). There are limits placed by AASHTO on the allowable rotation of the bearing to prevent rupture.

2.1.2 Inspection Items

To ensure that an elastomeric bearing is not failing, it should be inspected regularly. There are many symptoms which must be diagnosed. These symptoms must be understood to properly identify the condition of the bearing as well as if and how it is failing. Before an inspection, the design dimensions and whether the bearing allows expansion or if it is fixed should be known. Studying the as built plans before an inspection is critical to determining the condition of the bearing. Refer to Table 2.1.

Failure Modes	Notes	Inspection Items	Reference
Pad Deterioration	Results from large shear strains on plain pads.	1)Splitting and tearing at edges 2)Delamination between rubber and metal	NCHRP Report 449 - p 3
Slip	Results when the bearing was not directly connected to the piers using sole plates or other mechanical devices. Repeated slip occurred due to paraffin wax added to the rubber for Ozone protection.	1)walking of the bearing from its original position 2)Bond between rubber and the sole plate	NCHRP Report 449 - p 3
Creep/Bulging	There is significant creep for Electrometric Bearings. Bonded sole plates at the top and bottom of the bearing caused about 50% less creep. Bearings with a higher shear modulus have higher creep.	1)Excessive bulging of the pad	NCHRP Report 449 - p 45
Aging	Generally aging only affects the thin outer layer of the bearing. Old bearings which are exposed to severe temperatures will experience a change in the shear modulus.	1) Cracked edges (especially in bulges)	NCHRP Report 449 - p 51
Delamination	Occurs between the metal shim and rubber due to low or absent bond.	1)Splitting and tearing at edges 2)Delamination between rubber and metal	NCHRP Report 449 - p 81 Bridge Inspection and Structural Analysis - p 165
Poor Quality	A major cause of failure. Bearings will be damaged if the bridge superstructure rotates about any other axis than the line of the bearings.	1)Splitting and tearing at edges 2)Delamination between rubber and metal 3)Growth in pad length at the masonry plate	Bridge Inspection and Structural Analysis - p 159
Crushing	Compressive failure in the bearing. Hard to detect and noticeable by voids at the bottom of the bearing. Also increased bump in the road.	1) Voids beneath the pad 2)Bumps in the roadway	Bridge Inspection and Structural Analysis - p 165
Diagonal Tension Strains	Caused by the combined effect of compression, shear and rotation.	1)Growth in pad length at the masonry plate 2)Height differences in the pad or internal layers	Bridge Inspection and Structural Analysis - p 165
Rupture of Reinforcement	Caused by large shear strains.	1)Layer heights should be the same	Bridge Inspection and Structural Analysis - p 169

Table 2.1 - Inspection Items for Elastomeric Bearings

Chapter 3

Field Study Results and Findings

3.0 Field Study Findings

Data was collected from the field study and recorded on forms. Pictures were also taken so that the bearings could be analyzed at a later time. The data that was collected was organized by a spreadsheet which can be seen in Appendix B. The most common symptoms included bulging, creep and slip. The symptoms of each bearing were cross referenced with pictures along with the as-built dimensions in order to best identify how each bearing was failing. Once the modes of failure were identified for each bearing, they were rated using both the NBI Condition & Appraisal Ratings and the PONTIS Element Condition Rating to determine the degree of failure.

3.1 Failing Bearings by Mode

The data that was collected during the field study were organized in a spreadsheet so that each bearing could be analyzed for the symptoms observed in the field. The pictures taken in the field were used to help understanding the notes recorded in the field. Using both the notes and pictures, each bearing was placed into groups based on the different failure modes. Creep was separated from bulging when the bearings were grouped because excessive creep may be classified as a state of failure while bulging for the most part may not.

3.1.1 Pad Deterioration

Pad deterioration was observed in thirteen of the studied bearings. Most of the bearings studied were in good condition. Only in cases where there seemed to be an undersized bearing was there noticeable deterioration. Older bearings also had more problems with deterioration. In about half of the slab bridges, foam had been placed around the bearing to protect it from the effects of weather. The presence of the foam led to less deterioration. Below is a list of the bridges which were determined to have deteriorated beyond an acceptable limit.

010016001	160108031
010016901	160108041
010097001	170026001
070007001	190009001
070034001	220020001
080051041	230017001
100048001	

Below is an example of deterioration in bridge #1169.



Figure 3.1 - Pad Deterioration in Bridge #1169

3.1.2 Pad Slip

Pad slip was detected in twenty-two of the studied bearings; some situations are worse than others. The beginning stages of slip were detected in the majority of the diagnosed bearings. In a few cases the bearings had walked significantly. In these cases the

Maryland SHA was contacted and alerted to the condition of the bearings. Most of the cases of slip were determined to be in the acceptable limits of allowable slip. Below is a list of the bridges which were determined to have slipped from their original position.

010013001	090006001
010097001	090010001
020006001	090012001
020071001	090013001
030097001	090015001
040029001	130157001
060012001	190009001
070007001	210059001
080009001	230042011
080051031	230042021
090004001	230043001

Below in Figure 3.2 was the worst case of slip observed while performing the study. Notice that about fifty percent of the bearing has walked off of the sole plate. This is very dangerous as eventually the girder could fall when the bearing walks completely out.



Figure 3.2 - Bearing Slip in Bridge #9015

Less critical occurrences of slip were also observed such as the one displayed in Figure 3.3 below. Notice that the left side of the bearing is walking off of the edge of the sole plate.



Figure 3.3 - Bearing Slip in Bridge #2006

3.1.3 Creep

Creep was diagnosed in 26 of the bridges that were surveyed. The least critical cases of slip included those bearings whose edges were beginning to grow at the sole plate. This was drastically different from the most critical cases in which the bearing had been crushed due to creep. In this situation the section of the bearing directly underneath the girder or slab was much thinner than the section of bearing that had expanded beyond the extents of the girder. Bearings located at the piers of girder bridges tended to exhibit creep more than the bearings located at the abutments. Figure 3.4 shows creep at a pier in a girder bridge.



Figure 3.4 - Creep at a Pier in a Girder Bridge

This suggests that bearings located at piers may be undersized for the most part. Most bearings located at the abutments seemed to be adequately sized in general, but not in all cases. Figure 3.5 shows a bearing located at an abutment which has crept out from underneath the girder.



Figure 3.5 - Creep at an Abutment in a Girder Bridge

Crushing of the bearing can result from excessive creep as seen in Figures 3.4 and 3.5. Figure 3.6 shows the beginning stages of creep. Eventually the bearing will creep until it begins to be crushed similar to those shown in the above figures. Notice the excessive bulge in the bearing in Figure 3.6.



Figure 3.6 - Beginning Stages of Creep

Below is a list of bridges which experienced creep in the bearings.

010097001	090010001	070034001	200016001
020006001	090012001	080009001	210059001
020071001	090013001	080051031	220002011
030097001	090015001	080051041	230042011
040029001	100026001	090004001	230042021
060012001	130157001	090006001	230043001
070007001	190009001		

3.1.4 Bulging

Bulging was the most common symptom experienced by the bearings. Compressive loading causes bulging in elastomers. Moderate bulging is expected in bearings and is not a cause for rehabilitation. Only when bulging is excessive is it identified as a problem.

Excessive bulging can lead to creep and eventually crushing or it can lead to accelerated deterioration of the bearing. Excessive bulging also gives an indication that a bearing has been undersized. Bulging in laminated pads is generally less than in plain pads because the steel reinforcement doesn't allow the elastomer to expand where it is in contact with the steel. Plain pads do not have that confinement and will tend to bulge uniformly over

the entire thickness of the pad. This is displayed in Figure 3.6. Figure 3.7 shows bulging in a laminated bearing. Notice that bulging occurs in between the reinforcement at each individual pad and not uniformly over the entire thickness. A total of 40 bearings shows bulging.



Figure 3.7 - Bulging in a Laminated Bearing

Below is a list of bridges which experienced bulging.

010013001	090012001	060016001	190012021
010016001	090013001	070007001	200016001
010097001	090015001	070034001	200017001
010169001	100026001	080009001	200024001
020006001	100048001	080051031	210059001
020071001	120045001	080051041	220005011
030015001	120046001	090003001	220002011
030097001	130157001	090004001	230017001
040029001	170027001	090006001	230042011
060012001	190009001	090010001	230042021

3.1.5 Aging

Aging is experienced by all bearings, although the process of aging accelerates as stress increases on the bearing. Exposure to UV radiation and ozone are the other factors which contribute to aging. Aging can be identified by small cracks in areas of concentrated stresses. Four bearings were identified as having an aging problem. This was not a

common problem as most of the bearings investigated were not directly exposed to the weather. Below is a list of bridges which experienced aging.

010097001
160108031
160108041
190009001

3.1.6 Delamination

Delamination was not a major symptom found during the field study. This suggests that the bearings were not loaded to the point where the elastomer debonded from the laminate. Cracks that form at areas of concentrated stresses tend to propagate to the bond between the laminate and elastomer. This is a major source of delamination along with poor manufacturing. Figure 3.8 shows the top elastomeric pad moving past the extents of the laminate. This is rarely seen as most laminated bearings are fully encased by the elastomer.

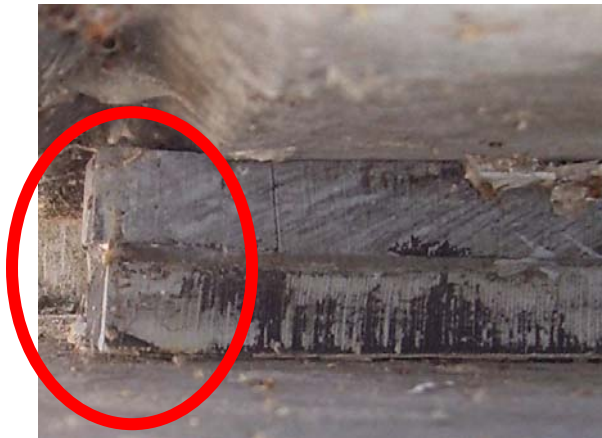


Figure 3.8 - Delamination of an Elastomeric Pad

Below is a list of the three bearings which had problems with delamination.

010097001
230017001
090010001

3.1.7 Poor Quality

Diagnosing a bearing for poor quality is difficult for two reasons. Poor quality rarely poses problems in elastomeric bearings and poor quality is hard to distinguish when the bearing is failing by other modes. Today's manufacturers implement high quality control practices to ensure maximum performance. During the field study three bearings were found to have substandard quality. Figure 3.9 shows a bearing which has deteriorated, most likely due to an inferior elastomer.



Figure 3.9 - Deterioration Due to Poor Quality

The bearing in figure 3.9 was installed in 1996 which leads one to believe that the pad hasn't deteriorated or aged. Below is a list of the three bearings which had problems with poor quality.

010097001
100048001
230017001

3.1.8 Crushing

Crushing is a result of a bearing being excessively loaded. Signs of crushing include high creep beyond the extents of the girder and a size difference between two elastomeric pads in the same bearing. Creep beyond the extents of the girder can be seen in figure 3.10.

Notice the height difference between the edge of the bearing not under the slab and the area of the bearing which is under the slab. The bearing shows a height difference of 33% between the two areas. Crushing of this nature tends to be found in plain bearings with thicknesses less than two inches. Crushing in laminated bearings is less frequent as laminated bearings generally have higher strength.



Figure 3.10 - Crushing in a Slab Bridge

A total of nine total bridges which had crushed bearings were found during the field investigation. They are listed below.

010097001	080009001	200024001
030097001	160108031	230042011
060012001	160108041	230042021

3.1.9 Rupture of Reinforcement

There was one questionable case of rupture of reinforcement in bridge 23017. Rupture of reinforcement did not tend to be a problem in the laminated bearings studied. This suggests that the steel shims used to reinforce laminated bearings are adequately sized per AASHTO standards.

3.2 Group and Ranking of Failing Bearings

After the diagnosis of the symptoms, the condition of each bearing was rated (Minnesota DOT 2004). The PONTIS scale was used to rate each bearing. The PONTIS scale is based on the “AASHTO Guide for Commonly Recognized Structural Elements”.

PONTIS was created to comply with the 1991 Inter-Modal Surface Transportation Efficiency Act (ISTEA) which required each state to implement a comprehensive bridge inspection program. PONTIS is a comprehensive inspection system which breaks the bridge into different “elements”, each element representing an individual structural component commonly found in bridges.

The PONTIS scale is based on a rating of one to three for element #310, Elastomeric Bearings. Each rating represent a different condition state, condition state 1, 2 and 3, each state corresponding to a rating.

Condition State 1 or a rating of 1 indicates that the bearing is virtually free of any damage. The bearing should be in the proper position with the expected deformation and orientation for the temperature at the time of the inspection. Limited minor cracking or splitting is permissible while still achieving a rating of 1. No action is needed to refurbish or replace the bearing.

Condition State 2 or a rating of 2 indicates that there may be slight damage but generally in tact as installed. This rating may also indicate that the bearing has moved slightly from its original position or that the current temperature is imposed an unacceptable deformation or orientation. Splitting, laminations being exposed, excessive bulging and medium sized gaps between the bearing and the sole plate will also deem a rating of 2.

The bearing should be refurbished to an acceptable condition, or the bearing should be replaced. Immediate action is not necessary as the bearing is still functioning.

Condition State 3 or a rating of 3 indicates that there is failure or excessive damage. Crushing, excessive bulging, walking, tearing of the elastomer, large deformations due to rotation or compression are all part of this condition state. The steel reinforcement in the bearing could also have failed or be deteriorating. A bearing in this condition should be given a rating of 3. Danger could be imminent and the bearing should be replaced immediately.

The bearings studied produced 40 bearings with a rating of 1, 17 bearings with a rating of 2 and 2 bearings with a rating of 3. The two bearings which were rated a 3 had excessive damage and action to replace them should be taken immediately.

The 2 bridges which had bearings with a PONTIS rating of 3 are listed below.

10097001
90015001

The 17 bridges which had bearings with a PONTIS rating of 2 are listed below.

10169001	190009001
30097001	200017001
40029001	220020001
60012001	100026001
80009001	100048001
80051041	230017001
90012001	230042011
130157001	230042021
160108041	

Chapter 4

Overview and Progression of AASHTO Codes and Design Methods

4.0 Evolution of AASHTO Codes and Industry Practices

Elastomeric bridge bearing design is governed by AASHTO (formerly AASHO) in the “Standard Specifications for Highway Bridges” and lately, “LRFD Bridge Design Specifications.” There have been numerous editions of the AASHTO requirements, each addition, theoretically, improving bearing design based on the improved knowledge of neoprene/steel composite action. These editions must be investigated for the specific improvements and other differences. Beyond design of the bearing there are other factors which may contribute to the ill performance of a bearing. Industry practices for manufacturing and construction play an important role in the performance of elastomeric bearings.

4.1 Approach

To properly analyze the studied elastomeric bearings, enough information had to be collected or generated so that comparisons could be made. The data which was obtained from the field study was not enough to analyze the bearings. These data only shed light on the current physical condition of the bearings. Properties such as hardness and shear modulus could not be obtained from the field study. To analyze each bearing, as many of the properties, loads, and design criteria needed to be collected in order to be able to make comparisons between different factors affecting the bridge.

It is expected that each successive design should provide a more accurate or “better” design for the same loading conditions. For example, if a failing bearing were to comply

with the requirements for the 10th edition of the AASHTO code but not the 14th edition, it may be concluded that if the same bearing had been designed using 14th edition standards that it might not be failing. The evolution of AASHTO codes through the years was studied to see what requirements had changed, as this could provide insight as to why bearings may or may not be failing.

After each bearing was compared to the design requirements of each of the AASHTO codes, an investigation to determine if there were any relationships between geometric properties (such as length, width and height), loads and deflections were made. These results can be seen in chapter 3. The thought behind this analysis was that there may be certain trends with failing bearings and the bearings which were not failing. The analysis was done on the entire group of studied bearings, as well as bearings in girder bridges and slab bridges separately to determine whether either type of bridge displayed trends for failing. The findings from both analyses gave insight into what is causing the degradation of bearings.

4.2 Data Collection

The collection of data was an important part of the analyses performed. Data was collected in a few different ways. To begin the study, background information about each bridge had to be collected. Using the bridge background information a field study was performed to verify all of the background data as well as to gather new data about the bearing and its performance. Other information needed to be collected about the designs of the bearings in order to perform analyses. Available design files were collected from the SHA in order to get an idea of how bearings have been designed over the last 50 years. Less than a quarter of the studied bridges had applicable design files for their

bearings so the design loads were calculated for each bridge that did not have a design file.

4.2.1 Bridge Background

The bridge background for the selected bridges was provided by the SHA database. Items which were included were bridge number, the county location, structure type (items 43a and 43b), the features under each bridge (item 55a), minimum vertical clearance underneath the bridge (item 54b), the number and length of spans (items 210 -218) and the type of loading (item 66a). The item numbers in parentheses above correspond to the “Guide for Completing Structure Inventory and Appraisal Input Forms” produced by the Maryland Department of Transportation (MDOT 2003). Information that could not be collected from this book was obtained from the “2005 Bridge Inventory” produced by the MDOT and SHA.

Other information was collected from as built plans of the bearings. The plans were provided by the SHA and are in electronic form. Data collected from the as built plans included the bearing material, length, width, height, hardness, whether the bearing was laminated or not and the reinforcements inside the bearings. Not all of this information could be extracted from the plans as some sets of plans were incomplete or lacked the types of information above. Also based on its age, each bearing was categorized by the AASHTO edition which governed the design of the bearing.

4.2.2 Field Study

Information that could not be collected from the as built plans, such as bearing dimensions, was collected from the field study. This helped to complete or verify the

information collected from as-built plans and other sources. Other information collected during the field study had to do with the condition of the bearing, whether the bearing was in good condition and what symptoms of failure (if any) were being displayed. Each bearing was then rated using the PONTIS rating scale as discussed in chapter three.

4.2.3 SHA File Search

Information dealing with the physical attributes of the bridges and their bearings was collected during the field study but no information was known about the loading conditions or the bearing design. To collect information about the bearing designs, files at the SHA were searched for the design files. The contract numbers for each bridge were found and as many design files were located as possible. 23 (of the 81 possible) bridge files had complete bearing designs. The remaining 58 bridges had no design calculations or design loads. To perform a complete analysis, the load on each bearing was needed.

4.2.4 Load Generation

Since 23 of the bridges had design files, design loads could be taken directly from those files. The remaining 58 bridges required the loads to be generated manually. Using the as built plans and the program DASH/PSB, created by the BEST Center, design loads were developed for the remaining 58 bridges. For the 23 bridges which had design files, design loads were verified.

4.2.5 File Organization

To perform the analyses on the bearings, all data were gathered and manipulated in various spreadsheets. Different parts of each spreadsheet were combined into more

spreadsheets in order to be able to make comparisons and graphs for the different analyses. The spreadsheets can be seen in Appendix B.

4.2.6 Evolution of AASHTO Codes

The governing body for the design of elastomeric bearings is American Association of State Highway and Transportation Officials (AASHTO, formerly AASHO). Many editions of AASHTO have been used in bearing design over the years. Every successive edition theoretically provides a “better” design methodology, although for this study that was left in question. Statistics taken from the data which was collected revealed that this was not the case. The later editions of AASHTO showed the same percentage of failed bearings as did earlier editions. The results are seen in Figure 4.1.

AASHTO Design Edition	PONTIS Rating = 1	PONTIS Rating = 2,3
Prior to the 10th Edition	66.67%	33.33%
10th Edition	66.67%	33.33%
11th Edition	No Data	No Data
12th Edition	0.00%	100.00%
13th Edition	33.33%	66.67%
14th Edition	66.67%	33.33%
15th Edition	87.50%	12.50%
16th Edition	62.50%	37.50%
17th Edition	No Data	No Data

Table 4.1 - Percentage of Bearings by PONTIS Rating and AASHTO Design Edition

Table 4.1 reveals that nearly 2/3 of the bearings which were studied consistently had a PONTIS rating of 1 (no problems) excluding the 12th and 13th editions. No consistent improvement is seen from the 10th to the 17th edition as was expected. This may mean that although changes have been made, the actual design of bearings have not become “better” for later editions of AASHTO. To verify this hypothesis an analysis was done to

compare the different editions of the AASHTO design guides and their design criteria. For each edition, changes from previous design criteria were noted. Graphs were made to compare the different design criteria visually.

Spreadsheets were created for design bearings using the 10th, 12th, 14th and 17th editions of AASHTO. This was done so that each bearing design could be checked against the later AASHTO design criteria with the thought that bearings with PONTIS ratings of 2 or 3 may not be in such bad condition if they had been designed by using a more recent AASHTO design standard. Based on figure 4.1, the initial thought would be that there are no significant changes in bearing designs over the years.

4.2.7 10th Edition

The oldest edition of the AASHTO design standards for elastomeric bearings that could be found was the 9th edition, in 1961. The DuPont Company was responsible for much of the research of elastomeric bearing behavior to this point. The research that had been completed was focused on plain (unreinforced) elastomeric pads. (Roeder et al. NCHRP 325, 1989) This was the starting point of elastomeric bearing design in AASHO. The 10th edition did not include any improvements to the bearing designs. The 10th edition was published in 1969 and was used until 1972. The design standards were brief, only discussing major design issues such as the maximum bearing pressure, compressive strain, stability and the allowable dimensions of bearings. Section 1.12.2 of the AASHTO code outlines the design specifications for elastomeric bearings. It relies heavily on manufacturers' data to determine the physical capabilities of the elastomers although AASHO provided basic guidelines for the properties of the elastomers. Either virgin

natural polyisoprene (natural rubber) or 100% virgin chloroprene (neoprene) was able to be used so long as it met the requirements of the AASHTO code.

4.2.7.1 Design Criteria

The 10th edition design criteria were taken as being at a base level design as they proved to have the least stringent design criteria of all of the editions of AASHTO. Below is a bulleted summary of the design criteria of the 10th edition.

- Bearings may be plain (elastomer only) or laminated (natural rubber or neoprene)
- Elastomer compounds of nominal 70 durometer hardness shall not be used in laminated bearings
- Plain bearings shall be restricted to applications where little movement is anticipated
- $S =$ Shape factor (the area of the loaded face divided by the side area free to bulge
- $S = \frac{LW}{2t(L+W)}$ for rectangular bearings
- $S = \frac{R}{2t}$ for circular bearings
- The strain is dependent on the unit compressive stress, the hardness of the elastomer and the shape factor
- The maximum compressive stress of each layer is 800 psi for the combination of dead and live load (not including impact)
- The maximum compressive stress of each layer is 500 psi for dead load
- The maximum allowable uplift is 200 psi
- Stability for
 - Plain Bearings

- Min. Length = 5T
- Min. Width = 5T
- Min. Radius = 5T
- Laminated Bearings
 - Min. Length = 3T
 - Min. Width = 2T
 - Min. Radius = 3T

4.2.8 12th Edition

The 12th edition of AASHTO was published in 1977 and was used until 1982. Section 1.12.2 of the AASHTO code outlines the design specifications for elastomeric bearings. Studies by the National Cooperative for Highway Research (NCHRP) were performed to bring light to the design of elastomeric bearings. Up to this point AASHTO relied heavily on manufacturer data and specifications to provide guidelines for their design procedure. In 1970, the NCHRP published their Report #109 which began to reveal the factors which governed the behavior of elastomers when used in a bearing application.

Before 1970, research had been limited to bearings with a shape factor less than 4. Compressive stress had been limited to 800 psi for no rational/scientific basis and designs were based on the hardness of the elastomer. The research performed by the NCHRP was used to develop standard curves to relate initial compressive stress to hardness and shape factor. Research also showed that the shear modulus changed based on the surrounding temperature. The crystallization of the elastomer at low temperatures was investigated to an extent. Shear loading was identified as a major design issue and it was identified that

the shape of the bearing played a more important role than previously thought. Bearing failures to that point were attributed to low quality elastomers. Investigation showed that the amount of filler in the elastomer compound determined the hardness of the rubber. The more filler that was present, the harder the bearing became. It was also discovered that the amount of filler present (the hardness of the bearing) determined the long term creep behavior of the elastomer. Elastomers with more filler were found to creep more. It was also found that softer bearings did not crystallize as quickly as harder bearings did. (Minor et al. 1970)

Even with all of these discoveries, the design criteria in the 12th edition were the same as the 10th edition except for the stability of bearings. The lack of change between the 10th and 12th editions leads one to believe that the 11th edition was similar to its predecessor and successor. The change in the design criteria are listed below.

4.2.8.1 Design Criteria

The changes between the 10th and 12th editions are listed below.

- Plain Bearings
 - Min. Length = 5T
 - Min. Width = 5T
 - Min. Radius = 3T
- Laminated Bearings
 - Min. Length = 3T
 - Min. Width = 2T
 - Min. Radius = 2T

4.2.9 14th Edition

The 14th edition of AASHTO's "Standard Specifications for Highway Bridges" was published in 1989. This edition introduces a few new factors into bearing designs, such as shear modulus, and a strength reduction factor for bearings with holes. Much more emphasis was put on shear modulus and the effects of shear modulus than in previous editions.

By the time this edition was published all of the research reported in the NCHRP Report #109 was included in the design of elastomeric bearings. Also another large study was undertaken by the NCHRP to develop better design parameters for the AASHTO code. Elastomeric bearings had great performance to this point. Although when a bearing did fail, it was major, usually causing problems in the substructure. Bearing replacement tends to be expensive so research was done to better understand the behavior of bearings so that failures would occur less frequently. It was determined that the existing design method did not have a rational basis and that it was geared to the design of plain bearings, not laminated steel bearings. (Stanton et al. 1982)

In 1980, the NCHRP began a three phase research project to improve the design of elastomeric bearings. Other countries around the world had incorporated less conservative designs based on scientific research of elastomers, while the U.S. was depending on manufacturer data. Phase one of the research project was to improve the design procedure that was being used at that time. Phase two set out to identify the failure modes of bearings and to create a more sophisticated bearing design procedure which would take into account the material properties of the elastomer. Phase three of the

project was intended to bring light to the low temperature behavior of elastomeric bearings and to then analyze/verify the findings. (Roeder et al. 1989)

Phase one, as stated earlier, was undertaken in the interest of refining the existing AASHTO design procedure. NCHRP Report #248 was published in 1982 with the results of the research. It was found that manufacturers did not perform adequate quality control checks on bearings as they were produced. (Stanton et al. 1982) It was also found that the tensile stresses developed in the elastomer caused failure of the bearings. (Stanton et al. 1982) The shape factor of bearings could not capture the geometric dependence of the bearings behavior. Also the 7 percent compressive strain limit, 800 psi compressive stress limit and the frictional limits which controls slip of the bearing were identified as having no rational or scientific basis. Empirical manufacturer data was the only rational for these requirements. Because of the problems listed above, the NCHRP set out to improve the current design method, called Method A. (Method B is developed by Phase two of the project) It was recognized that the current design procedure was developed for plain (unreinforced) bearings, yet designers were required to use this method for the design of reinforced bearings. Strength increases were not given to reinforced bearings even though they were known to have greater strength. The compressive strength of the bearings became dependent on the shape factor as well as the shear modulus of the elastomer. Compressive deflection became a design parameter as it was identified to have great impact on the serviceability of the bridge. Rotation, strength of reinforcement and horizontal slip all became part of the design standard of Method A. (Stanton et al. 1982)

Phase two set out to develop an alternate procedure, to Method A, based on the findings of tests performed by the NCHRP. The NCHRP Report #298 was published in October of

1987. The researchers involved in this study recognized that there were different design procedures as well as rationales in different countries of the world. (Stanton et al. 1987) Many of these procedures contradicted each other. It was the goal of the research team to fully understand the parameters that should control the design of the elastomeric bearings. First on the list was to understand the low temperature behavior of elastomeric bearings. It was found that crystallization of elastomers began at temperatures below 32°F and that the rate of crystallization of the elastomer was greatest at 14°F. (This would later be refuted in Phase three of this study). (Stanton et al. 1987) Other key findings included the idea that larger shape factors lead to stiffer bearings as well as higher strains. (Stanton et al. 1987) Related to this idea, it was found that smaller shape factors were associated with higher deflections and strains in the bearings. (Stanton et al. 1987) It was also found that the shear force experienced by the bearings and eventually transferred to the substructure could increase by up to four times as temperature decreased and the shear modulus becomes higher. It was suggested in this study that the U.S. be divided into separate regions defined by different characteristic temperature patterns. (Stanton et al. 1987) From these findings Method B was developed and implemented into the AASHTO design standard.

Phase three of the research project dealt with the effects of low temperature behavior of elastomeric bearings. Findings of this research project can be found in the NCHRP Report #325, published in December 1989. When elastomeric bearings experience low temperatures, they stiffen, causing greater force to be transferred to the substructure. (Roeder et al. 1989) Previous research identified the hardness and compression set as the proper way to describe the low temperature behavior of bearings. The research conducted

in phase three of this study refuted that, identifying the shear modulus as the key factor in describing the behavior of elastomers at low temperatures. (Roeder et al. 1989) As stated before, it was believed that the maximum rate of crystallization occurred at 14°F.

However, studies done during phase three showed that the rate of crystallization of the elastomer increases as temperature decreases. (Roeder et al. 1989)

4.2.9.1 Design Criteria

The changes in design criteria between the 12th and 14th editions of AASHTO are listed below. Design criteria can be found in section 14 of the AASHTO design code. New additions to the 14th edition include specific sections in the code for each element of design. For example, material properties, compressive stress, etc., have their own dedicated sections for design in the AASHTO code. Edition 14 has a more comprehensive design standard calling for the design for rotation of the bearing, design of the reinforcement in laminated bearings, anchorage of the bearing and even the installation of the bearing. In previous editions, manufacturer data was used to find the compressive strain of bearings. This edition has its own standard charts which are to be used, rather than having many varying manufacturer- produced charts. Also standard maximum values for shear modulus and long term creep are given in this edition.

- **Hardness**, the maximum permissible hardness for any bearing was lowered to 60 durometer in laminated bearings. In previous editions, 70 durometer was the maximum allowable hardness. Figure 4.2 below shows the allowable values for shear modulus and creep deflection at 25 years.

Hardness (Shore 'A')	50	60	70
Shear Modulus at 73°F (psi)	85-110	120-155	160-260
<u>Creep Deflection at 25 years</u> Instantaneous Deflection	25%	35%	45%

Table 4.2 - Allowable Shear Modulus and Creep Deflection per AASHTO
(Reference Table 14.2.2A, Standard Specification 14th Edition, 1989)

- **Maximum Shear Deformation** is limited to $T/2$ where T is the total thickness of the elastomer. This clause was limited to the maximum deflection due to temperature in previous editions. The 14th edition expands this to the total shear deflection of the bearing due to creep, shrinkage, post-tensioning and thermal effects.
- **Shear Modulus** becomes more stringent as more requirements based on the hardness were added. The compressive design is also affected by the shear modulus. The limits of the shear modulus can be seen in figure 4.2.
- **Compressive Stress** requirements become more stringent for plain bearings. Higher allowable stresses for laminated bearings are introduced. The factor β is introduced as the modification factor for compressive strength. The β factor reduces the allowable compressive stress in plain and laminated exterior bearings. Laminated interior bearings are allowed the full value of GS for compressive strength. The allowable compressive stress is allowed to be increased by 10% in bearings where shear translation is prevented.

The maximum allowable compressive stress must be taken as the minimum of

- For Plain Bearings (maximum allowable compressive stress)
 - 800 psi

- $\frac{GS}{\beta}$

- For all Laminated Bearings (maximum allowable compressive stress)

- 1000 psi

- $\frac{GS}{\beta}$

Where,

- G= Shear Modulus

- S = Shape Factor

- β = Modification Factor for Compressive Stress

- = 1.8 for Plain Bearings

- = 1 for Laminated Interior Layers

- = 1.4 for Laminated Exterior Layers

- **Rotation** limits are given for the first time in the 14th edition. The relative rotation between the top and bottom surfaces are limited by

- $L\alpha_L + W\alpha_W \leq 2\Delta_c$ for rectangular bearings

- α_L = relative rotation of bearing parallel to traffic

- α_W = relative rotation of bearing perpendicular to traffic

- Δ_c = instantaneous compressive deflection of the bearing

- **Compressive Deflection** is limited to 1/8" over the entire bearing. The compressive deflection is based on the instantaneous compressive strain and the total elastomer thickness. The instantaneous compressive strain is based on the shape factor, compressive

stress and hardness of the bearing. An example of an instantaneous compressive strain chart can be seen in Chapter 6.

- **Creep** deflection, plus the instantaneous compressive deflection is limited to 1/8". The 25 year creep is given in a figure 4.2 and based on the hardness of the elastomer.
- **Rotational Capacity of Bearing**, which can be defined as $2\Delta_c$ should be greater than the design rotation of the bearing. Rotation is given by 2 factors, α_L and α_W , explained above.
- **Reinforcement** in bearings must be designed for A36 steel. The fatigue strength of A36 must also be considered (24 ksi). The effects of holes in the bearings must also be accounted for by a hole factor which is defined by the engineer. The strength of the steel laminate must be greater than the working stresses in the steel. The steel must be checked for LL + DL as well as LL taking into account the fatigue strength when checking just the LL.
- DL + LL

- Working Stress = $1700 \times t_i \times F_h$ (lb/in)

- T_i = average thickness of elastomer layers around steel
 - F_h = Hole Factor

- Strength of Laminate = $F_y \times h_s$ (lb/in)

- h_s = thickness of steel laminate (in)

- LL

- Working Stress = $1700 \times t_i \times F_h \times \frac{\sigma_{LL}}{\sigma_{TL}}$ (lb/in)

- T_i = average thickness of elastomer layers around steel
- F_h = Hole Factor
- Strength of Laminate = $F_{sr} \times h_s$ (lb/in)
 - F_{sr} = Fatigue Strength of steel (psi)
 - h_s = thickness of steel laminate (in)
- **Stability**, the minimum ratio between the total thickness of the elastomer and the length and width change to:
 - Plain Bearings
 - Min. Length = 5T
 - Min. Width = 5T
 - Laminated Bearings
 - Min. Length = 3T
 - Min. Width = 3T
- **Shear Deformation**: Limits for shear deformation are defined in this edition and are based on the shear force and the resistance given by the dead load reaction on the bearing, multiplied by the coefficient of static friction. If the shear force is greater than the resistance, a positive slip apparatus will be required to keep the bearing from moving.
- $F_s = G \frac{A}{T} \Delta_s$
 - G = Shear Modulus
 - A = plan area of the bearing
 - T = total elastomer thickness
 - Δ_s = shear deflection of the bearing

4.2.10 15th Edition

The 15th edition introduces a new design method in addition to the classical bearing design method. Method A was the typical design method that has been used in all previous AASHTO bridge design methods. Method B (the new design procedure) was introduced as an alternate design method for steel laminated bearings. Method B tended to allow smaller bearings than Method A, as well as in previous editions of AASHTO, for any load, due to the presence of the steel reinforcement.

4.2.10.1 Design Criteria

4.2.10.1.1 Method A

- **Hardness**, the maximum permissible hardness for any bearing is raised to 70 durometer in plain bearings only. The maximum allowable shear modulus is only 300 psi in these bearings.
- **Shear Modulus** of the elastomers have a higher maximum value and a larger range than the 14th edition for each respective hardness.
- **Compressive Stress** requirements become less stringent. A 10% strength increase is allowed for fixed bearings (no shear deformations). The maximum allowable compressive stress must be less than the minimum of:
 - For Plain Bearings
 - 800 psi
 - $\frac{GS}{\beta}$
 - For Laminated Bearings
 - Laminated Interior Bearings

- 1000 psi
- $\frac{GS}{\beta}$
- Laminated Exterior Bearings
 - 1000 psi
 - $\frac{GS}{\beta}$

where

- G = Shear Modulus
- S = Shape Factor
- β = Modification Factor for Comp. Stress
 - = 1.8 for Plain Bearings
 - = 1 for Laminated Interior Layers
 - = 1.4 for Laminated Exterior Layers
- **Rotational Capacity of Bearing** is limited to a maximum of

$$\frac{2\Delta_c}{L} \text{ and } \frac{2\Delta_c}{W}$$

in the longitudinal and transverse directions respectively, for rectangular bearings.

Rotation is given by a factor θ_{TL} . Rotation is considered for both the longitudinal and transverse directions for the first time in this edition.

- **Reinforcement**, no changes except for notations
- DL + LL

- Working Stress = $1700 \times h_r i \times F_h$ (lb/in)

- h_{ri} = average thickness of elastomer layers around steel
- F_h = Hole Factor
- Strength of Laminate = $F_y \times h_s$ (lb/in)
- h_s = thickness of steel laminate (in)
- LL
- Working Stress = $1700 \times h_{ri} \times F_h \times \frac{\sigma_{LL}}{\sigma_{TL}}$ (lb/in)
- h_{ri} = average thickness of elastomer layers around steel
- F_h = Hole Factor
- Strength of Laminate = $F_{sr} \times h_s$ (lb/in)
- F_{sr} = Fatigue Strength of steel (psi)
- h_s = thickness of steel laminate (in)

4.2.10.1.2 Method B

Method B was the optional design procedure for steel reinforced bearings. Generally, bearings with smaller plan areas and smaller thicknesses were allowable by this method. The presence of steel laminates in bearings theoretically reduces the shear deformations and allows for higher compressive stress in the bearing.

- **Compressive Stress** – Different restrictions are given to fixed (no shear deformations) and expansion bearings. Also, the β factor is redefined in this method.
- Fixed Bearings (no shear deformations)

- Laminated Bearings
- Laminated Interior Bearings – the maximum compressive stress shall be the minimum of
 - $\sigma_{c,TL} \leq 1,600$ psi
 - $\sigma_{c,TL} \leq 1.66 \frac{GS}{\beta}$
 - $\sigma_{c,LL} \leq 0.66 \frac{GS}{\beta}$
- Expansion Bearings (shear deformations occur)
 - Laminated Bearings
 - Laminated Interior Bearings – the maximum compressive stress shall be the minimum of
 - $\sigma_{c,TL} \leq 1,600$ psi
 - $\sigma_{c,TL} \leq 2.00 \frac{GS}{\beta}$
 - $\sigma_{c,LL} \leq 1.0 \frac{GS}{\beta}$

where

- G= Shear Modulus
- S = Shape Factor
- β = Modification Factor for Comp. Stress
 - = 1 for Interior Layers
 - = 1.4 for Exterior Layers

- **Combined Compression and Rotation** – If the bearing undergoes both compression and rotation about the transverse axis of bearing, the average compressive stress ($\sigma_{c,TL}$) is limited for both fixed and expansion bearings.

- For Expansion Bearings

$$\bullet \sigma_{c,TL} \leq \left(\frac{1.66GS}{\beta} \right) \frac{1}{1 + \frac{L\theta_{TL,x}}{4\Delta_c}}$$

- For Fixed Bearings

$$\bullet \sigma_{c,TL} \leq \left(\frac{2.0GS}{\beta} \right) \frac{1}{1 + \frac{L\theta_{TL,x}}{4\Delta_c}}$$

where, Δ_c = Instantaneous Compressive Deflection.

- **Stability** requirements in Method B change to being controlled by stress as opposed to size. Free translation of the deck in the horizontal direction becomes a factor in the determination of the bearings stability.

If the bridge deck is free to translate

$$\bullet \sigma_{c,TL} \leq \frac{G}{\left\{ \frac{3.84 \left(\frac{h_r}{L} \right)}{S \sqrt{1 + 2 \frac{L}{W}}} - \frac{2.67}{S(S+2) \left(1 + \frac{L}{4W} \right)} \right\}}$$

- If the bridge deck is not free to translate horizontally

$$\bullet \quad \sigma_{c,TL} \leq \frac{G}{\left\{ \frac{1.92 \left(\frac{h_{r1}}{L} \right)}{S \sqrt{1 + 2 \frac{L}{W}}} - \frac{2.67}{S(S+2) \left(1 + \frac{L}{4W} \right)} \right\}}$$

- **Reinforcement** – thickness of the steel laminate is defined by new equations for both total load (DL + LL + I) and Live Load (LL). This is a change from the working stress requirements present in the Method A design procedure.

- For DL + LL + I

$$\bullet \quad h_s \geq \frac{1.5(h_{r1} + h_{r2})\sigma_{c,TL}}{F_y} F_H$$

- For LL

$$\bullet \quad h_s \geq \frac{1.5(h_{r1} + h_{r2})\sigma_{c,LL}}{F_{sr}} F_H ; \quad F_{sr} = \text{Fatigue Strength of Steel}$$

$$\bullet \quad F_H = \text{Hole Factor} = \frac{2 \times \text{gross width}}{\text{net width}}$$

4.2.11 4th Edition LRFD

The 4th edition of the “AASHTO LRFD Bridge Design Specifications” has the latest design standards for the design of elastomeric bearings. Similarly to the 15th edition, Method A and Method B are the available design procedures. Most of the changes occur in Method B as today’s research is concentrated on the design procedures in Method B. Method A remains virtually unchanged except for compressive deflection criteria for

cotton-duck pads (CPD's). The compressive deflection shall be calculated using the average compressive strain, which is given by the following equation, $\sigma_s/10000$.

4.2.11.1 Method B

Since the inception of Method B (AASHTO 15th edition 1992), the NCHRP has done research to improve the design method. Changes concerning the serviceability of the bearing were implemented along with changes dealing with the design standards. The first change from the 15th edition is in the rotational capacity of the bearing. The LRFD states that the rotational capacity shall include a .005 radian tolerance along with being able to accommodate the rotation due to the dead and live loads.

- **Rotational Capacity**

- $\theta_s \leq (\theta_L + \theta_D + .005)$ radians

- **Characteristics** The table below is a new addition to the LRFD. It shows a bearing suitability for the different situations when designing a bridge. (The table below is incomplete as it only addresses elastomeric bearings) This table will guide the design engineer to properly assess whether and which kind of elastomeric bearing is appropriate for design.

Type of Bearing	Movement		Rotation about Bridge Axis Indicated			Resistance to Loads		
	Long.	Trans.	Long.	Trans.	Vert.	Long.	Trans.	Vert.
Plain Elastomeric Pad	S	S	S	S	L	L	L	L
Fiberglass-Reinforced Pad	S	S	S	S	L	L	L	L
Cotton-Duck-Reinforced Pad	U	U	U	U	U	L	L	S
Steel-Reinforced Elastomeric Pad	S	S	S	S	L	L	L	S

S = Suitable for the situation

U = Unsuitable for the situation

L = Suitable for limited applications

Table 4.3 – Bearing Suitability
(Reference Table 14.6.2-1, AASHTO/LRFD 4th Edition, 2007)

- Tapered elastomeric layers are prohibited from use because they tend to cause larger shear strains in the elastomer.
- **Horizontal Force and Movement**
 - A new stipulation was added to this edition which addresses seismic forces. The code requires that expansion bearings must be able to accommodate seismic forces as well as displacements along with gravity forces. Seismic forces will now have to be considered may begin to control the design of elastomeric bearings in Maryland.
 - The Sliding Friction force is defined as
 - $H_u = \mu P_u$
 - H_u = lateral load from worst loading case
 - μ = coefficient of sliding friction
 - P_u = factored compressive load
 - The force due to elastomer deformation
 - $H_u = GA(\Delta_u/h_{rt})$
 - G = shear modulus of the elastomer
 - A = plan area of bearing
 - Δ_u = factored compressive load
 - h_{rt} = total elastomer thickness
- **Moment**
 - The definition of Ultimate Moment
 - $M_u = 1.60(0.5E_cI)(\theta_s/h_{rt})$
 - I = moment of inertia of the plan shape

- E_c = effective elastic modulus
- θ_s = design rotation
- **Material Properties** - The shear modulus of all bearings must be between 80 and 175 psi. It must also conform with all of the listed material specifications in the LRFD.
- **Compressive Deflection** – Initial and long term dead load deflections become a consideration in the design process
 - $\delta_d = \sum \varepsilon_{dl} h_{ri}$
 - δ_d = initial dead load deflection
 - ε_{dl} = initial compressive strain
 - $\delta_{lt} = \delta_d + a_{cr} \delta_d$
 - δ_{lt} = long term compressive deflection
 - a_{cr} = creep deflection divided by the initial dead load deflection
- **Combined Compression and Rotation** – The more recent editions of the AASHTO design code take into account the fact that edge uplift has a great effect on the fatigue life of the elastomer. To ensure that bearings do not experience uplift or high compression at the edges the 17th edition of AASHTO and 4th edition of the LRFD require these checks on the compressive stress in the elastomer, σ_s .
- Uplift requirement for all bearings
 - $\sigma_s > 1.0GS \left(\frac{\theta_s}{n} \right) \left(\frac{B}{h_{ri}} \right)^2$
- Additional uplift requirement for Expansion Bearings

- $\sigma_s < 1.875GS \left[1 - 0.200 \left(\frac{\theta_s}{n} \right) \left(\frac{B}{h_{ri}} \right)^2 \right]$

○ Additional uplift requirement for Fixed Bearings

- $\sigma_s < 2.25GS \left[1 - 0.167 \left(\frac{\theta_s}{n} \right) \left(\frac{B}{h_{ri}} \right)^2 \right]$

Figure 4.1 was produced to show the acceptable range for bearings to prevent uplift at the edges.

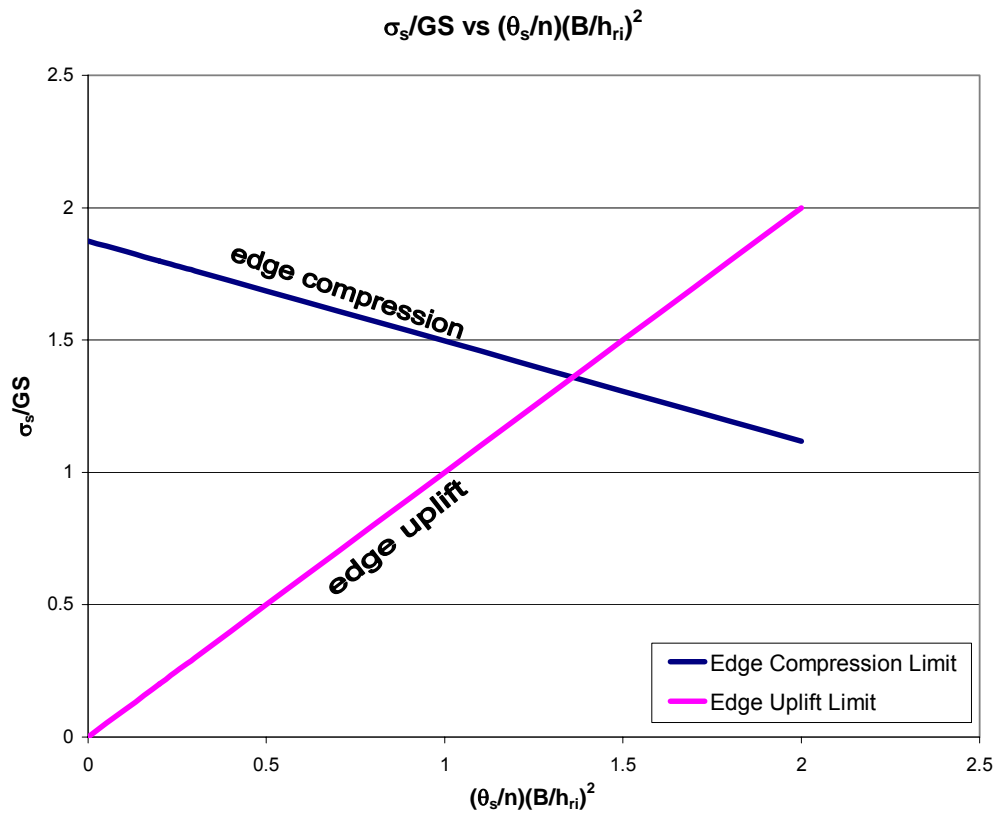


Figure 4.1 – Combined Compression and Rotation Limits
(AASHTO/LRFD 4th Edition, 2007)

4.2.12 Comparisons of Different Editions of Standard Specifications for Highway Bridges

The following graphs show important relationships between load and either plan area or thickness of the elastomeric bearings. The data represents only steel laminated expansion bearings. A dead load to live load ratio of .62 to .38 was used based on the average of the loads developed by DASH for all bridges. A hardness of 60 durometer, shape factor of 5.12, shear modulus of 130 psi, $W = 2.32L$ and β value of 1 (for interior layers of a bearing, when applicable) were used to create the graphs. All values were based on the average values for the 80 bridges which were studied.

4.2.12.1 Plan Area vs. Total Load

In all of the editions of the AASHTO design code, the minimum plan area of all bearings is proportional to the total load. The allowable compressive stress controls this relationship. As can be seen in figure 4.1, the 14th and 15th editions (Method A) require the highest plan area of a bearing. The 10th and 12th editions each had the same compressive stress requirements and required less plan area than the 14th edition. The 14th edition requires 17 percent more plan area than the 10th and 12th editions and 40 percent more plan area than the 15th edition (Method B).

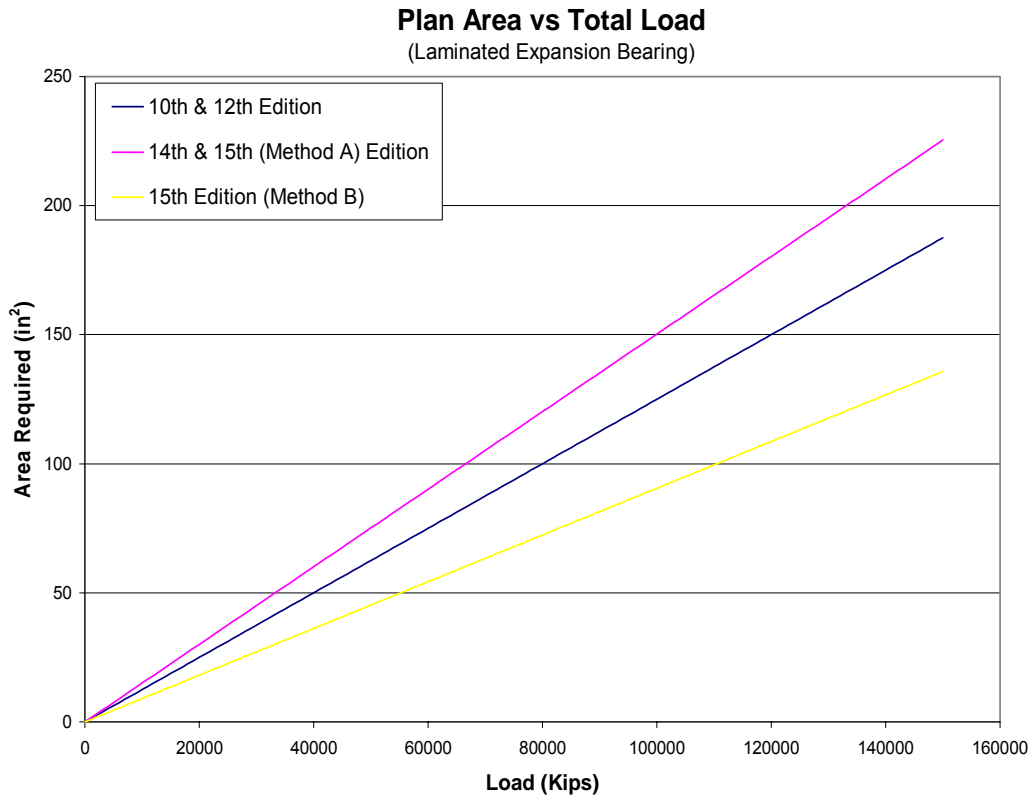


Figure 4.2 – Plan Area vs. Total Load by AASHTO Editions

4.2.12.2 Elastomer Layer Thickness vs. Total Load

The elastomer thickness can be estimated based on the total load if a length to width ratio of a bearing is assumed. The average length to width ratio was 1 to 2.32. The required

thickness based on the load can be found by the equation $t = \frac{A}{2S \left(4 \sqrt{\frac{A}{2.32}} \right)}$

where $A = \frac{\text{Load}}{\sigma_{allowable}}$. The graph shows the minimum thickness to allow the bearing to

bulge freely. Again the 14th and 15th editions (Method A) showed the greatest restrictions.

The 14th and 15th editions (Method A) show an 8.7 percent difference over the 10th and

12th editions' requirements and 22.3 percent over the 15th edition (Method B). Figure 4.2 shows the results.

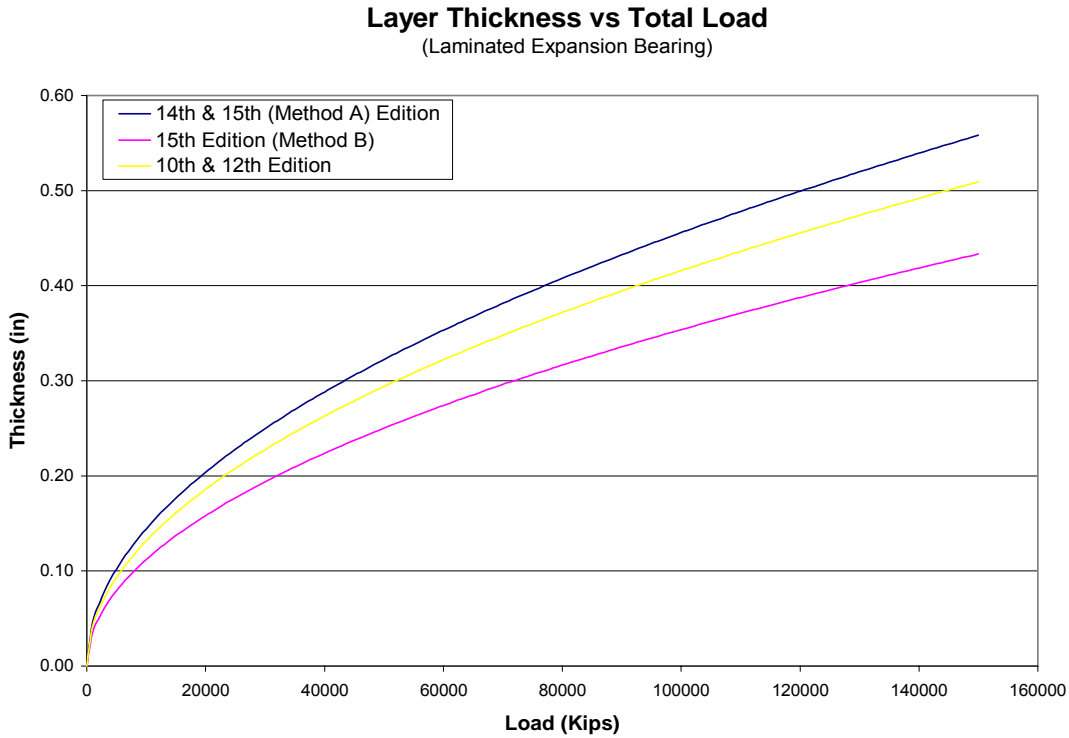


Figure 4.3 – Layer Thickness vs. Total Load by AASHTO Editions

4.2.12.3 Plan Area vs. Total Load by Shape Factor

The shape factor of a bearing is defined as $S = \frac{\text{Plan Area}}{\text{Area of Perimeter Free to Bulge}}$.

Depending on the shape factor of a bearing the allowable loads for that bearing are affected. In figures 4.3 and 4.4, the effect of shape factor on the minimum plan area of an elastomeric bearing is shown. For the 14th and 15th editions (Method A), as the shape factor increases the minimum plan area decreases. For the 15th edition (Method B) the

same trend occurs although the values for the required plan area are less for every given load and shape factor. The 15th edition (Method B) is a less conservative design method.

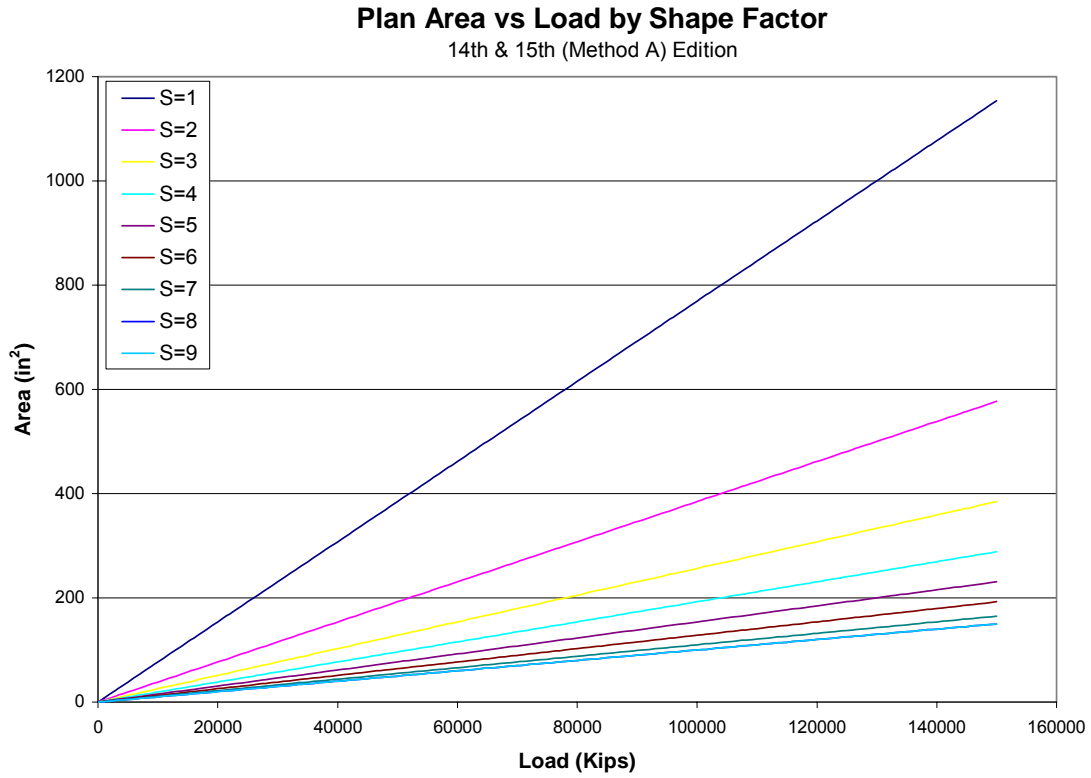


Figure 4.4 – Plan Area vs. Load by Shape Factors (Method A)

Plan Area vs Load by Shape Factor

15th Edition (Method B)

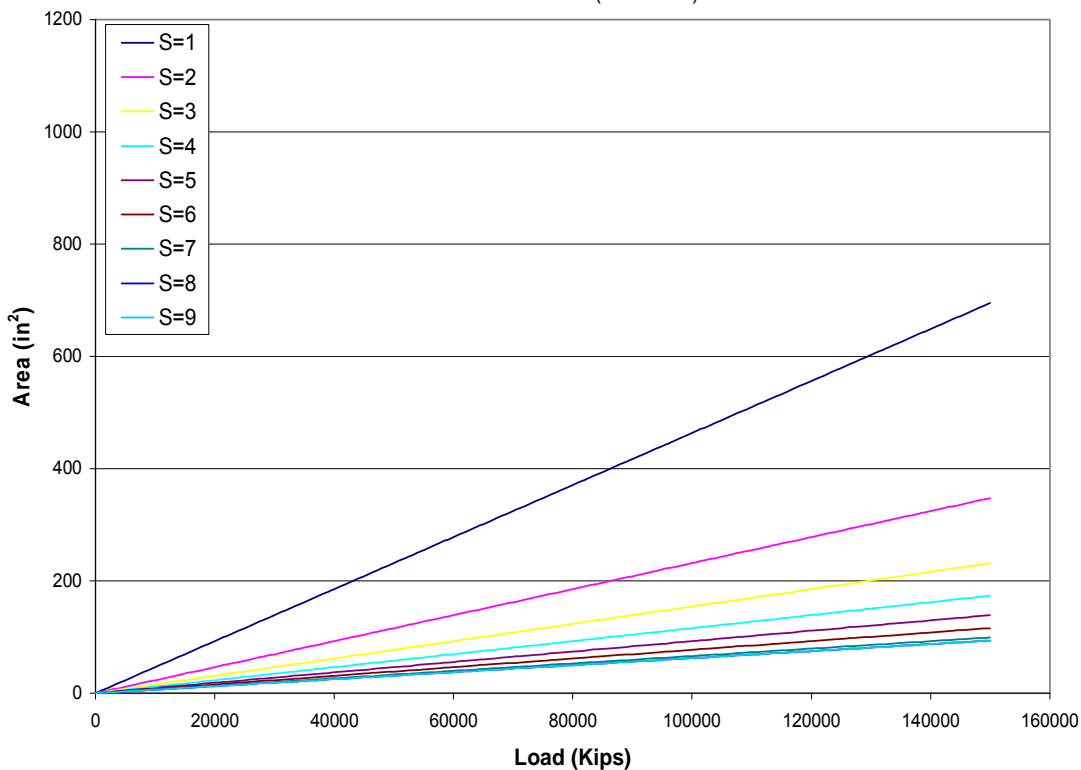


Figure 4.5 – Plan Area vs. Load by Shape Factors (Method B)

4.2.12.4 Layer Thickness vs. Total Load by Shape Factor

The same assumptions as above for minimum layer thickness were made to develop figures 4.5 and 4.6. The 14th and 15th (Method A) editions of AASHTO, require a greater layer thickness, for the same load and shape factor as compared to the 15th edition (Method B). Once the shape factor becomes greater than 4 the requirements for the required layer thickness become close. For shape factors between 4 and 6 (most typical) the minimum layer thickness varies between $\frac{1}{2}$ and $\frac{3}{4}$ of an inch for typical loads. Most of the bearings studied in both slab and girder bridges had layers of elastomer in this range.

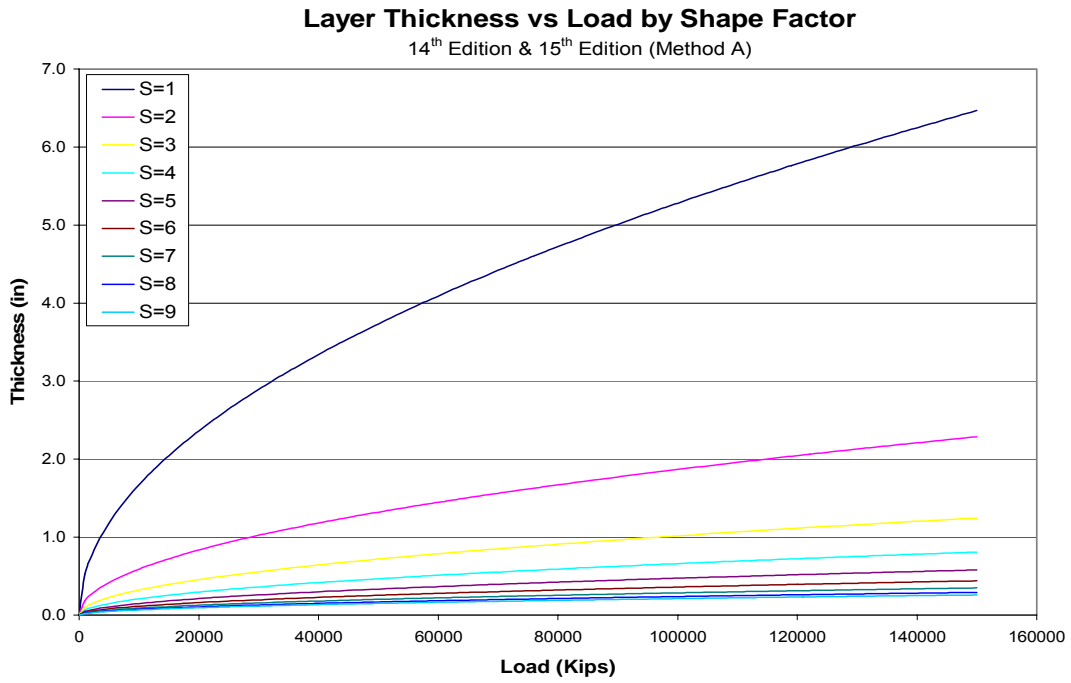


Figure 4.6 - Layer Thickness vs. Load by Shape Factor (Method A)

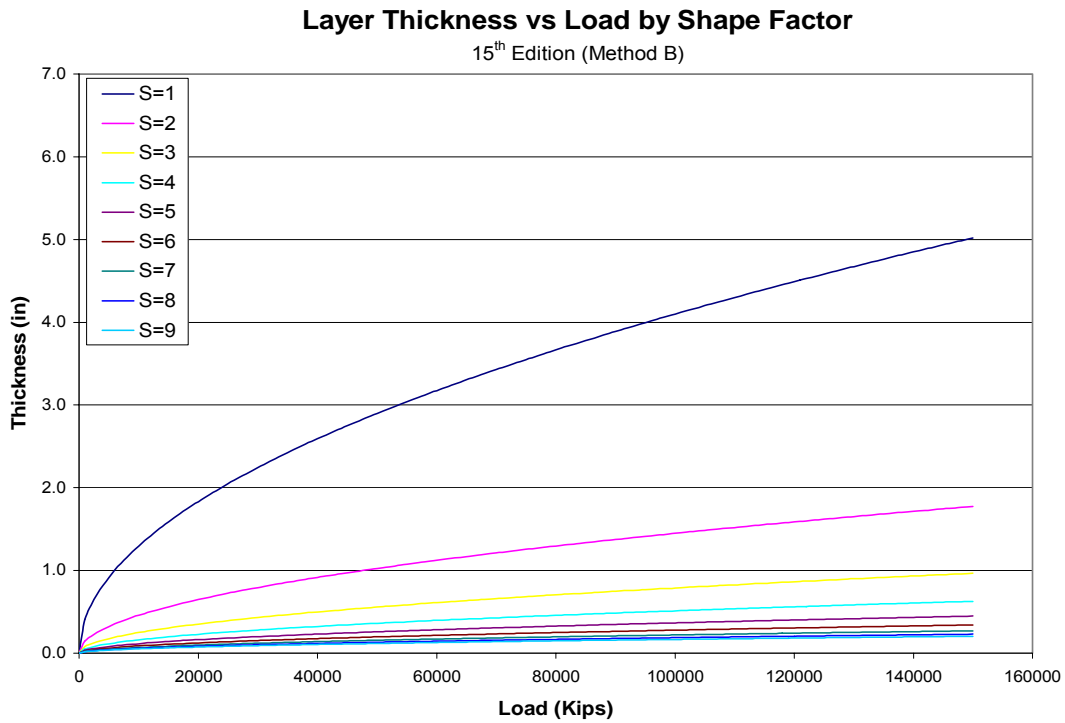


Figure 4.7 – Layer Thickness vs. Load by Shape Factor (Method B)

Chapter 5

Multi-Variable Regression Analysis

5.0 Introduction

The goal of this research is to isolate factors which have a strong influence on the design of elastomeric bearings. Further, to identify potential problems on design procedures based on empirical data collected during the field study. The data set which is being analyzed had over 750 inspected bearings from 76 bridges. A representative sample from each of the 76 bridges was selected to form the sample pool. Of the 76, 51 samples are representative of a PONTIS rating of 1, 23 samples have a rating of 2 and 2 have a rating of 4. For the regression modeling any rating of 2 or higher was considered a deteriorating bearing. To properly analyze whether the design factors have correlation to the deteriorated condition of the bearing a logistic regression procedure was selected to be used.

5.1 Logistic Regression Process

Logistic regression is a statistical tool which is used to analyze discrete sets of data. Typically, many independent variables, X_i , are tested against a single dependent variable, Y , to determine whether each independent variable is statistically significant to the outcome of the dependent variable. Generally, the dependent variable, Y , has two possible values, 0 for good condition and 1 for bad condition, for the case at hand; not deteriorating and deteriorating will be the subsets of the dependent. Because of the dichotomous nature of the dependent it is also referred to as a binary variable. For the dependent variable, X_i , the probability of deterioration can be described as θ and the probability of not deteriorating can be described as $1-\theta$. Because there is no prior

knowledge of the independent variables, logistic regression analysis is a prime candidate for this study as it assumes no single type of distribution on the set.

The approach for the logistic regression is known as a “backward stepwise regression”. This method begins with analyzing all of the variables to begin and then eliminating variables which show no significance. Once the initial run is made, all possible combinations of the significant and insignificant variables should be made to further explore if these combinations show significance. All significant variables from the first run should be monitored during the subsequent runs to ensure that they still show significance. After this process is complete, a final list of significant variables can be produced. If a variable proves significant through the regression, the exploratory assumptions for this variable may be confirmed (Logistic Regression 2007)

5.2 Studied Variables

To test whether elements of the field study showed correlation to the condition of the bearing, a logistic regression was performed on a number of variables. The variables were chosen based on their presence in the AASHTO design criteria as well as combinations of those variables, called mega-variables. Initial exploratory investigations were done by plotting the different factors against on another and separating them into two groups (good condition and bad condition). If the investigation of a variable showed the expected trend with good correlation to its condition, the variable was then included in the logistic regression analysis.

5.2.1 Exploratory Investigation

To determine the set of variables to perform logistic regression analysis on, an initial look to determine which variables showed some correlation to the bearings condition was done. These variables were taken from the AASHTO/LRFD design methodologies as well as published articles written about the performance of elastomeric bearings. A total of 25 variables were initially investigated for their correlation to the bearings condition, based on PONTIS rating. These 25 variables included 9 individual variables as well as 16 mega-variables (combination of two or more variables). The variables were investigated by separating the data sets into two categories, bearings in good condition and bearings in bad condition, and then plotted using Microsoft Excel. Regressions for all of the graphs were calculated and those graphs which showed the expected trends were investigated further. Figure 5.1 shows a typical graph that would be investigated further while figure 5.2 shows a graph that would not be investigated further.

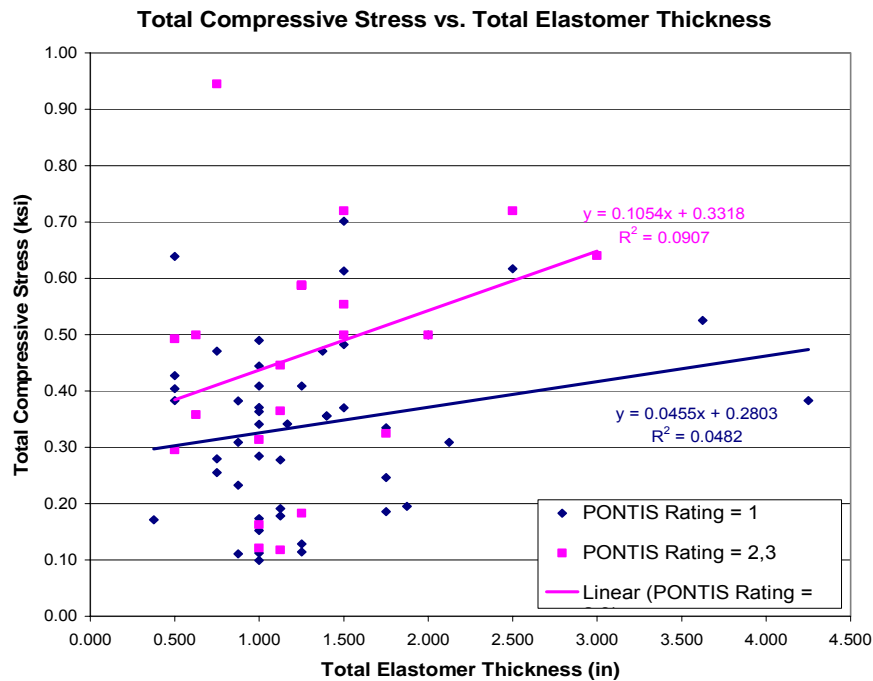


Figure 5.2 – Example of a Usable Exploratory Comparison

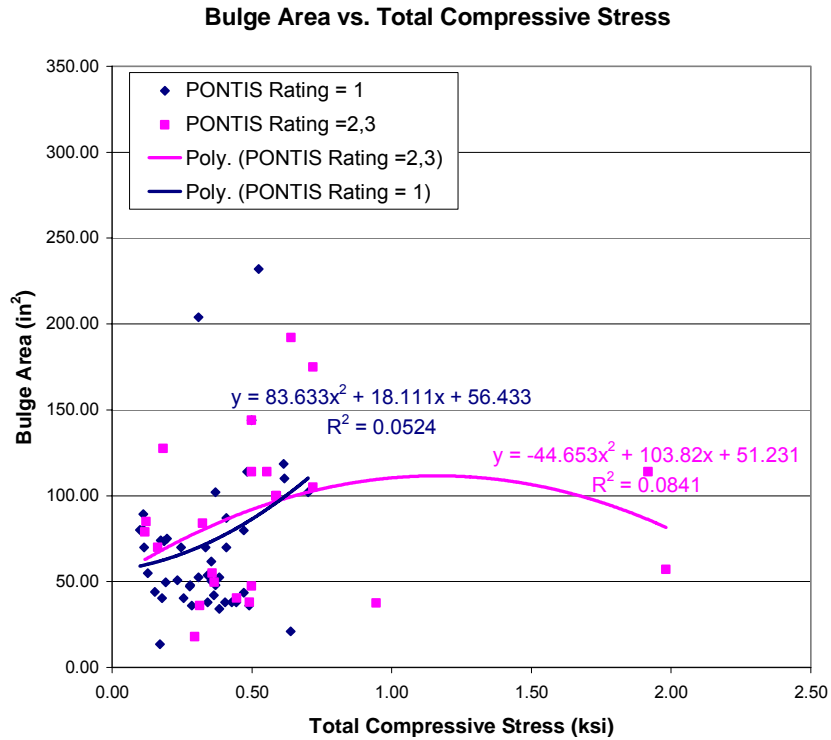


Figure 5.2 – Example of an Unusable Exploratory Comparison

Figure 5.1 shows the expected trend of bad bearings having higher compressive stresses. The regression lines shown represent the best fit for the two data sets (PONTIS Rating = 1 and PONTIS Rating = 2, 3). Figure 5.2 shows two data sets which should not be pursued for their correlation to the condition of the bearing. The two regressions show no definitive behavior and no hypothesis can be drawn from these relationships. After similar analysis for the other variables, a final list of 9 was compiled for the logistic regression.

5.2.2 X1 – Shape Factor, S

The shape factor is an important factor in the design process of elastomeric bearings. It is a mega-variable as it is a combination of other variables. Shape factor is defined by

AASHTO as $S = \frac{LW}{2h_{ri}(L+W)}$, where L denotes length, W denotes width and h_{ri} denotes

thickness of an elastomeric layer. In all of the editions of AASHTO the shape factor dictates the compressive strain that is expected in the bearing. In the 15th edition and later, the shape factor becomes a design parameter which controls the compressive stress allowance and the initial compressive strain of the elastomer. It has been recognized as an important design parameter in the AASHTO design methods as well as in reports produced by the Transportation Research Board (Minor et al. NCHRP 109 1970). The initial studies for the shape factor show high correlation to deterioration.

5.2.3 X2 – Elastomer Thickness, h_{ri}

Elastomer thickness is a primary design parameter in both AASHTO Design Methods A and B. Shear strains are directly proportional to the thickness of the elastomer ($\epsilon_s = \Delta_{\text{thermal}}/h_{ri}$). Thermal shear strains produce high stresses in the elastomer and are emphasized as important design loads. Elastomer thickness also plays a part in the mega-variables Shape Factor, Bulge Area, Shear Strain and Shearing Area. Preliminary investigation showed that the thickness of the elastomer may have some effect on bearing condition.

5.2.4 X3 – Plan Area, A

The plan area of a bearing is simply the length, L, multiplied against the width, W, of the bearing. For a given load, the amount of compressive stress a bearing experienced is solely dependent on the plan area. Plan area showed some correlation in the initial study and was selected for the logistic regression.

5.2.5 X4 – Shear Area

The term shearing area refers to the cross-sectional area, $L \times h_{ri}$, through the length of the bearing. Figure 5.3 shows a deformed bearing due to temperature loading with the shearing area in orange. The shear area needs to be able to develop the shear stresses caused by thermal deflection or the bearing may experience failure due to high shear strains. The greater the shear area, the lower the shear strains will be in a bearing. Some relationships between the shear area and bearing condition seemed strong so it was included in the logistic regression.

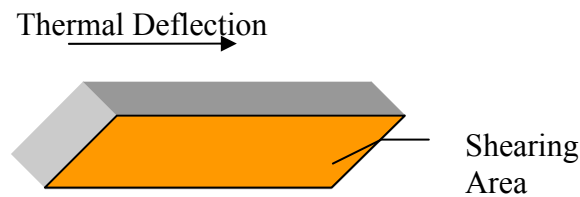


Figure 5.3 - Deformed Bearing Due to Temperature Loading

5.2.6 X5 – Bulge Area

The bulge area is another mega-variable which the AASHTO code uses in its design standard. It is defined as the area which will experience bulging when a compressive load is applied or $A_{bulge} = 2h_{ri}(L + W)$. Due to the hyper-elastic properties of neoprene and natural rubbers there can be no gain or loss of volume in the bearings. As the bearings are compressed the bearing needs changes shape and the elastomer tries to reposition itself outside its normal boundaries. The volume which the bearing must displace or bulge is dependent on the compressive load being applied. The greater the load the greater the required volume displacement will be. Adequate bulge area is required to prevent high

stress concentrations along the perimeter of the bearing. During initial investigation, the bulge area showed some correlation to the bearing condition.

5.2.7 X6 – Shear Strain, ϵ_s

Shear strains are present in bearings because of the thermal expansion of the slab and girders supporting the slab. Shear strain is defined as the thermal deflection divided by

the thickness of the elastomer or $\epsilon_s = \frac{\Delta_{thermal}}{h_{rt}}$. Shear strains can induce high stresses

throughout the bearing and must be taken into consideration when designing. Shear strains showed a positive correlation to deterioration of the bearing and was studied in the logistic regression.

5.2.8 X7 – Compressive Stress, σ_s

Compressive stress is a primary factor in the design of bearings. Because transferring dead and live loads is one of the main functions of the elastomer, one must ensure the adequacy of the bearing to resist these forces. Compressive stress controls the plan dimensions of the bearing. The bearing condition had a good correlation to the compressive stress acting on the bearing. In the majority of cases in the preliminary study, compressive stresses were typically higher in bearings with a PONTIS rating of 2 or more than in bearings rated 1.

5.2.9 X8 – Combined Compression and Rotation, $\frac{\sigma_s}{GS}$

The 15th edition of the AASHTO design standard was the first to include the effects of combined compression and rotation. The mega-variable $\frac{\sigma_s}{GS}$ was created to describe the compression interaction with rotation. More recent editions have contributed a bearings condition heavily to this factor. Preliminary studies have aligned with the AAHSTO findings and this mega-variable was investigated further in the logistic regression.

5.2.10 X9 – Compressive Stress divided by Bulge Area, $\frac{\sigma_s}{2h_{rt}(L+W)}$

This mega-variable was investigated as a possible factor having to do with bearing deterioration. Similar to the discussion above, the bearing must have enough area to bulge when under going compressive stresses due to dead and live loading. The initial investigation showed that there could be a relation between this factor and the condition of the bearing.

5.3 Logistic Regression Results

The logistic regression was performed using TSP International, a program used to provide forecasts when given data sets. For all the different analyses performed, TSP provided P-values and t-statistics. Based on these and the estimate of the slope of the regression, certain variables were confirmed as having substantial correlation to the condition of the bearing. The table below presents all of the meaningful variables.

	Variable	Standard Error	t-statistic	P-value
Individual Factors	X1 - Shape Factor	4.06E-03	-2.22891	0.026
	X2 - Thickness	0.013227	-1.62967	0.103
	X3 - Plan Area	5.77E-03	-1.4124	0.158
	X6 - Shear Strain	7.58E-03	-2.02574	0.043
	X7 - Compressive Stress	0.010109	-1.94961	0.051
	X8 - σ_s /GS	0.010109	-1.9498	0.051
	X9 - σ_s /Bulge Area	0.011668	-1.5172	0.129
Combined Factors	X2,X5 – Thickness, Bulge Area	0.011668	-1.5172	0.129
		0.081024	2.42732	0.015
	X4,X5 – Bulge Area, Shear Area	0.083594	1.42837	0.153
		0.062727	-1.579	0.114
	X7,X8 - Compressive Stress, σ_s /GS	78.8921	1.86283	0.062
		78.8932	-1.86306	0.062

Significance Level = .15

Table 5.1 – Logistic Regression Summary of Meaningful Variables

Factors which seem to be the most significant are X1, X6, X7 and X8. The P-values are about .05 or less. X7 and X8 are very similar. The only difference is the t-statistic which only varies by .00019. These variables should be considered statistically dependent and significant. Variables with a more moderate correlation include X2, X9 and the combination of X2 with X5. Variables with an acceptable but lower correlation are X3 and the combination of X4 with X5. The initial exploratory analysis of these variables and these variable combinations are now validated.

Chapter 6

Finite Element Modeling

6.0 Overview of Finite Element Modeling

Finite element models were created to confirm field data and provide further insight into problems with past design standards. The commercial finite element program, SAP 2000[®], was used to perform the analysis. Bridge 1097 was selected for the analysis due to its poor performance in the field. Analysis was performed on the bearing using the as built design, and then using a new suggested design.

6.1 Models

Two models were analyzed for bridge 1097, as stated previously. One model represented the as-built bearing and the other represented a suggested bearing for the bridge. For all models, the same stress-strain responses were used for the neoprene found in typical 60 durometer elastomeric bearings. Thermal deflections and gravity loading were taken into consideration. Based on the span of the bridge and current AASHTO standards, the maximum thermal deflection was .12 inches. A total compressive load of 119 kips was used to simulate the gravity loads. Loads for the bridge were found using Merlin-Dash program.

The neoprene was modeled using 8-node, solid/brick elements with 3 translational degrees of freedom at each node. The neoprene was modeled as an orthotropic-hyperelastic material with an elastic modulus of 360 psi and shear modulus of 120 psi with a poisson's ratio of .4995.

For laminated bearings, the steel shims were modeled using 8-node, solid/brick elements with 3 translational degrees of freedom at each node. The steel was modeled as an

isotropic material with an F_y value of 42 ksi, an elastic modulus of 29000 ksi and a Poisson's ratio of .3.

All models were automatically meshed with 9 divisions in the x direction, 5 divisions in the y direction and .25" and .125" slices vertically for neoprene and steel respectively using the FEM program. The small vertical divisions helped to capture the shape changes in the elastomer accurately.

6.1.1 As-Built Bearing for Bridge 1097

Bridge 1097 is located in Allegany County Maryland. It is a 4 span, concrete girder bridge. Span lengths are 33', 70', 70' and 50'. The bridge was designed for HS-44 loading has 2 lanes and an overall width of 35'. The bridge was constructed in 1968, making the bearings 40 years old. The bearing pads present at the north abutment are plain, 60 durometer, 26" x 7" x 3/4" neoprene pads. These pads have not performed well succumbing to the effects of compression and thermal deflections. Major tearing in the pad indicates that the compressive stress is too high, while excessive creep indicates that the pad is undersized for dead load. The creep in bridge 1097 can be seen in figure 6.1. The shape factor for the bearing is 3.68 which is lower than the average by about 1.25. A shape factor this low tends to increase the stresses at the edge of the bearing.



Figure 6.1 – Bearing Creep in Bridge 1097

The failure of this bearing has led to overstressed piers and abutments. Cracking and spalling are the results of the bearing failure.

6.1.1.1 Performance of Finite Element Model for As Built Situation

As expected, the model for the as built condition for bridge 1097 did not perform well in the analysis. The maximum combined stress from thermal deflection and compression was 1671 psi. The suggested maximum compressive stress for this bearing by AASHTO design standards is 800 psi while the stress due strictly to compression was 1029 psi. Shear strain was an acceptable .16 in/in but added to the overall stress experienced by the bearing. The maximum compressive deflection for the model was roughly 1/16 of an inch. (Model does not account for long term creep effects.) Stress contours can be seen in the figures below.

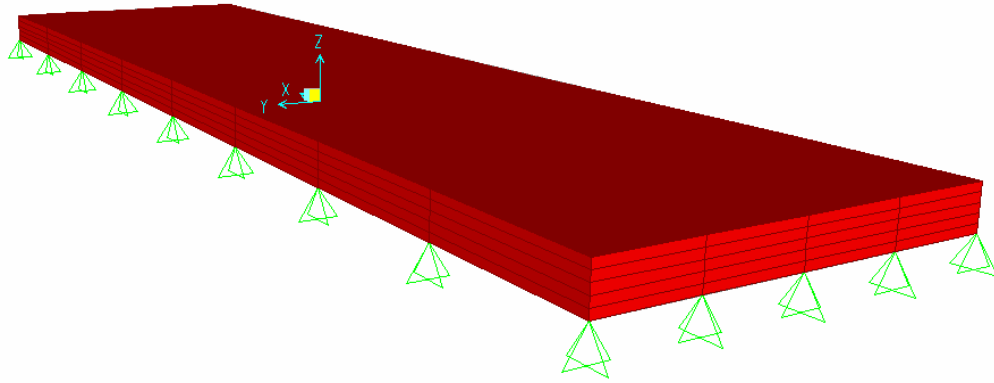


Figure 6.2 – Undeformed Model (3-D View)

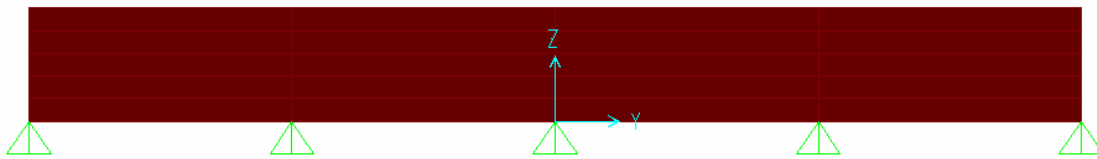


Figure 6.3 – Undeformed Model (Side View)

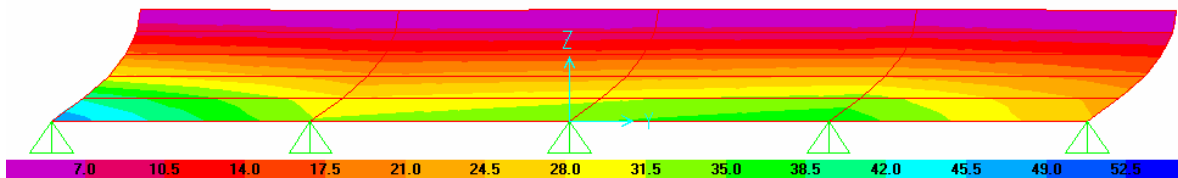


Figure 6.4 – Stress Contours for Thermal Loading

Notice the high stress concentration at the corners and along the bottom edge. This may be due to having a low shape factor.

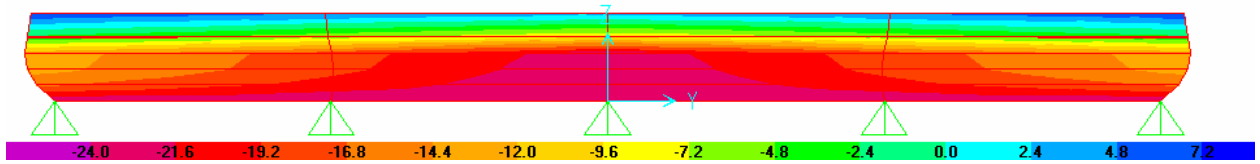


Figure 6.5 – Stress Contours for Compressive Loading

Compressive loading causes bulging as well as stress concentrations at the top corners as well as the bottom edge.

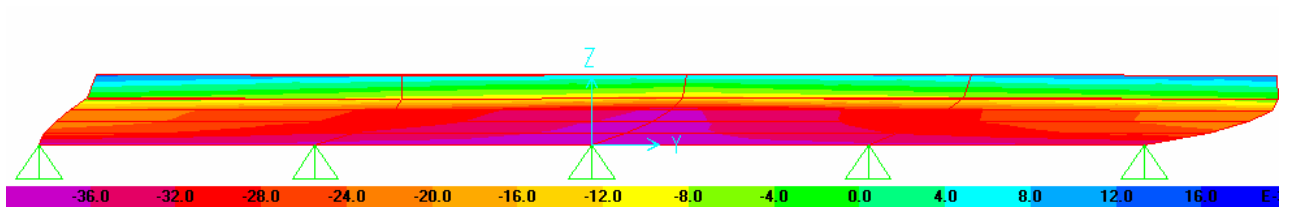


Figure 6.6 – Stress Contours from Thermal and Compressive Loading

The highest stresses when the bearing is subjected to shear and compression are found along the bottom edge and in the corners of the plain pad.

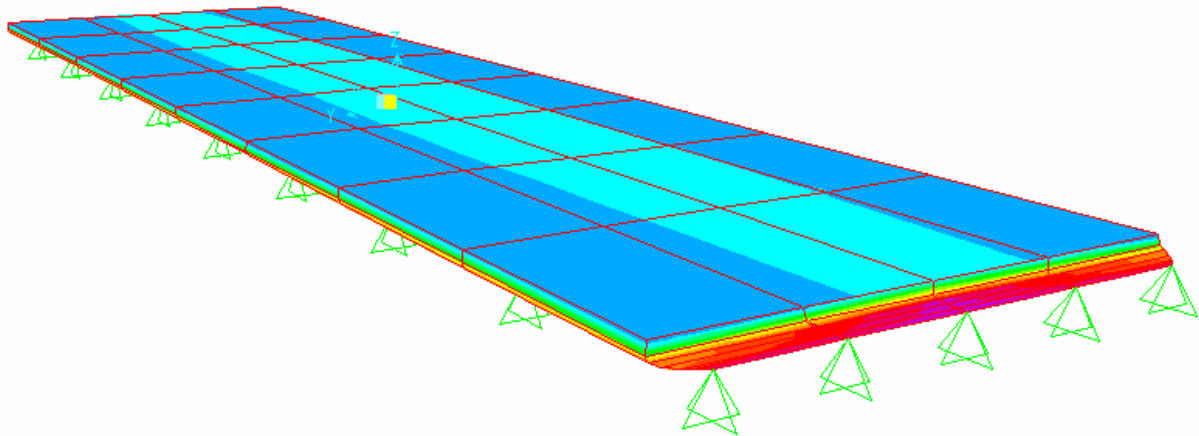


Figure 6.7 – Stress Contours from Thermal and Compressive Loading (3D)

6.1.2 Suggested Bearing for Bridge 1097

Based on the suggestions outlined in chapter 7 and the current LRFD design standards, a new bearing was designed for bridge 1097. Knowing the condition of the existing bearings, a laminated bearing was picked. Parameters such as the shape factor and compressive stress controlled the initial size of the bearing (26x16x2.25). Method B of the LRFD (4th edition, 2007) was used to design the bearing.

6.1.2.1 Design

To design the elastomeric bearing, the 4th edition of the LRFD Bridge Design Standards was used.

Inputs:

$$S = \frac{LW}{2t(L+W)} = \frac{26 \times 16}{2 \times 1(16+26)} = 4.95$$

$$G = .130ksi$$

$$\sigma_s = \frac{\text{Service Load}}{\text{Plan Area}} = \frac{119kips}{26 \times 16} = .286ksi$$

$$\sigma_L = \frac{\text{Live Load}}{\text{Plan Area}} = \frac{38.08kips}{26 \times 16} = .092ksi$$

$$a_{cr} = .35\% \quad \text{Table 14.7.6.2-1}$$

$$\Delta_s = \alpha_c L_{span} = .00006(50 \times 12) = .12in$$

$$\theta_s = .0025 rad$$

$$h_{rt} = 1 in$$

$$h_{rt} = 2 in$$

$$A = \frac{1.92 \frac{h_{rt}}{L}}{\sqrt{1 + \frac{2L}{W}}} = \frac{1.92 \frac{2}{16}}{\sqrt{1 + \frac{2 \times 16}{26}}} = .108$$

$$B = \frac{2.67}{(S + 2)\left(1 + \frac{L}{4W}\right)} = \frac{2.67}{(4.95 + 2)\left(1 + \frac{16}{4 \times 26}\right)} = .333$$

$$F_y = 50 \text{ksi}$$

$$F_{TH} = 24 \text{ksi}$$

Design:

Check Compressive Stress

Check Compressive Stress due to Service Load

$$\sigma_s \leq 1.66GS \leq 1.6 \text{ksi}$$

$$1.66GS = 1.66 \times .130 \times 4.95 = .986 \text{ksi}$$

$$\sigma_s = .286 \leq .986 \text{ksi} \quad \text{O.K.}$$

Check Compressive Stress due to Live Load

$$\sigma_L \leq .66GS$$

$$.66GS = .66 \times .130 \times 4.95 = .392 \text{ksi}$$

$$\sigma_s = .092 \leq .392 \text{ksi} \quad \text{O.K.}$$

Check Compressive Deflection

Check Live Load Deflection

$$\delta_L = \sum \varepsilon_{Li} h_{ri}$$

$$\delta_L = 1(.02) + 1(.02) = .04$$

Check Dead Load Deflection

$$\delta_D = \sum \varepsilon_{Di} h_{ri}$$

$$\delta_D = 1(.02) + 1(.02) = .04$$

Check Long Term Dead Load Deflection

$$\delta_D = \delta_D + a_{cr} \delta_D$$

$$\delta_D = .04 + .35(.04) = .054 \text{ in}$$

Check Shear Deformation

$$h_{rt} \geq 2\Delta_s$$

$$2 \geq 2(.12) = .24 \quad \text{O.K.}$$

Check Combined Compression and Rotation

Check Uplift

$$\sigma_s > GS \left(\frac{\theta_s}{n} \right) \left(\frac{B}{h_{ri}} \right)^2$$

$$\sigma_s > .130 \times 4.95 \left(\frac{.0025}{2} \right) \left(\frac{16}{1} \right)^2$$

$$.286 > .19 \text{ksi} \quad \text{O.K.}$$

Check Edge Compression

$$\sigma_s < 1.875GS \left[1 - .2 \left(\frac{\theta_s}{n} \right) \left(\frac{B}{h_{ri}} \right)^2 \right]$$

$$\sigma_s < 1.875 \times .130 \times 4.95 \left[1 - .2 \left(\frac{.0025}{2} \right) \left(\frac{16}{1} \right)^2 \right]$$

$$.286 < 8.68 \text{ksi} \quad \text{O.K.}$$

Check Stability

$$2A \leq B$$

$$.216 \leq .333 \quad \text{O.K.}$$

Check Reinforcement

Check Service Limit State

$$h_s \geq \frac{3h_{\max} \sigma_s}{F_y}$$

$$h_s \geq \frac{3 \times 1 \times .286}{50} = .02 \text{ in}$$

$$.125 \geq .02 \text{ in.} \quad \text{O.K.}$$

Check Fatigue Limit State

$$h_s \geq \frac{2h_{\max}\sigma_s}{F_{TH}}$$

$$h_s \geq \frac{2 \times 1 \times .286}{24} = .0077 \text{ in}$$

$$.125 \geq .0077 \text{ in.} \quad \text{O.K.}$$

16"x26"x2.125" laminated bearing will work for Bridge 1097.

6.1.2.2 Performance of Finite Element Model for Suggested Bearing

The model for the suggested bearing condition for bridge 1097 performed much better in the analysis than the existing bearing. The bearing being analyzed is a 16"x26"x2.125" with a single steel lamination at mid height. The maximum combined stress from thermal deflection and compression was reduced from 1671 to 784 psi. The suggested maximum compressive stress for this bearing by AASHTO design standards is 986 psi while the stress due strictly to compression was 700 psi. Shear strain was reduced by half to .08 in/in. The maximum compressive deflection for the model was roughly 1/18 of an inch, a little less than the existing model. (Model does not account for long term creep effects) Stress contours can be seen in the figures below.

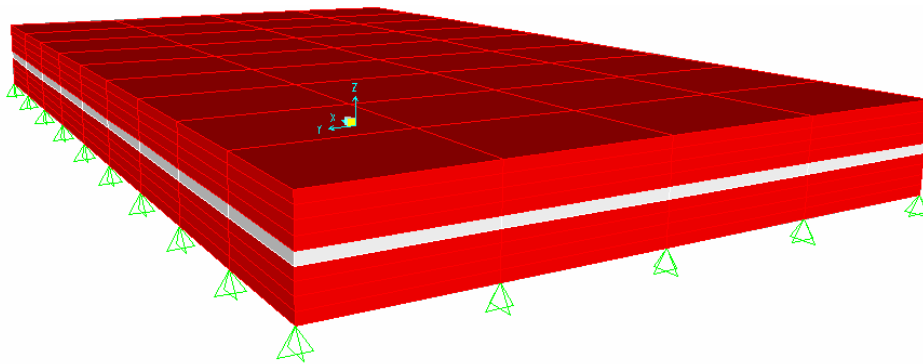


Figure 6.8 – Undeformed Model (3-D View)

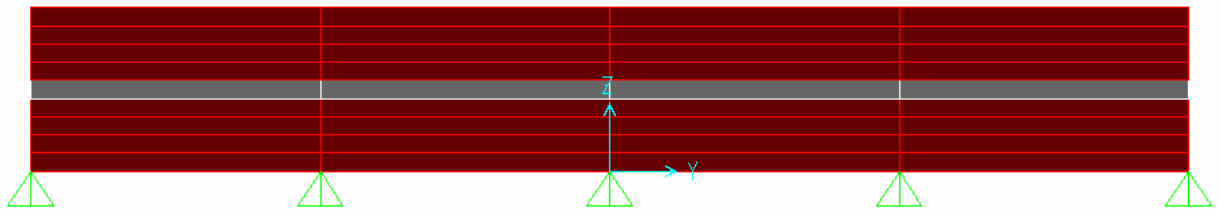


Figure 6.9 – Undeformed Model (Side View)

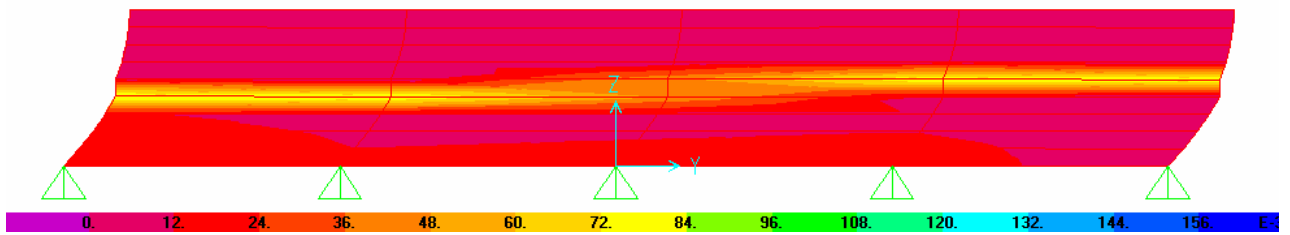


Figure 6.10 – Stress Contours for Thermal Loading

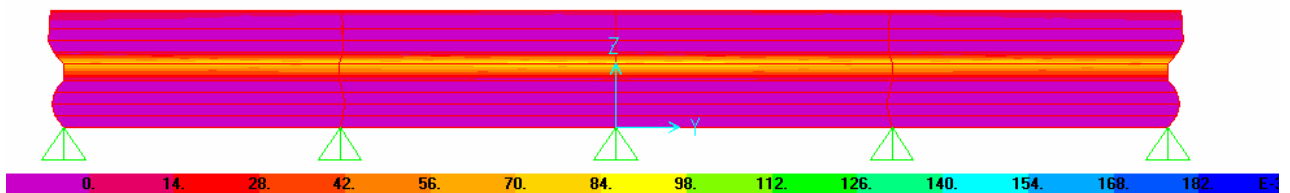


Figure 6.11 – Stress Contours for Compressive Loading

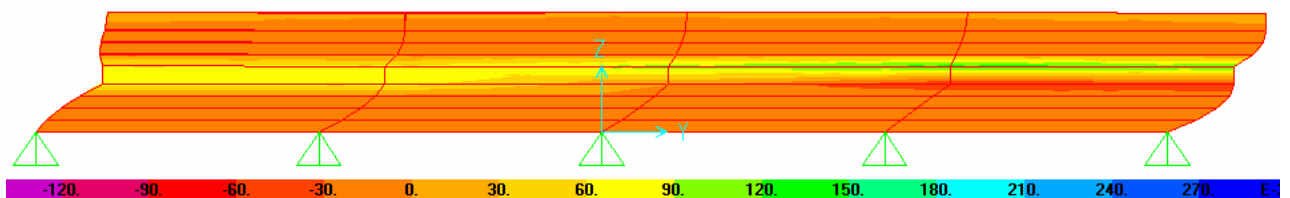


Figure 6.12 – Stress Contours from Thermal and Compressive Loading

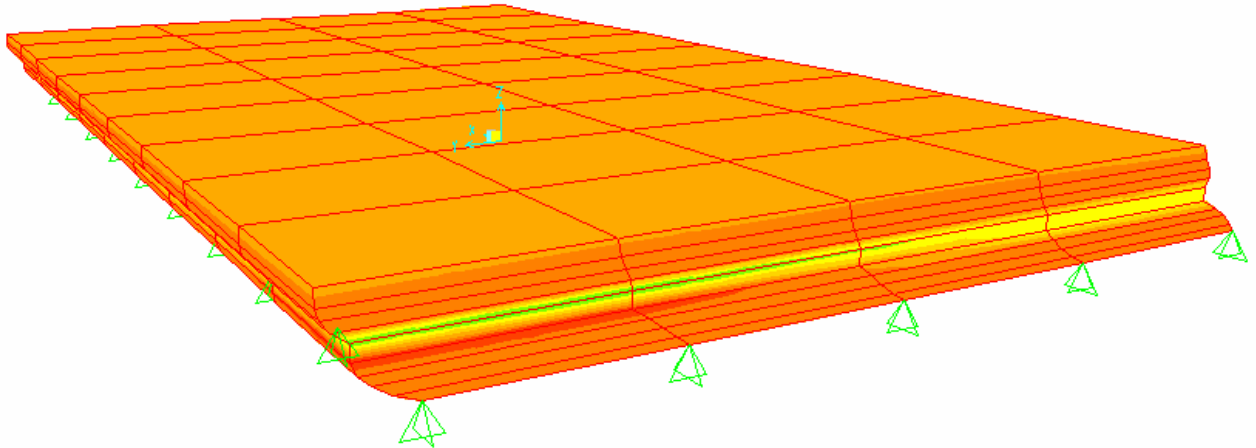


Figure 6.13 – Stress Contours from Thermal and Compressive Loading (3D)

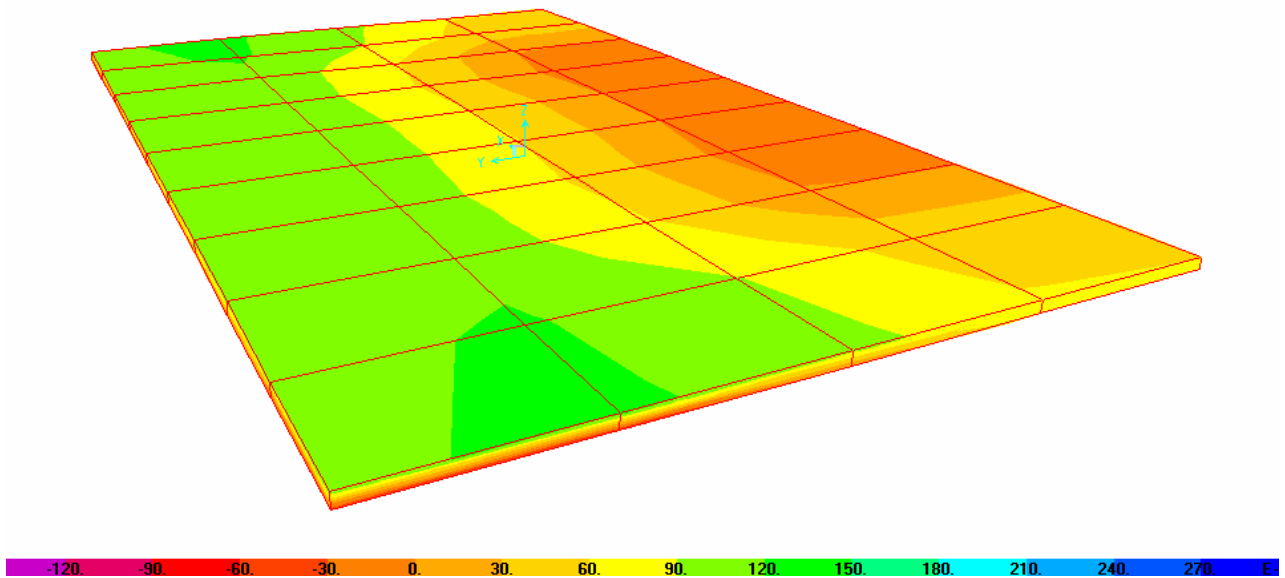


Figure 6.14 – Steel Stress from Thermal and Compressive Loading (3D)

6.2 Results (Graphs)

Simulations were run using a similar laminated bearing; a set width of 26 inches and a set height of 1.625 inches were used while the length of the bearing was varied in order to

vary the shape factor. Table 6.1 below shows the results of the analysis and figure 6.15 shows a plot of the resultant stresses for each situation.

		26x7x.75 As Built	26x7x1.625 Lower SF Limit	26X9X1.625 Mid-Low SF	26x12x1.625 Mid-High SF	26x16x1.625 Upper SF Limit	26x16x2.125 Suggested Shape
Length	(in)	26.0	26.0	26.0	26.0	26.0	26.0
Width	(in)	7.0	7.0	9.0	12.0	16.0	16.0
Total Elastomer Thickness	(in)	0.75	1.50	1.50	1.50	1.75	2.00
Minimum Layer Thickness	(in)	0.75	0.75	0.75	0.75	0.75	1.00
Shape Factor		3.68	3.68	4.46	5.47	6.60	4.95
Max. Stress due to Compression	(psi)	1029.0	1387.0	1017.0	734.0	540.0	700.0
Max. Stress due to Deflection	(psi)	64.0	269.0	240.0	181.0	126.0	149.0
Max. SVM Stress	(psi)	1671.0	1595.0	1198.0	867.0	629.0	784.0
Shear Strain	(in/in)	0.160	0.080	0.080	0.080	0.080	0.060
Shear Stress	(psi)	352.0	112.0	101.7	130.7	205.4	72.0
Max. Compressive Deflection	(in)	0.0623	0.0851	0.0638	0.0478	0.0363	0.0575

Table 6.1 – Results of Finite Element Analysis

Figure 6.15 shows the relation of stress and the shape factor for different types of stresses. Stress due to compression and total stress follow a similar pattern of decreasing as the shape factor increases. The difference between the two lines represents the stress due to shear forces and thermal deflections. As the shape factor increases, shear stress increases which is expected as increasing the shape factor is equivalent to reducing the thickness of the pad in terms of shear stress. The stress due to thermal deflections decreases as the shape factor increases. The AASHTO/LRFD limit is also shown on the plot. For this situation, to meet the AASHTO service load stress requirements, the shape factor must be greater than 4.66. Different bearings in different situations will have different allowable shape factors.

Stress vs. Shape Factor

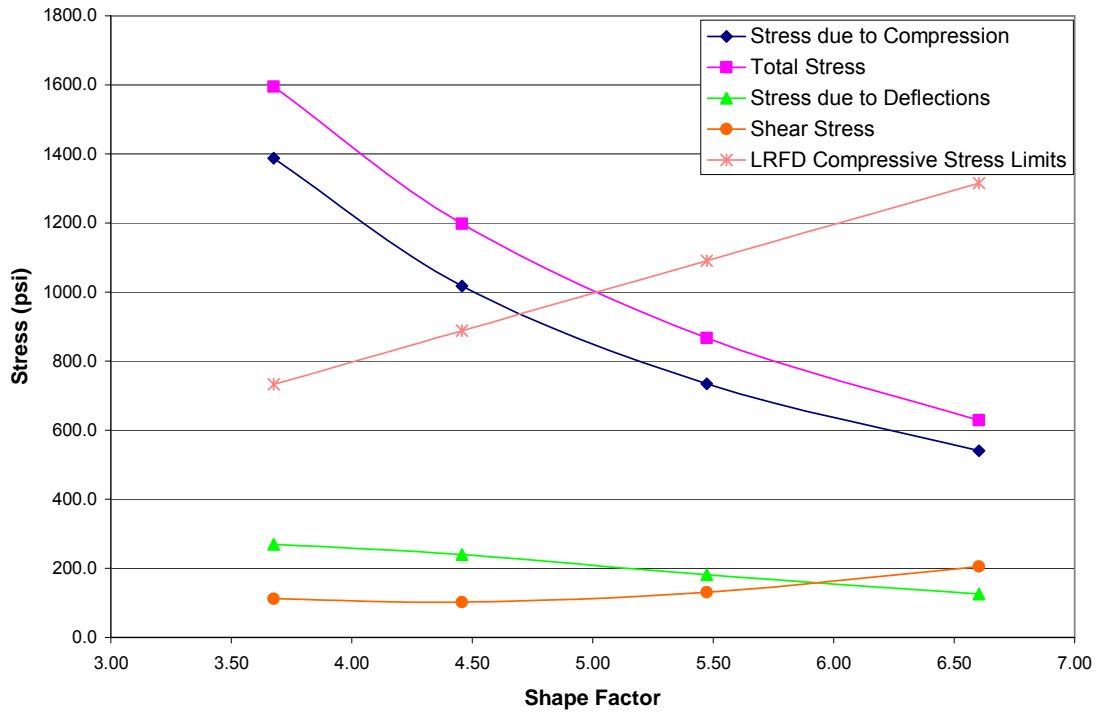


Figure 6.15 – Stress vs Shape Factor for 16x26x1 5/8” Laminated Bearing

Chapter 7

Overview and Recommendation

7.0 Overview of Statistical Analysis Summary

To determine the controlling factors for the condition of elastomeric bearings a field study was conducted to collect in-situ data. Spreadsheets were created to perform exploratory studies in order to gain some insight into the problems with the bearings. Once initial hypotheses had been formed, the technique of logistic regression was employed in order to determine the statistical significance of each variable.

7.1 Overview

Logistic regression determined whether each variable had statistical significance to the condition of elastomeric bearings. If a variable was found to be significant, the validity of the expletory hypothesis could be strengthened. Discussions of each significant variable are presented below.

7.2 Results and Discussion

Logistic regression determined whether each variable had statistical significance to the condition of elastomeric bearings. If a variable was found to be significant, the validity of the expletory hypothesis could be strengthened. Discussions of each significant variable are presented below.

7.2.1 Shape Factor

Shape Factor has been recognized by AASHTO as an important design parameter. Exploratory studies showed that there may be a relation between the condition of

bearings and their shape factor. Logistic regression verified this as a strongest relationship observed. Further, former studies by the Transportation Research Board (Minor et al. NCHRP 109 1970) have had similar results. The shape factor of an elastomeric bearing should be considered as a critical variable in design as it relates to compressive stress allowances, and combined compression and rotation. Figure 7.1 below shows the relation between shape factor as well as failure.

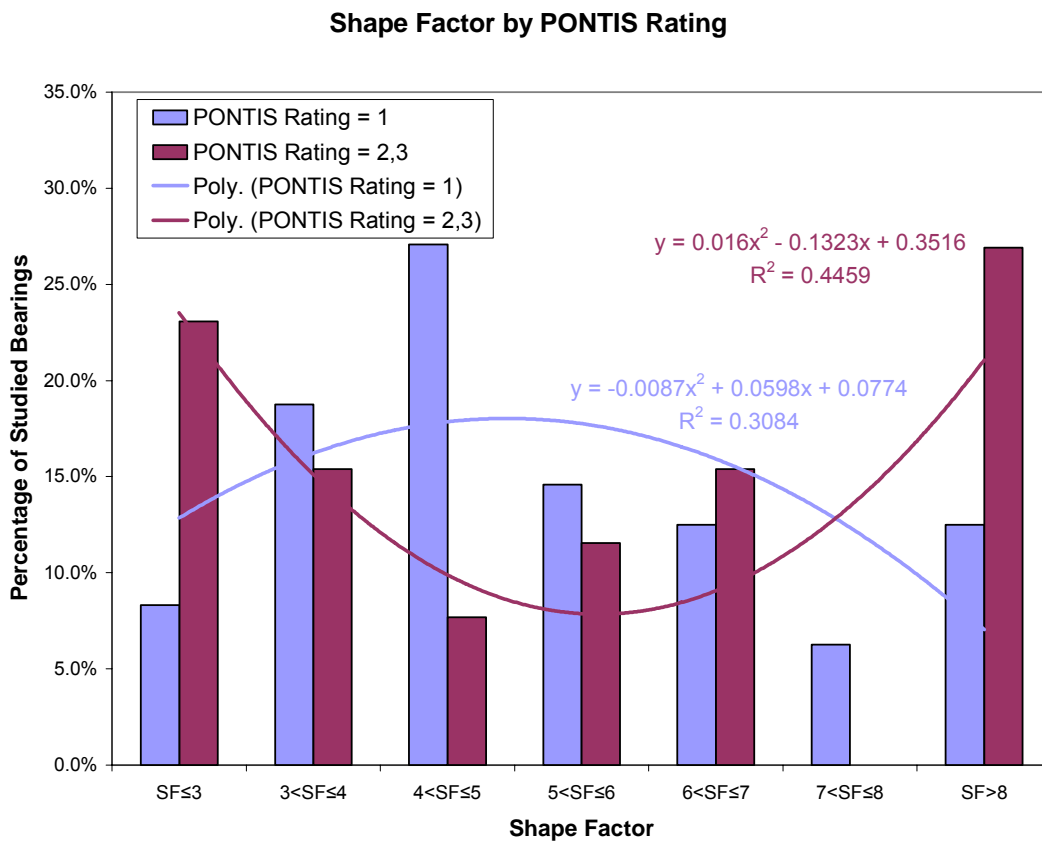


Figure 7.1 – Bearing Condition by Shape Factor

Bearings with a PONTIS rating of 2, 3 or 4 tend to be concentrated at the extremes of the graph while bearings with a PONTIS rating of 1 are concentrated in the center of the range. This shows that bearings with shape factor below 3.5 and above 6.5 have a higher probability of being in degraded condition and vice versa for bearing with shape factors

between 3.5 and 7.5. Although previous reports do not give a range of shape factors to design between, they do say that bearings with lower or higher shape factors tend to have problems in the field. Figure 7.1 is consistent with these findings.

Figure 7.2 shows bearings with PONTIS ratings greater than 1 tend to have higher compressive stresses inside the elastomer. This may be expected that bearing in a deteriorating state may be subject to higher compressive stresses, but should not be assumed. From logistic regression this is verified.

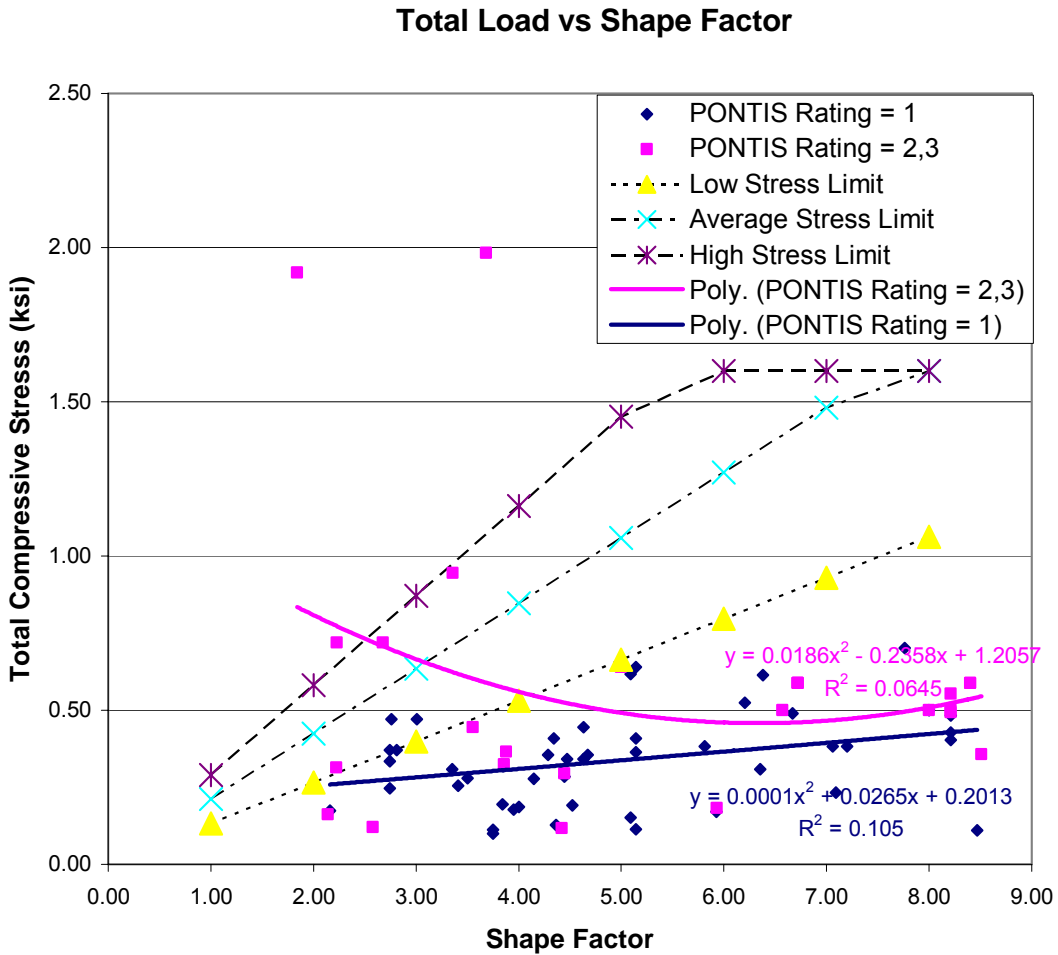


Figure 7.2 – Total Compressive Stress vs. Shape Factor

The graph in the above figure does not show the relation between the shape factor and elastomer condition but rather the combined effect between compressive stress and shape factor in relation to the condition of the bearing.

Three lines are plotted on the graph in figure 7.2, the “Low Stress Limit”, the “Average Stress Limit” and the “High Stress Limit” lines. These lines represent the maximum allowable compressive stress based on the range of shear modulus’ allowable for 60 durometer bearings (.8 ksi – 1.75 ksi). Bearings with a PONTIS rating of 1 stay primarily below the lower limit indicating that bearings in good condition do not exceed even the lowest of the allowable compressive stress limits. Bearings rated 2 or 3 can be observed above the average stress limit line and even above the maximum stress limit of elastomeric bearings. This implies that bearings are deteriorating due to excessive compressive stresses. This graph helps to further verify the results from the logistic regression.

7.2.2 Shear Strain

Shear strains were found to be statistically significant both in the exploratory study as well as in the logistic regression. Shear strains are highly dependent on the thermal expansion and contraction of the bridge deck and girders. Figure 7.3 shows the distribution of shear strains for the 2 groups, PONTIS rating equal to 1 and PONTIS rating greater than or equal to 1.

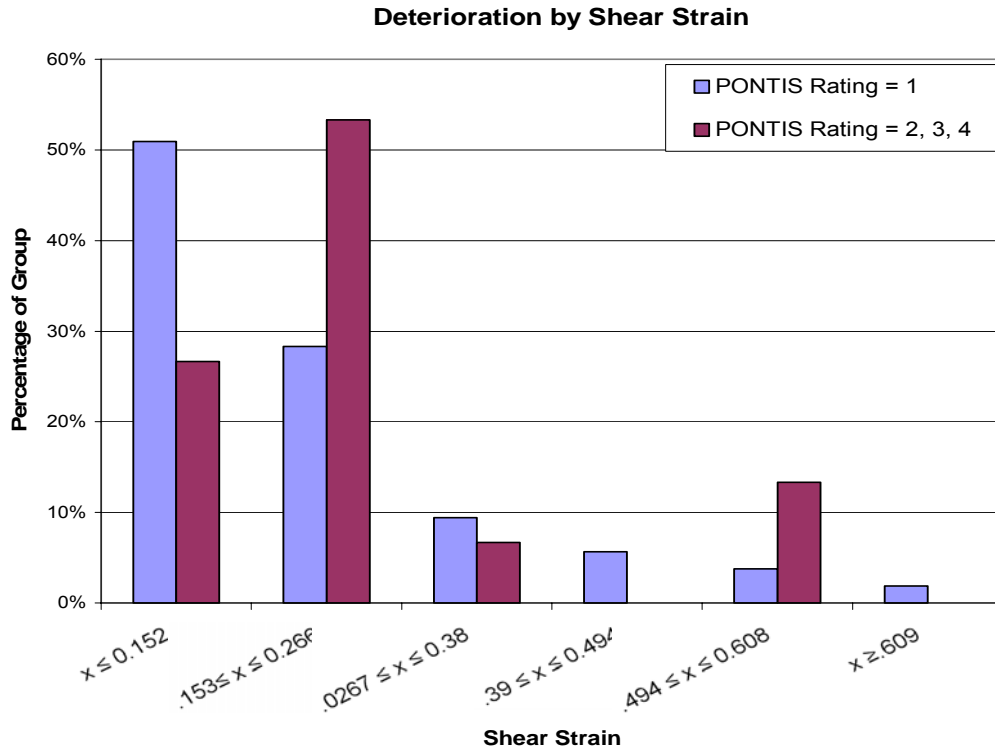


Figure 7.3 – Bearing Condition by Shear Strains

The above figure shows that the majority of bearings with a PONTIS rating of 1 have shear strains less than .152 in/in while the majority of bearings with a PONTIS rating of 2, 3 or 4 have shear strains between .153 and .266 in/in. Shear strains alone can cause the deterioration of the bearing but are not usually the sole cause of deterioration. With this stated, shear strains seem to be a heavy contributor to the overall condition of the bearing. The combination of shear strains, compressive stresses and rotation on the bearing can lead to the failure of the bearing.

Figure 7.4 for all sample bridges, including slab and girder bridges, shows that higher shear strains are associated with bearings that have begun or are beginning to deteriorate. According to the regression lines in figure 7.4, bearings with a higher PONTIS rating show 28.4% higher shear strains on average.

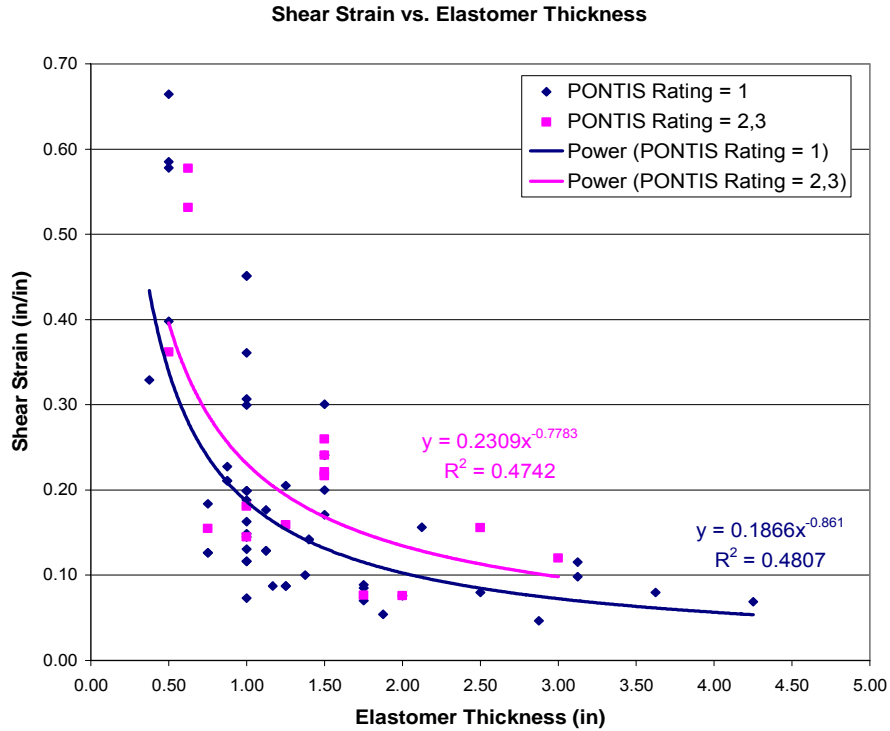


Figure 7.4 – Shear Strain vs. Elastomer Thickness for All Sample Bridges

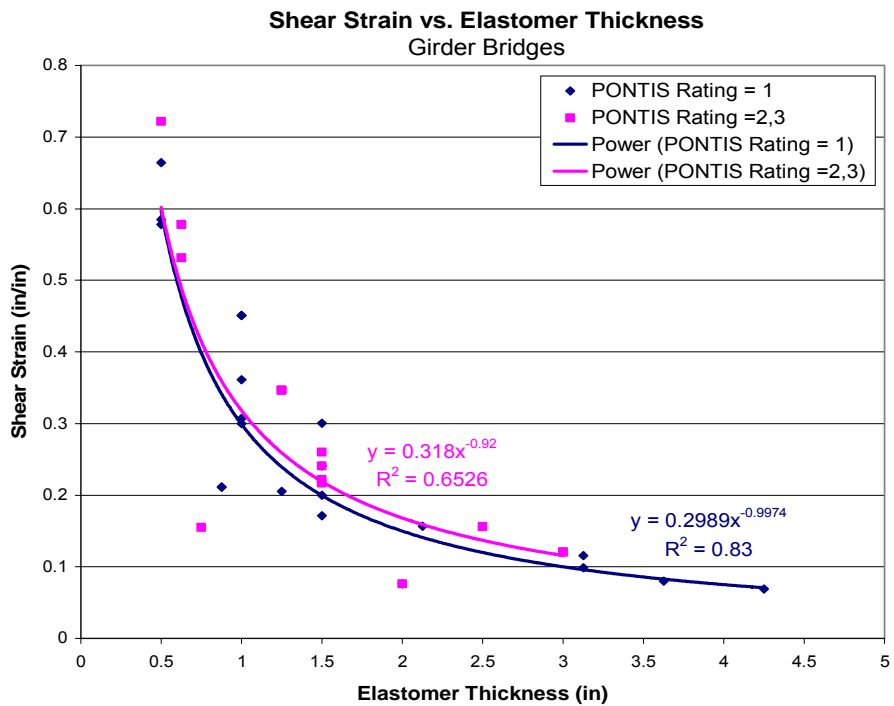


Figure 7.5 – Shear Strain vs. Elastomer Thickness for Girder Bridges

Figure 7.5 shows the relationship between shear strains and the elastomer thickness for girder bridges. For the studied girder bridges bearings with higher PONTIS ratings had slightly higher shear strains by 11.6%. The trend of this graph follows closely with that of the graph for all sample bridges implying there is a consistent tendency for bearings that are beginning to deteriorate or have already to have higher strains due to thermal deflection.

7.2.3 Compressive Stress, σ_s

Compressive stresses were found to have a statistically significant impact on the condition of a bearing through the processes of logistic regression as well as in the exploratory studies. Figure 7.6 shows the distribution of the two groups of bearings with relation to compressive stress.

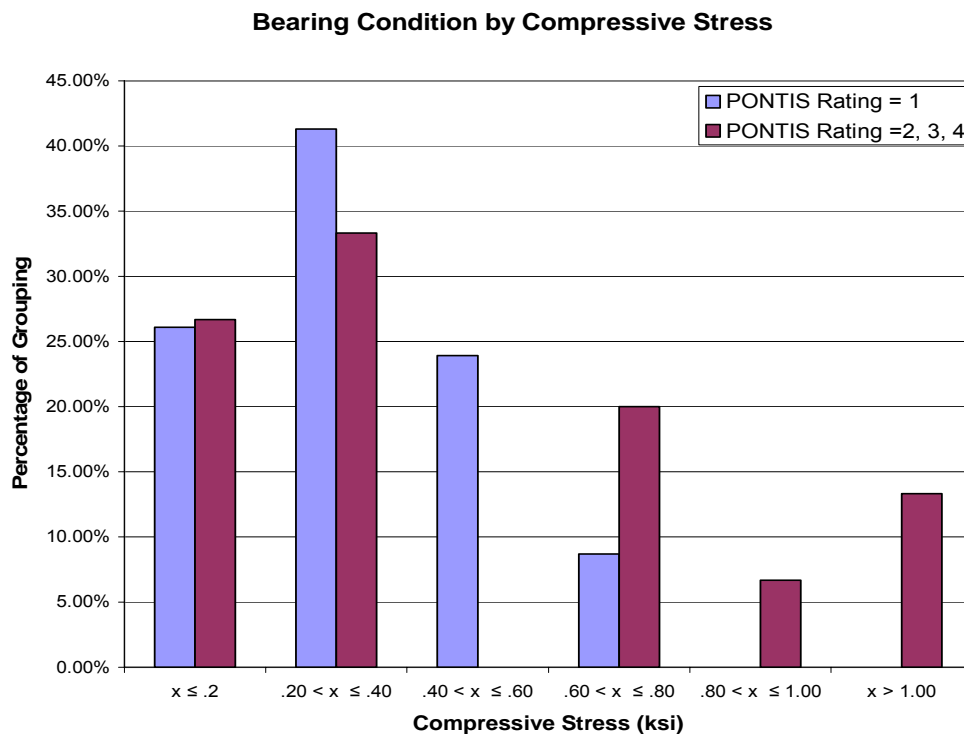


Figure 7.6 – Bearing Condition by Compressive Stress

Bearings in either PONTIS group seem to have a similar rate of occurrence when compressive stresses are below .4 ksi. Of the bearings studied, ones with a PONTIS rating of 1 had compressive stresses concentrated below .6 ksi with a maximum of .7 ksi. Conversely, bearings with a PONTIS rating of 2, 3 or 4 do have instances of compressive stresses above .8 ksi. In the editions of the AASHTO “Standard Specifications” prior to the 14th edition, .8 ksi was the upper limit for allowable compressive stress for elastomeric bearings. Approximately 40% of bearings with a rating of 2, 3 or 4 have compressive stresses approaching or exceeding this criterion. Later editions of the “Standard Specifications” give higher allowable stresses in “design method B”. As can be seen in figure 7.4, the majority of bearings have compressive stresses below .6 ksi. It seems that if possible, the designer should decrease the compressive stress of the bearing as much as possible. High compressive stresses coupled with thermal strains and rotations may be critical in the overall condition of the bearing.

Figure 7.7 for all sample bridges shows the relation between compressive stress and elastomer thickness. Bearings with PONTIS ratings of 2, 3 or 4 show higher compressive stresses than bearings with a rating of 1. Based on the regression lines in figure 7.7, bearings with a PONTIS rating of 2, 3 and 4 have an average of 93% higher compressive stress than bearings with a rating of 1. The same trend is found in the study for girder bridges. Figure 7.8 for girder bridges shows a similar result. Consistent results between the two graphs imply that the deteriorated condition of elastomeric bearings may be correlated to the compressive stresses.

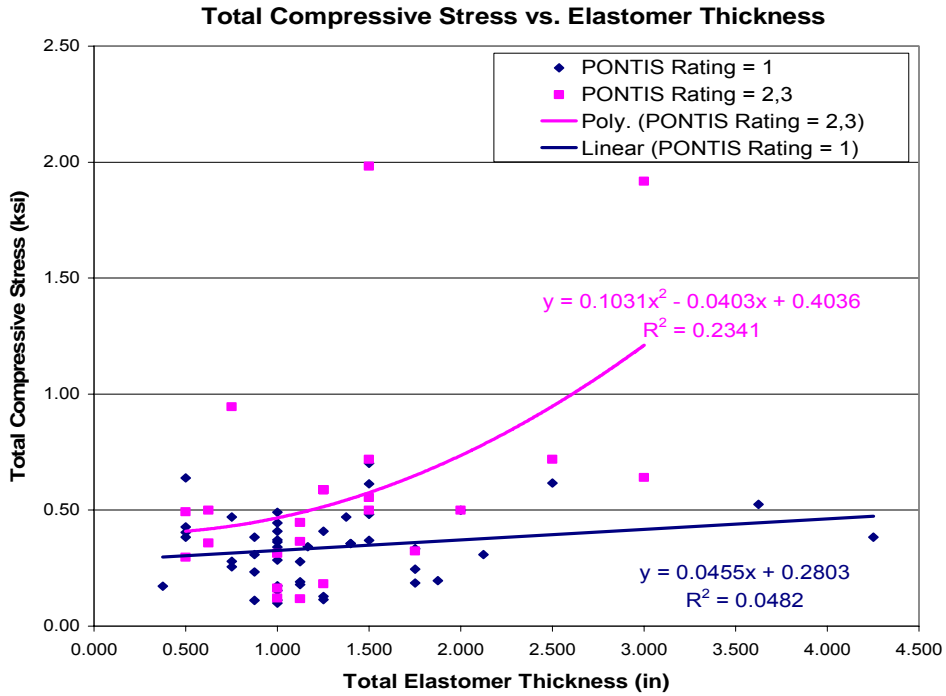


Figure 7.7 – Compressive Stress vs. Elastomer Thickness for All Sample Bridges

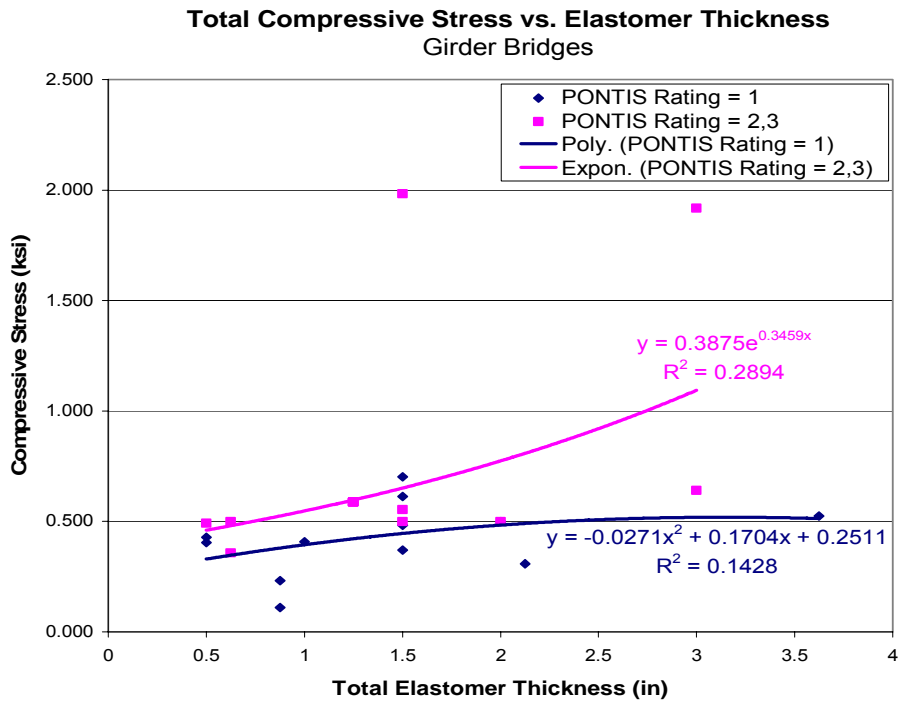


Figure 7.8 – Compressive Stress vs. Elastomer Thickness for Girder Bridges

7.2.4 Combined Compression and Rotation σ_s/GS

Combined compression and rotation were brought to the attention of designers via the 15th edition of the “Standard Specifications” published by AASHTO. “Method B” was introduced to accurately account for the material properties of the elastomer. With this method came the consideration of combined compression and rotation in the bearing. Higher allowances for compressive stress were introduced as well. Compression coupled with rotation will cause high edges stress and strains which lead to tearing and cracking of the elastomer. Special attention was paid to the state of the bearings at the edges in the 15th edition. Figure 7.9 shows a graph which has been presented in the commentary of the “Standard Specifications” since the 17th edition.

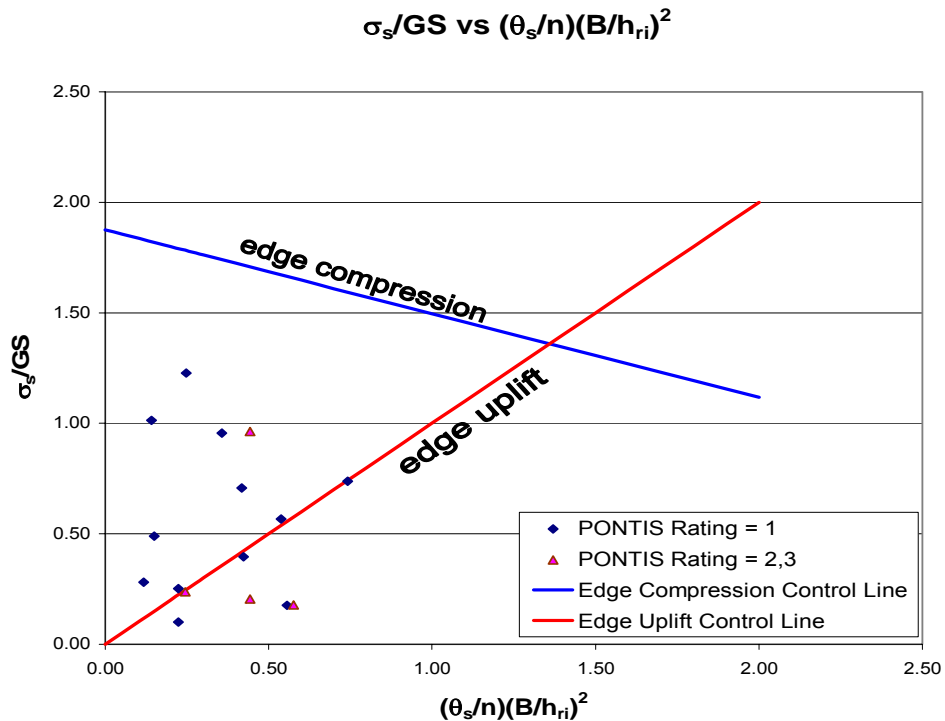


Figure 7.9 – Combined Compression and Rotation Limits of Elastomeric Bearings

The two lines in the above figure represent the edge compression limit and the edge uplift limit for elastomeric bearings. Bearings should be above the edge uplift line to prevent tearing or delamination of the elastomer and below the edge compression line to prevent crushing at the edges. The data from the field study with known compressive stresses and rotations follow this requirement for the most part and are shown in the same figure. The bearings with ratings of 2, 3 or 4 are lower than the edge uplift line for the most part and bearings with a rating of 1 are above it. The strong significance from the logistic regression implies that the graph is a good measure of the condition of the bearing.

7.3 Recommendations

7.3.1 Shape Factor

The shape factor of elastomeric bearings showed the highest correlation and strongest significance of all of the variables which were studied. Based on previous studies as well as this study, higher and lower shape factors seem to have a detrimental effect on the condition of elastomeric bearings. It is recommended that the shape factor of all bearings be kept between 3.5 and 6.5 in accordance to the findings summarized by figure 7.1.

7.3.2 Shear Strain

Shear strain was another significant factor which was related to the condition of elastomeric bearings. Higher shear strains were consistently found in bearings with ratings of 2, 3 or 4 when compared with other critical factors associated with the design of the bearing. Based on the findings of this study it is recommended that the shear strains present in the elastomer be limited to .21 in/in. Further, the design parameters

(design temperatures and the associated change in shear modulus) for the thermal deflection of elastomeric bearings should be standardized. This measure is important as the design procedures vary between engineers causing inconsistencies among the designs of similar bridges. For the majority of designs the worst thermal loading will be associated with the coldest temperatures as the elastomer becomes more brittle.

7.3.3 Combined Compression and Rotation

Based on the findings of this study and the current AASHTO design standards, combined compression and rotation were found to have strong correlation to the condition of elastomeric bearings. Figure 7.9 is based on the AASHTO requirements for edge uplift and edge compression. The results of the field study fit well with the AASHTO requirements. It is recommended that the current AASHTO requirements be followed in this regard.

This being the case, considering the above recommendation for the shape factor of a bearing is combined with the edge requirement graph of AASHTO and is based on the range of shear modulus for 60 durometer bearings and an .8 ksi compressive stress limit, a stricter recommendation can be asserted. Figure 7.10 combines the recommendation for shape factors and edge uplift/edge compression.

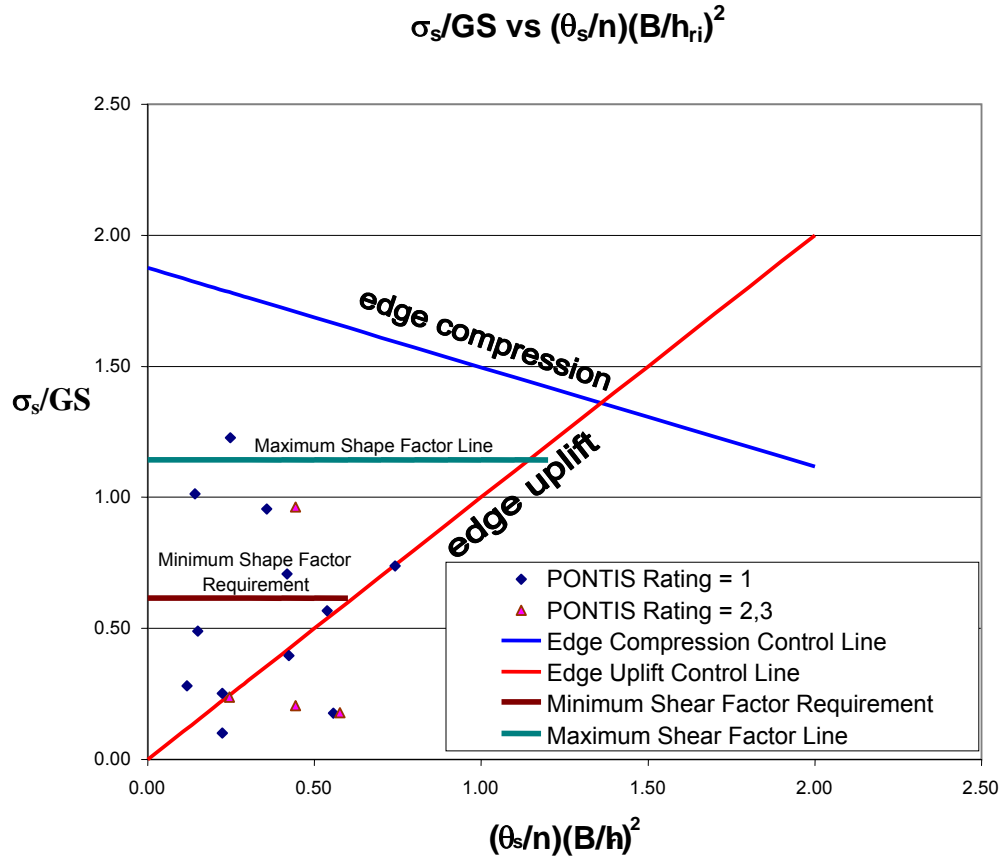


Figure 7.10 – Combined Compression and Rotation Limits of Elastomeric Bearings

To satisfy both recommendations for the shape factor and the combined compression and rotation it is recommended that all designs of 60 durometer elastomeric bearings coincide with figure 7.10. The limiting design criteria shall be the “maximum shear factor line”, the “minimum shear factor line” and the “edge uplift line as described by AASHTO.

Chapter 8

Conclusions and Future Research

Elastomeric bearings have been used in the concrete bridge structures in the state of Maryland for the last 50 years. Bridge bearings provide the bridge with a way to transfer gravity loads from the super-structure to the sub-structure without transferring the forces due to the thermal deflections of the super-structure. Although cost effective and reliable, some bearings are experiencing deterioration. The goal of this thesis was to identify the problems and to make recommendations for the future design.

Background information was collected on all of the bridges in Maryland using elastomeric bearings. Modes of deterioration were determined using textbooks, TRB reports and the AASHTO “Standard Specifications” and “LRFD Specifications”. A field study was then conducted to evaluate the condition of the bearings. Pictures, notes and measurements were taken so that analysis could be performed. All of the collected data was compiled into spreadsheets so that exploratory studies could be performed and preliminary hypotheses could be made. The validity of each hypothesis was evaluated by means of the logistic regression analysis. This statistical method determined whether different design parameters could be related to the condition of the elastomeric bearings. After each hypothesis was tested it was determined that the shape factor, shear strains and combined compression and rotation had the greatest correlation and statistical significance to the performance of elastomeric bearings.

Based on these findings, three recommendations were made. The first recommendation was to limit the range of the shape factor ($S = LW/[2h_r(L+W)]$ for rectangular bearing) to between 3.5 and 6.5. Designing using this range will help to control edge uplift in the

bearing. This conclusion is based on the findings in figure 7.1. Secondly, to limit the shear strains ($\epsilon_s = \Delta_{\text{thermal}}/h_{ri}$) to .21 in/in. The current limit for shear strains is .5 in/in. Limiting the shear strains will help to reduce the amount of deterioration due to the effects of thermal radiation. Lastly, to abide by the design recommendation of AASHTO for combined compression and rotation, σ_s/GS vs $(\theta_s/n)(B/h_{ri})^2$, and as shown in figure 7.10. Using this figure will allow the engineer to check the validity of their design as well as optimize the design. To satisfy both recommendations for the shape factor and the combined compression and rotation it is recommended that all designs of 60 durometer elastomeric bearings coincide with figure 7.10. The limiting design criteria shall be the “maximum shear factor line”, the “minimum shear factor line” and the “edge uplift line” as described by AASHTO. The implementation of these recommendations will reduce the variability of design between engineers as well.

Additional work recommended includes finding the interaction between shear strain, compression and rotation. Finite element models as well as laboratory testing could be used to determine their relation with one another. The effect of tall piers is a concern of bridge engineers and could be studied to understand the effect on the stresses in the bearing. Other works to be completed include standardizing a design method for elastomeric bearings in the state of Maryland. This will eliminate the variability of design between engineers for similar bridges.

Appendix A – Google Screenshots

Planned Trips

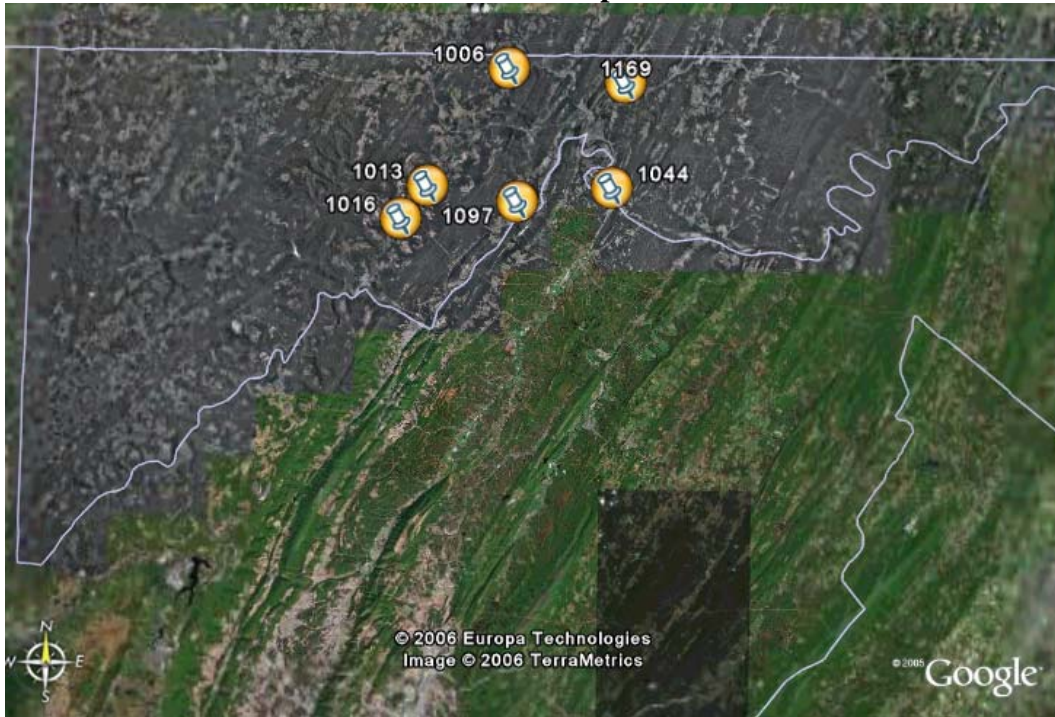


Figure A.1 – West

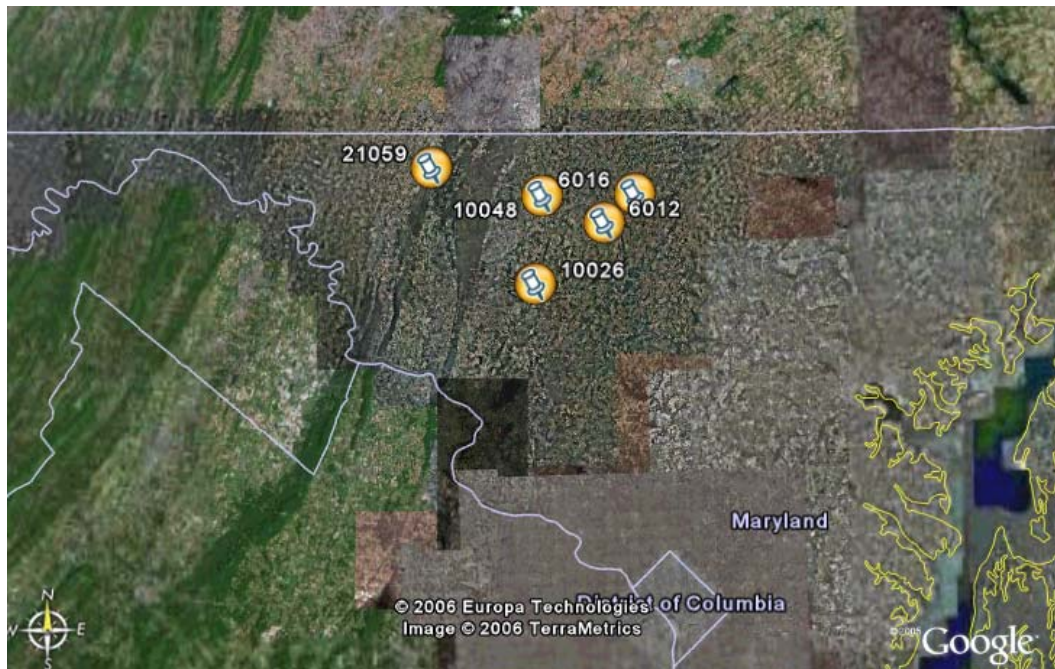


Figure A.2 – Midwest



Figure A.3 – Southeast 1

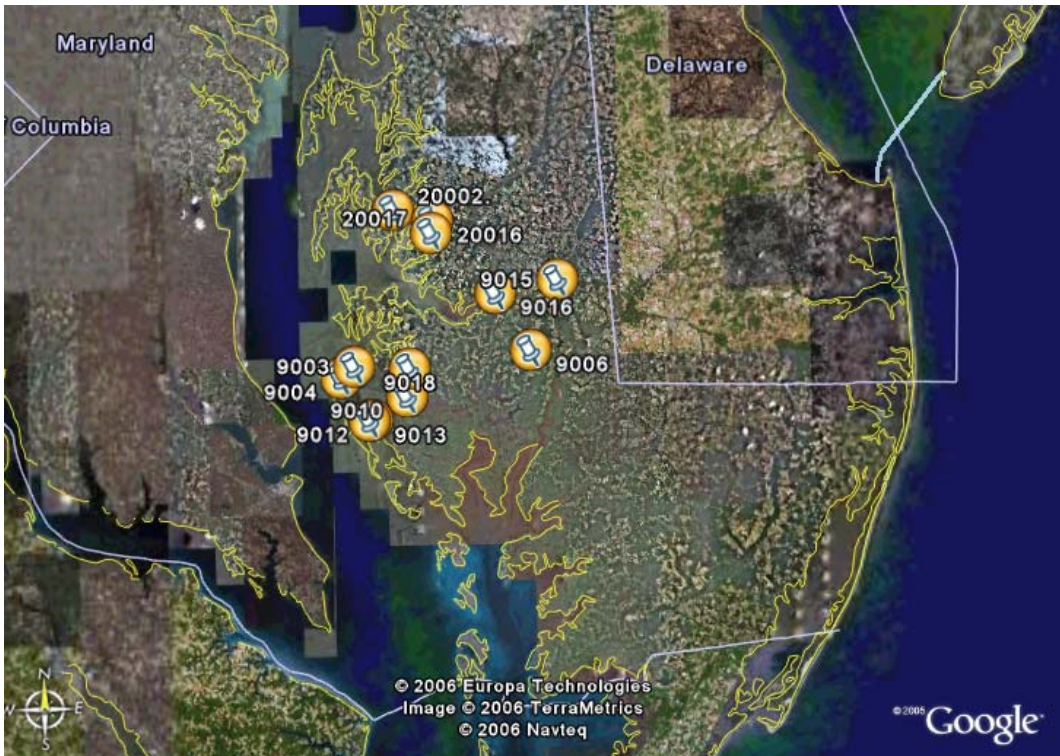


Figure A.4 – Southeast 2



Figure A.5 – South

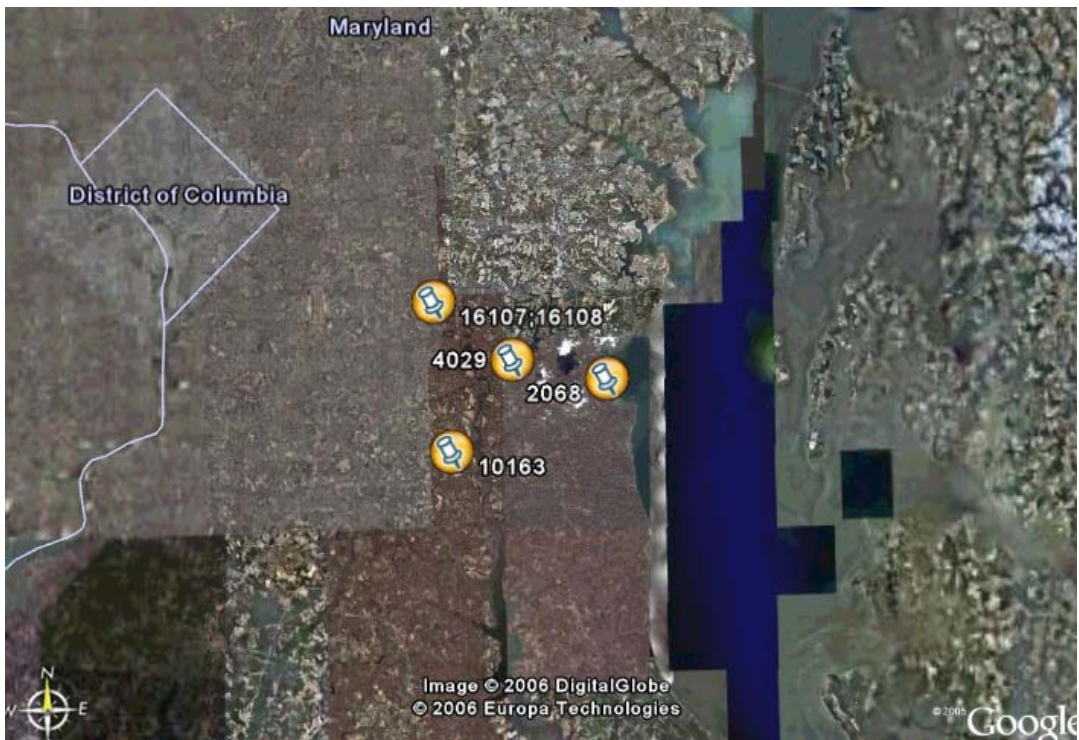


Figure A.6 – Mid-South

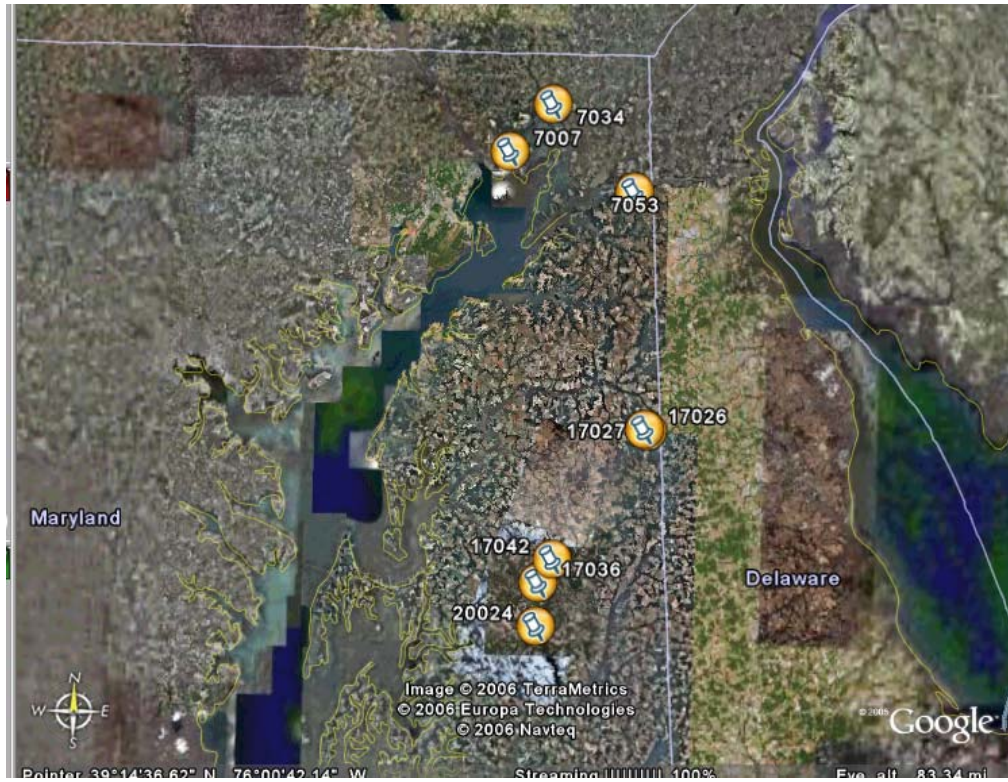


Figure A.7 – East 2

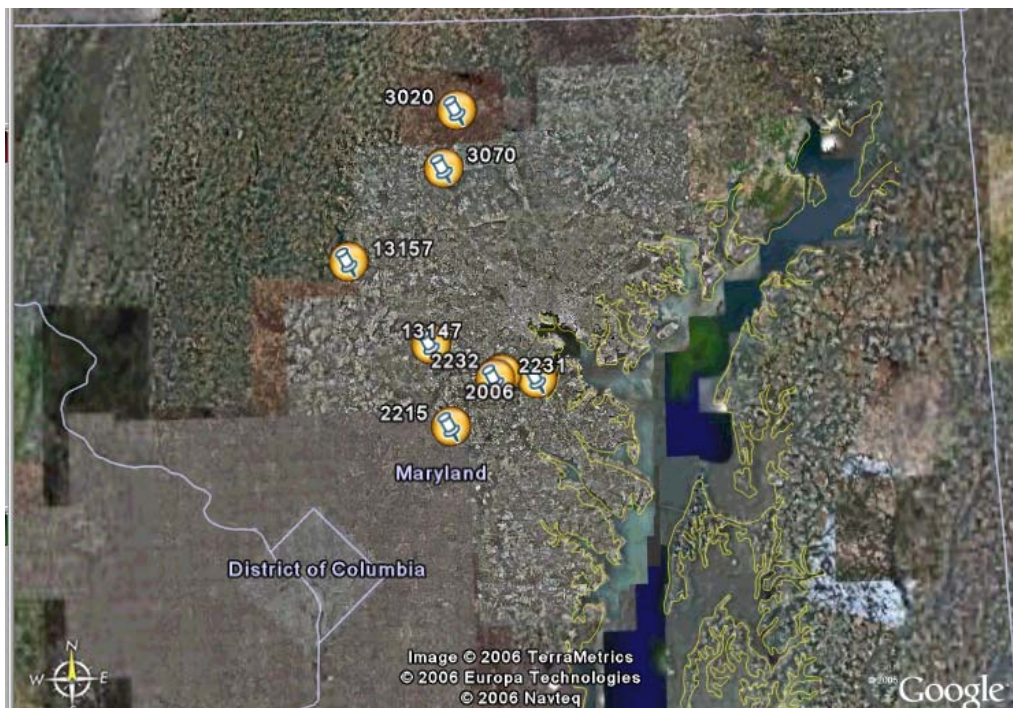


Figure A.8 – North 1



Figure A.9 – North 2

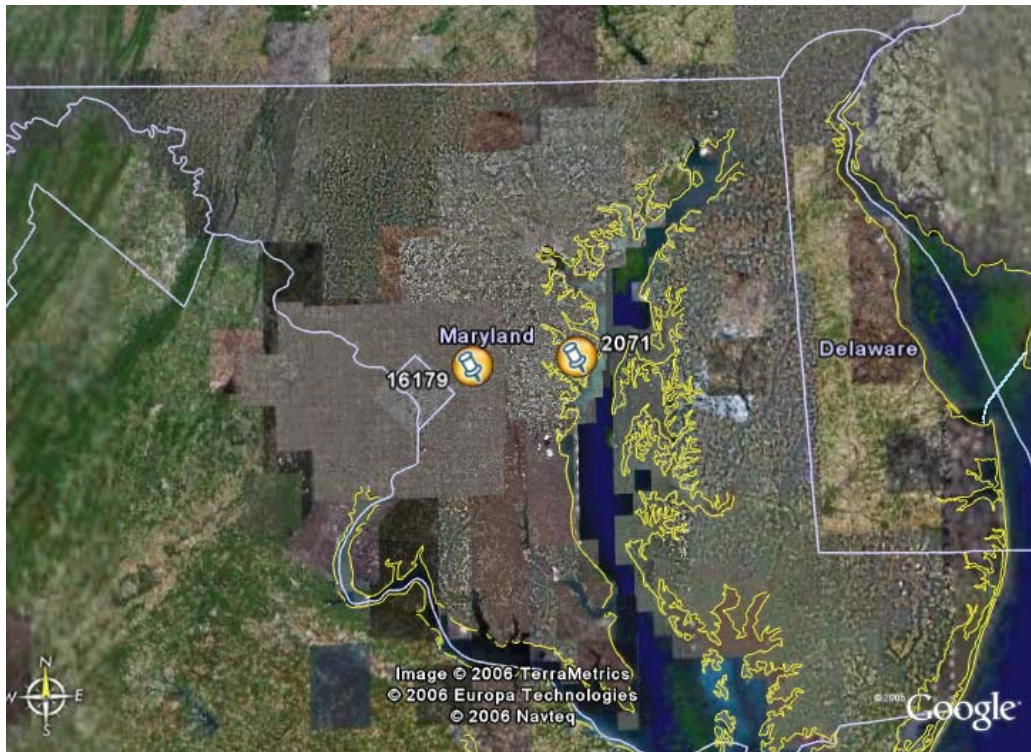


Figure A.10 – Central

Actual Inspections



Figure A.11 – May 19th : Mid-South

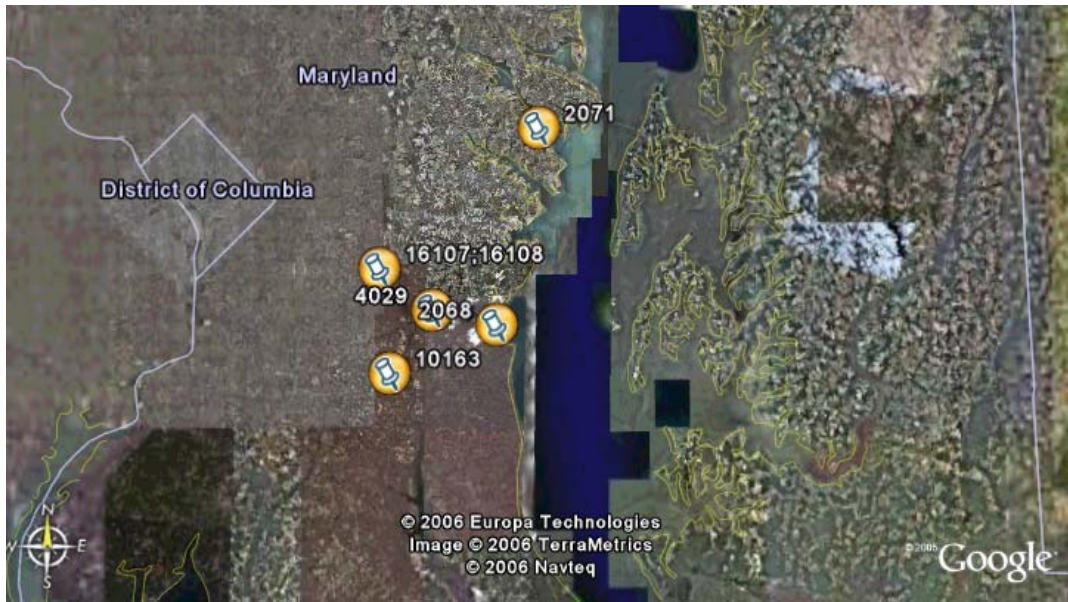


Figure A.12 – May 20th : North 2



Figure A.13 – May 21st : East



Figure A.14 – May 23rd : Southeast 1

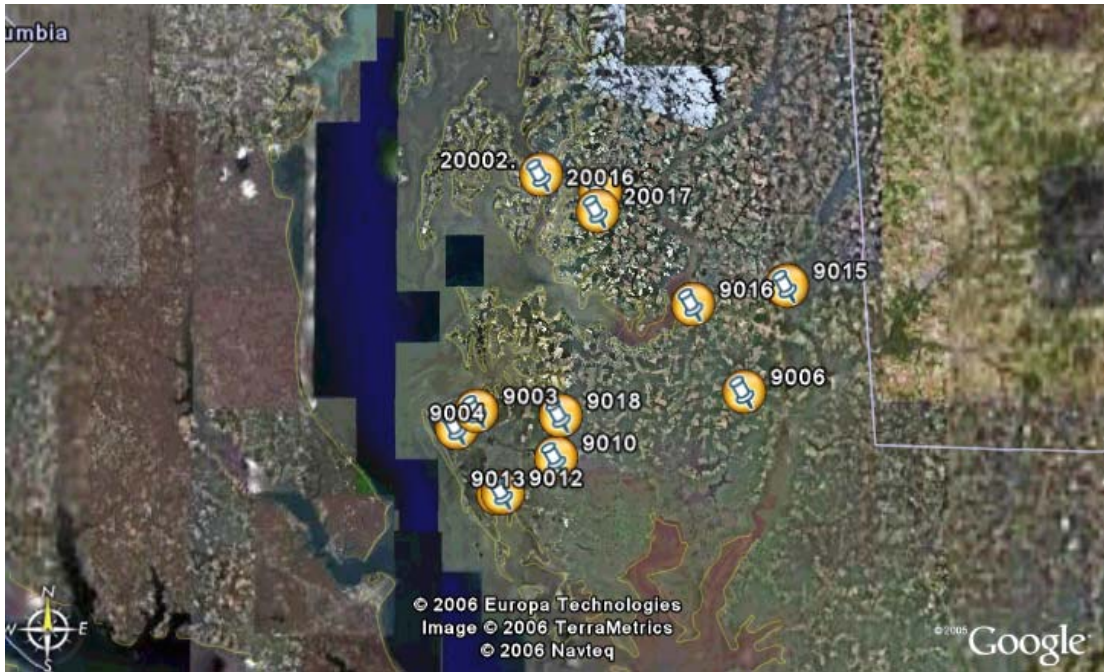


Figure A.15 – May 24th : Southeast 2

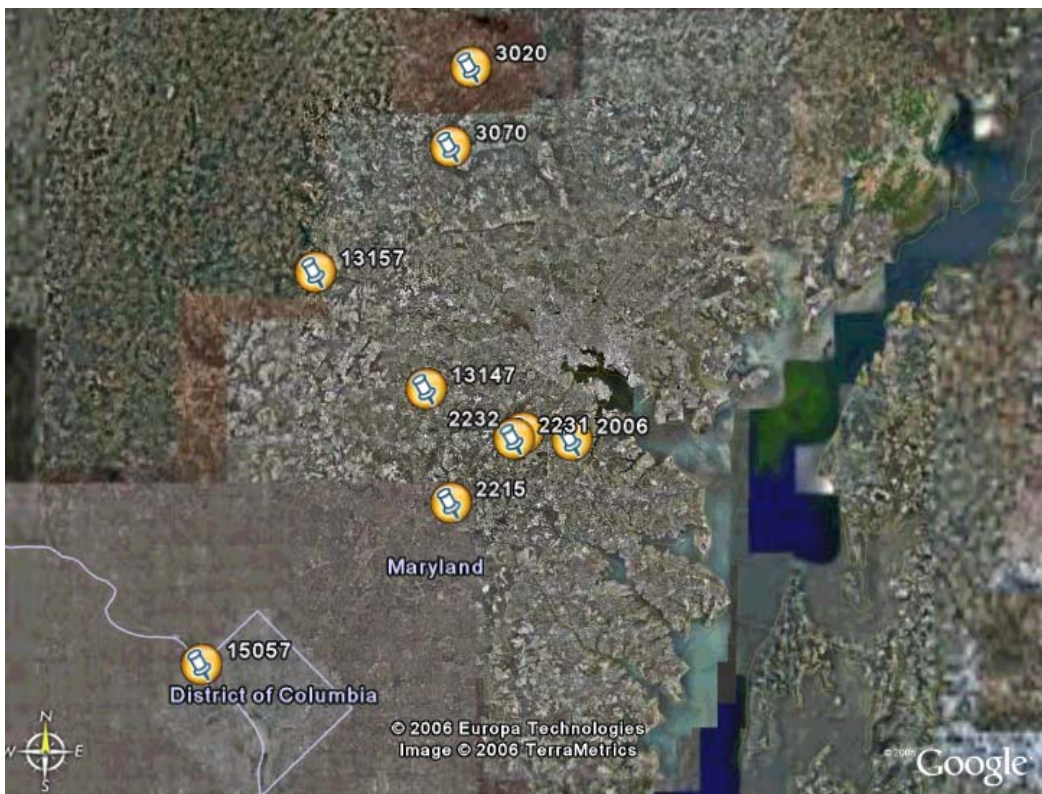


Figure A.16 – May 25th : North 1



Figure A.17 – May 30th : West

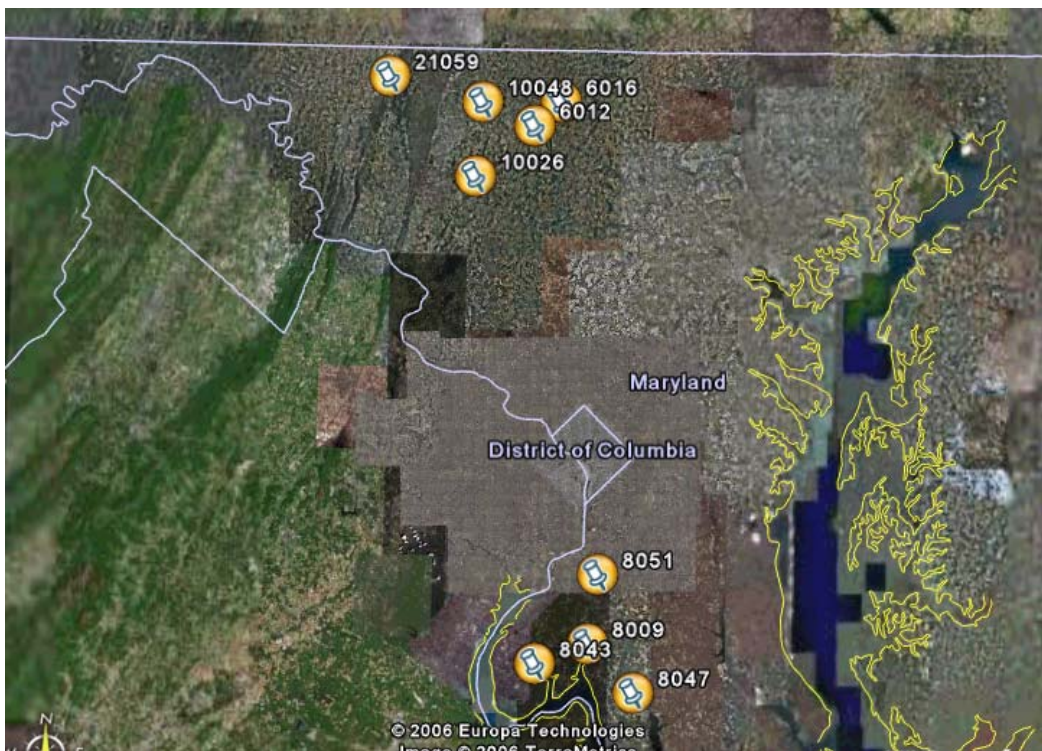


Figure A.18 – May 31st : Midwest



Figure A.19 – June 1st : South

Appendix B - Data Sets
Basic Bridge Information

item#	43a	43b	55a	54b				Good Bearings/Bad Bearings	AASHTO Design Manual
BRIDGE #	County	Structure Type	Structure Type	Feature Under Bridge	Min. Vert. Underclearance	Last Modified	Age		
010006001	Allegany	Pre-Ten	Slab Bridge	River or Grass	<10'	1996	10		15th Edition
010013001	Allegany	Pre-Ten	Slab Bridge	River or Grass	<10'			1	NO DATA
010016001	Allegany	Pre-Ten	Stringer/Girder	River or Grass	<10'				NO DATA
010044001	Allegany	Pre-Ten-Cont.	Slab Bridge	River or Grass	20' - 30'	1990	16		14th Edition
010097001	Allegany	Pre-Ten	Stringer/Girder	Railroad	23'-0"	1967	39	1	Previous to 10th Edition
010169001	Allegany	Pre-Ten-Cont.	Stringer/Girder	River or Grass	0'-0"	1999	7	1	16th Edition
020006001	Anne Arundel	Pre-Ten	Slab Bridge	River or Grass	<10'	1990	16	1	14th Edition
020068001	Anne Arundel	Pre-Ten	Slab Bridge	River or Grass	<10'	1989	17		14th Edition
020071001	Anne Arundel	Pre-Ten	Stringer/Girder Multiple Box	River or Grass	<10'	1987	19	1	13th Edition
020215031	Anne Arundel	Post-Ten-Cont.	Beams or Girders Multiple Box	Highway	17'-0"	1992	14		15th Edition
020215041	Anne Arundel	Post-Ten-Cont.	Beams or Girders	Highway	16'-0"	1991	15		14th Edition
020231002	Anne Arundel	Pre-Ten-Cont.	Stringer/Girder	River or Grass	0'-0"	1998	8		16th Edition
020232002	Anne Arundel	Pre-Ten-Cont.	Stringer/Girder	Highway	16'-9"	1998	8		16th Edition
030015001	Baltimore	Pre-Ten	Slab Bridge	River or Grass	10' - 20'				NO DATA
030020001	Baltimore	Pre-Ten	Slab Bridge	River or Grass	<10'	1995	11		15th Edition
030039001	Baltimore	Pre-Ten	Slab Bridge	River or Grass	<10'	1997	9		16th Edition
030070001	Baltimore	Pre-Ten	Slab Bridge	River or Grass	<10'	1990	16		14th Edition
030097001	Baltimore	Pre-Ten	Stringer/Girder	River or Grass	10' - 20'	1988	18	1	13th Edition
030366002	Baltimore	Pre-Ten	Slab Bridge	River or Grass	<10'	2000	6		16th Edition
040020001	Calvert	Pre-Ten	Slab Bridge	River or Grass	<10'			1	NO DATA
040023001	Calvert	Pre-Ten	Slab Bridge	River or Grass	<10'				NO DATA
040029001	Calvert	Pre-Ten-Cont.	Stringer/Girder	River or Grass	10' - 20'				NO DATA
060012001	Carroll	Pre-Ten	Slab Bridge	River or Grass	<10'	1972	34	1	10th Edition
060016001	Carroll	Pre-Ten	Beams or Girders	River or Grass	<10'				NO DATA

070007001	Cecil	Pre-Ten	Stringer/Girder	River or Grass	<10'	1995	11	1	15th Edition
070034001	Cecil	Pre-Ten	Stringer/Girder	River or Grass	<10'			1	NO DATA
070053001	Cecil	Pre-Ten	Slab Bridge	River or Grass	<10'				NO DATA
080009001	Charles	Pre-Ten	Slab Bridge	River or Grass	<10'	1988	18	1	13th Edition
080032001	Charles	Pre-Ten	Slab Bridge	River or Grass	<10'	1991	15		14th Edition
080043001	Charles	Pre-Ten	Slab Bridge	River or Grass	<10'	1995	11		15th Edition
080047001	Charles	Pre-Ten	Slab Bridge	River or Grass	10' - 20'	1959	47		Previous to 10th Edition
080051031	Charles	Pre-Ten	Stringer/Girder	River or Grass	10' - 20'	1995	11	1	15th Edition
080051041	Charles	Pre-Ten	Stringer/Girder	River or Grass	10' - 20'	1995	11	1	15th Edition
090003001	Dorchester	Pre-Ten	Slab Bridge	River or Grass	<10'	1970	36		10th Edition
090004001	Dorchester	Pre-Ten-Cont.	Stringer/Girder	River or Grass	10' - 20'	1949	57	1	Previous to 10th Edition
090006001	Dorchester	Pre-Ten	Slab Bridge	River or Grass	<10'	1996	10	1	15th Edition
090010001	Dorchester	Pre-Ten	Slab Bridge	River or Grass	<10'	1991	15	1	14th Edition
090012001	Dorchester	Pre-Ten	Slab Bridge	River or Grass	<10'	1991	15	1	14th Edition
090013001	Dorchester	Pre-Ten	Slab Bridge	River or Grass	<10'	1991	15		14th Edition
090015001	Dorchester	Pre-Ten-Cont.	Stringer/Girder	River or Grass	<10'	1999	7	1	16th Edition
090016001	Dorchester	Pre-Ten	Slab Bridge	River or Grass	10' - 20'	1971	35		10th Edition
090018001	Dorchester	Pre-Ten	Slab Bridge	River or Grass	<10'	1968	38		Previous to 10th Edition
100026001	Fredrick	Pre-Ten-Cont.	Stringer/Girder	River or Grass	<10'	2000	6	1	16th Edition
100048001	Fredrick	Pre-Ten	Slab Bridge	Railroad	23'-1"			1	NO DATA
100060001	Fredrick	Pre-Ten	Beams or Girders Multiple Box	River or Grass	<10'				NO DATA
100235X01	Fredrick	Pre-Ten	Beams or Girders	River or Grass	<10'	1998	8		16th Edition
120045001	Harford	Pre-Ten	Slab Bridge	River or Grass	<10'				NO DATA
120046001	Harford	Pre-Ten	Slab Bridge	River or Grass	<10'				NO DATA
130147001	Howard	Pre-Ten	Single Box Beam or Girder	Highway	17'-4"	1973	33		11th Edition
130157001	Howard	Pre-Ten-Cont.	Stringer/Girder	Railroad	25'-0"			1	NO DATA
150057001	Montgomery	Pre-Ten	Slab Bridge	River or Grass	<10'	1999	7		16th Edition
150131001	Montgomery	Pre-Ten	Stringer/Girder	River or Grass	12'-9"				NO DATA
160063001	Prince	Pre-Ten-Cont.	Slab Bridge	River or Grass	<10'	1960	46		Previous to 10th Edition

160108031	Georges Prince	Pre-Ten	Slab Bridge	Highway	14'-0"	1960	46	1	15th Edition
160108041	Georges Prince	Pre-Ten	Slab Bridge	Highway	14'-0"	1968	38	1	15th Edition
160179001	Georges	Pre-Ten	Stringer/Girder	River or Grass	10' - 20'	1995	11		16th Edition
170026001	Queen Annes	Pre-Ten	Slab Bridge	River or Grass	<10'	1995	11	1	16th Edition
170027001	Queen Annes	Pre-Ten	Slab Bridge	River or Grass	<10'	1997	9		16th Edition
170036001	Queen Annes	Pre-Ten	Slab Bridge	River or Grass	<10'				NO DATA
170042001	Queen Annes	Pre-Ten	Slab Bridge	River or Grass	<10'				NO DATA
180027001	St. Marys	Pre-Ten	Slab Bridge	River or Grass	<10'	1962	44		Previous to 10th Edition
190003021	Somerset	Pre-Ten	Slab Bridge	River or Grass	<10'	1974	32		11th Edition
190009001	Somerset	Pre-Ten	Slab Bridge	River or Grass	<10'	1980	26	1	12th Edition
190012021	Somerset	Pre-Ten	Slab Bridge	River or Grass	<10'	1965	41	1	Previous to 10th Edition
200002001	Talbot	Pre-Ten	Slab Bridge	River or Grass	20' - 30'	1998	8		16th Edition
200016001	Talbot	Pre-Ten-Cont.	Stringer/Girder	River or Grass	<10'	1998	8	1	16th Edition
200017001	Talbot	Pre-Ten-Cont.	Stringer/Girder	River or Grass	<10'	1960	46		Previous to 10th Edition
200024001	Talbot	Pre-Ten	Slab Bridge	River or Grass	<10'	2000	6		16th Edition
210059001	Washington	Pre-Ten	Stringer/Girder	Railroad	23'-0"	1995	11	1	15th Edition
220005011	Wicomico	Pre-Ten	Slab Bridge	River or Grass	0'-0"	1964	42		Previous to 10th Edition
220019001	Wicomico	Pre-Ten	Slab Bridge	River or Grass	<10'				NO DATA
220020001	Wicomico	Pre-Ten	Slab Bridge	River or Grass	<10'			1	NO DATA
220002011	Wicomico	Pre-Ten	Slab Bridge	River or Grass	10' - 20'			1	NO DATA
230018001	Worcester	Pre-Ten	Slab Bridge	River or Grass	30' - 40'	1996	10		15th Edition
230040002	Worcester	Pre-Ten-Cont.	Stringer/Girder	River or Grass	0'-0"				NO DATA
230017001	Worcester	Pre-Ten	Slab Bridge	River or Grass	<10'			1	NO DATA
230042011	Worcester	Pre-Ten	Stringer/Girder	Highway	17'-2"			1	NO DATA
230042021	Worcester	Pre-Ten	Stringer/Girder	Highway	17'-2"			1	NO DATA
230043001	Worcester	Pre-Ten-Cont.	Stringer/Girder	River or Grass	10' - 20'			1	NO DATA
230044001	Worcester	Pre-Ten-Cont.	Stringer/Girder	River or Grass	10' - 20'				NO DATA

Bearing Details

BRIDGE #	Location	File Number	Type	Length	Width	Height	Adhesive	Durometer	Steel
010006001	3' Trib Width of Slab	1026		10	18	1.375	epoxy	60	Y
	4' Trib Width of Slab	1026		10	18	1.375		60	Y
010013001		3094		7	14	1		60	Y
010016001		2043		10	18	1.375	Vulcanized		Y
010044001		2015,		11"	9"	1.75"		50	Y
010097001		1013,1011?	Neoprene	1'-6"	7"	.75"			
010169001		1017	Neoprene	26"	9"	1.5"		60	Y
		1016	Neoprene	26"	9"	2.5"		60	Y
020006001									
020068001		1014		1'-6"	12"	1"		60	Y
020071001		1029		2'-0"	10"	4.25"			Y
		1029		2'-0"	10"	.5"			Y
020215031	Fixed Bearing	3009, 3012	Neoprene	2'-0"	1'-8"	1"			N
		3012	Neoprene	1'-2"	10"	2 3/32"			Y
020215041	Fixed Bearing	3009, 3012	Neoprene	2'-0"	1'-8"	1"			N
		3012	Neoprene	1'-2"	10"	1 3/32"			Y
020231002		1018	Chloprene Virgin	1'-6"	10"	3.125"	vulcanized	60	Y
		1018	Chloprene Virgin	2'-0"	6"	1"	vulcanized	60	
020232002		1023	Chloprene Virgin	1'-6"	10"	3.125"	vulcanized	60	Y
		1023	Chloprene	2'-0"	6"	1"	vulcanized	60	
030015001	3' Trib Width of Slab	2036		8	14	2.5	epoxy	60	Y
	4' Trib Width of Slab	2036		8	10	1.25	epoxy	60	Y
030020001		3023		1'-3"	8"	1.75"		60	Y
030039001		3016		1'-2"	7"	1.75"		50	Y
030070001		1016	Neoprene	8"	6"	.75"		50	N
030097001		1029		2'-0"	1'-11"	9.5"	epoxy		Y
030366002		1007		8	18	0.75		150	Y

040020001	3' Trib Width of Slab	1026		8	14	1.125		60	Y
	4' Trib Width of Slab	1026		8	10	1.125		60	Y
040023001	Laminated	3035		8	12	1.375		60	Y
040029001	Expansion	1027		12	26	1.5		60	Y
	Laminated	1027		18	26	0.625			
060012001		1006		6	36.5	1"			
060016001	Laminated	2028		9	21	0.875		60	Y
070007001	Fixed Bearing	1027		20"	14"	1.5"	vulcanized	60	
070034001	Expansion	1036		12	31.5	1	vulcanized	60	N
	Fixed Bearing	1036		8	31.5	1.75	vulcanized	60	Y
070053001	3' Trib Width of Slab	1026		8	14	1.125		60	Y
	4' Trib Width of Slab	1026		8	10	1.125		60	Y
080009001	Abutment A	1015		8	10	.5"			
	Abutment B	1015		8	10	1"		70	
080032001									
080043001		1030		12	18	.625"		60	Y
080047001		2003		10		1			N
080051031		1017		12	24	.5"			
080051041		1017		12	24	.5"			
090003001		2044		9	15	1"	epoxy	60	Y
090004001	Everywhere but pier								
	7	1041		12	26	.5"	epoxy	60	N
	Peir 7	1041		12	36	2.125"	epoxy	60	Y
090006001	3 ft beams	1028	Neoprene	6	12	1.4"		60	Y
	4 ft beams	1028	Neoprene	6	16	1.4"		60	Y
090010001	Abutment	1020	Neoprene	5	24	1.375"			Y
	Pier	1020	Neoprene	5	24	.75"			N
090012001	Abutment	1021	Neoprene	6	18	1.75"		60	Y
	Pier	1021	Neoprene	6	16	1.125		60	Y
090013001	Abutment	1026	Neoprene	9	14	2.875"		60	Y
	Pier	1026	Neoprene	6	21	1.375"		60	Y
090015001		1078		14"	5"	1.5"		60	Y
090016001				5	32	1"	epoxy		Y
090018001				10	30	1"	epoxy		

100026001		1023		5	14	1"	vulcanized	60	
100048001	Abutment	1015, 1029		9	42	1.25	epoxy	60	Y
100060001		1026					epoxy		
100235001		1007		3'-6"	1'-0"	1"		60	
120045001				8	11	1.125		60	Y
120046001				8	11	1.125		60	Y
130147001		1006		3'-0"	8"	1.875"		60	Y
130157001	Fixed Bearing Expansion	1090		12	26	0.625	Vulcanized	60	N
		1090		12	26	1.5	Vulcanized	60	Y
150057001		2002			10"	1"			
150131001		4021		10	22	3.375		60	Y
		4021		12	16	3.375		60	Y
160063001		1038		22"	8"	7/8"		60	Y
160108031		1003			10	0.5			
160108041		1003			10	1			
160179001		2016		12"	9"	7/8"		60	Y
170026001		1031		12"	8"	1.75"		60	Y
170027001		1016		12"	8"	1.75"		60	Y
170036001		1023		9	12	1		60	Y
170042001		4023		9	12	1		60	Y
180027001		1019		16"	8"	.75"		60	Y
190003021		1002			8"	1"			
190009001		1008		5	30	1			
190012021		1003,1006		10	30	1			
200002001		1014		32"	18"	.25"			
200016001	Abutment	4051		20"	12"	3.625"		60	Y
	Pier	4051		26"	12"	.5"		60	N
200017001	Abutment	4105		20"	12"	3"		60	Y
	Pier	4105		26"	12"	.5"		60	N
200024001		1005		10		0.375			
210059001		2041		26"	12"	1.5"	clad	60	Y
220005011	3 ft beams	1026		9"	8"				
	4 ft beams	1026		12"	8"				

220019001	3 ft beams	2037		8	9	1.125		60	Y
	4 ft beams	2037		7	27	1.125		60	Y
220020001	3 ft beams	4037		6	12	1.125		60	Y
	4 ft beams	4037		6	29	1.125		60	Y
220002011	3 ft beams	2046		4	23	1		60	Y
	4 ft beams	2046		4	28	1		60	Y
230018001		1015		2'-6"	10"	1"	epoxy		
		1015		24"	8"	1"	epoxy		
230017001	Pier	1040		9	42	0.875		60	Y
	Abutment	1040		9	20	0.875		60	Y
230042011	Fixed	1026		12	28	1.375	vulcanized	60	Y
	Expansion	1026		12	28	1.875	vulcanized	60	Y
230042021	Fixed	1026		12	28	1.375	vulcanized	60	Y
	Expansion	1026		12	28	1.875	vulcanized	60	Y
230043001		1018		12	28	1.375		60	Y
230044001	Fixed	1026		12	22	1.875		60	Y

Appendix C – Field Study Trips

C.1 Bridge Location

Following the selection of the bridges suitable for study they had to be located. The two methods used to locate the bridges were by using the “2005 Office of Bridge Development Bridge Inventory” and then mapping the same bridges using Google Earth. The location of the bridges allowed for trips to be planned effectively.

C.1.1 Mapping in the Bridge Inventory Book

The first step to setting up trips for the field study was to locate the bridges in the “2005 Office of Bridge Development Bridge Inventory”. The Bridge Inventory breaks the bridges down by county. Locating a bridge required knowledge of the county and the bridge number. Locating bridges by this method gave an idea of surrounding roads and location in the county but was not able to provide a statewide look at the bridges. Another method of mapping was used to accomplish this.

C.1.2 Mapping on Google Earth

As stated in the previous section, mapping the bridges in Google Earth could provide a statewide relationship of the bridges. Setting up trips for the field study depended on this relationship. Google Earth is a program which allows one to view satellite imagery of the entire earth. Bridges can be easily identified with the resolution of the images as seen in figure C.1. This made it very easy to gain a statewide perspective of where the bridges are. The figure below is a look at the map of Maryland with all of the bridge locations for the study.

Using Google Earth, bridges were grouped based on their geographical location as opposed to grouping by county. An example of this is shown in figure C.2.

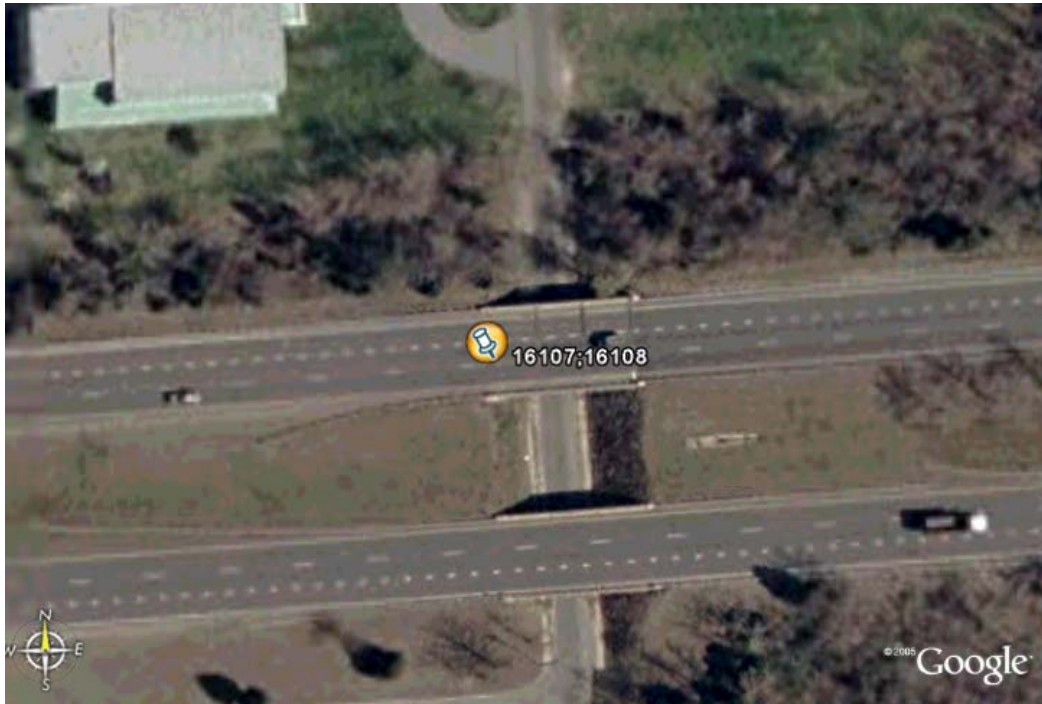


Figure C.1 – Sample image of bridges based on Google Earth

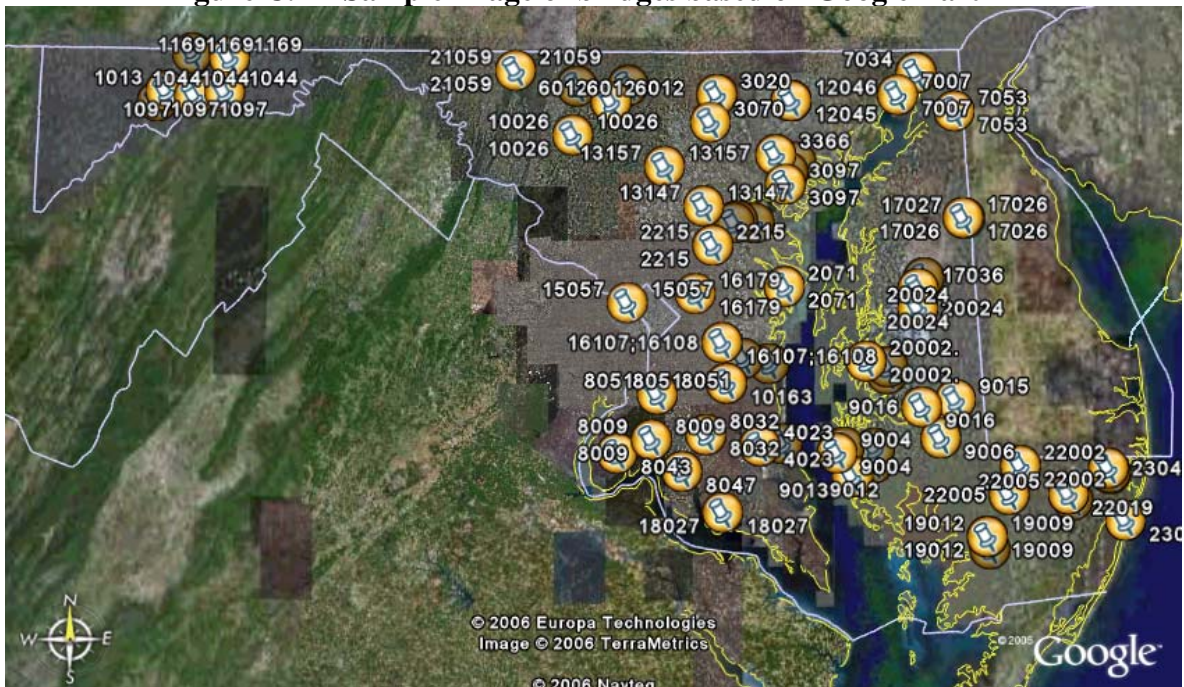


Figure C.2 – Image of Maryland bridges by geographical locations

C.2 Bridge Groupings

The bridges of interest were plotted on Google Earth to provide a global view, not restricted by county lines. Using this map the bridges were grouped together based on how close they were to each other. The bridges were broken down into the 10 groups listed below.

West – 1169, 1013, 1016, 1006, 1044, 1097

Midwest – 6012, 6016, 10026, 10048, 21059

Southeast 1 – 19003, 19012, 19009, 23018, 23044, 23017, 22002, 22020, 22019, 22005, 23043, 23042, 23040

Southeast 2 – 9013, 9004, 9003, 9010, 9012, 9016, 9018, 9006, 9015, 20016, 20017, 20002,

South – 8047, 18027, 8032, 8009, 8043, 4023, 4020, 8051

Mid South – 4029, 10163, 2068, 16107, 16108

East – 17026, 7053, 7007, 7034, 20024, 17027, 17036, 17042

North 1 – 3070, 13157, 2215, 2006, 2231, 2232, 13147, 3020

North 2 – 3366, 12045, 12046, 3097, 3015, 3039

Central – 2071, 16179

Figures C.3 to C.12 show Google Earth screenshots for each trip are below.

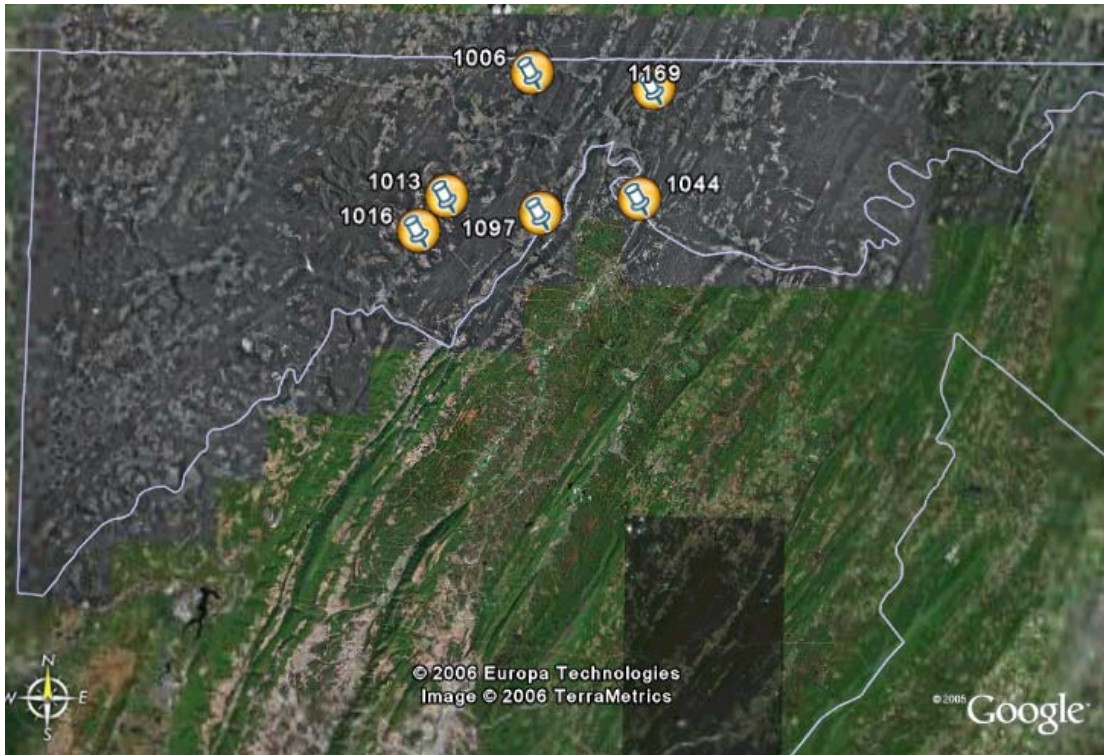


Figure C.3 - West Group

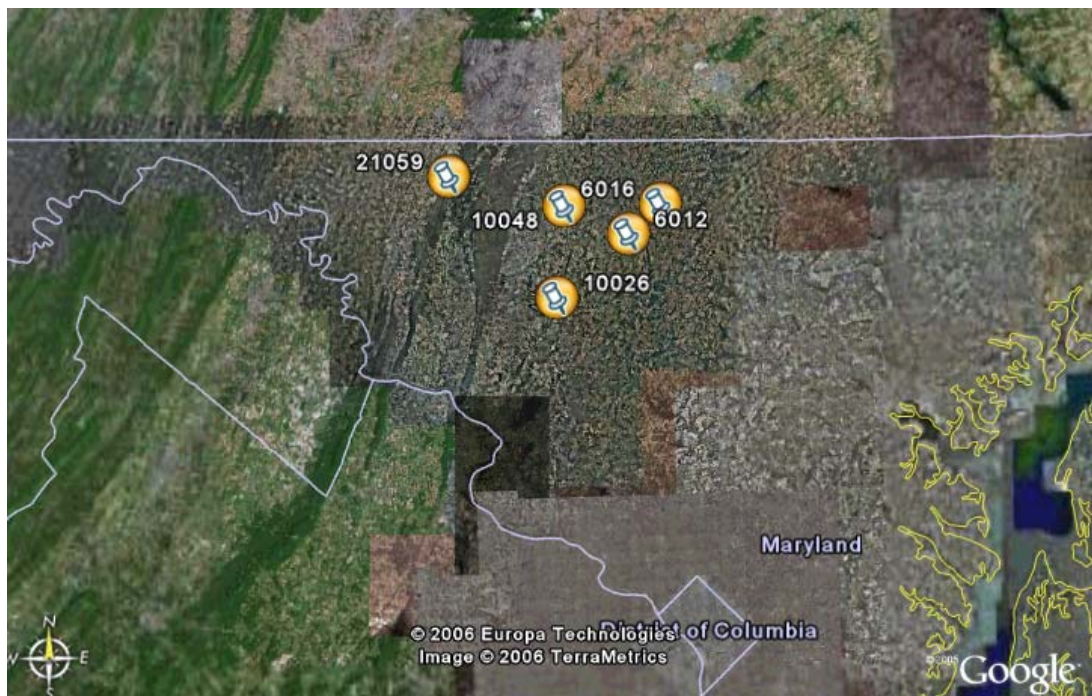


Figure C.4 - Midwest Group

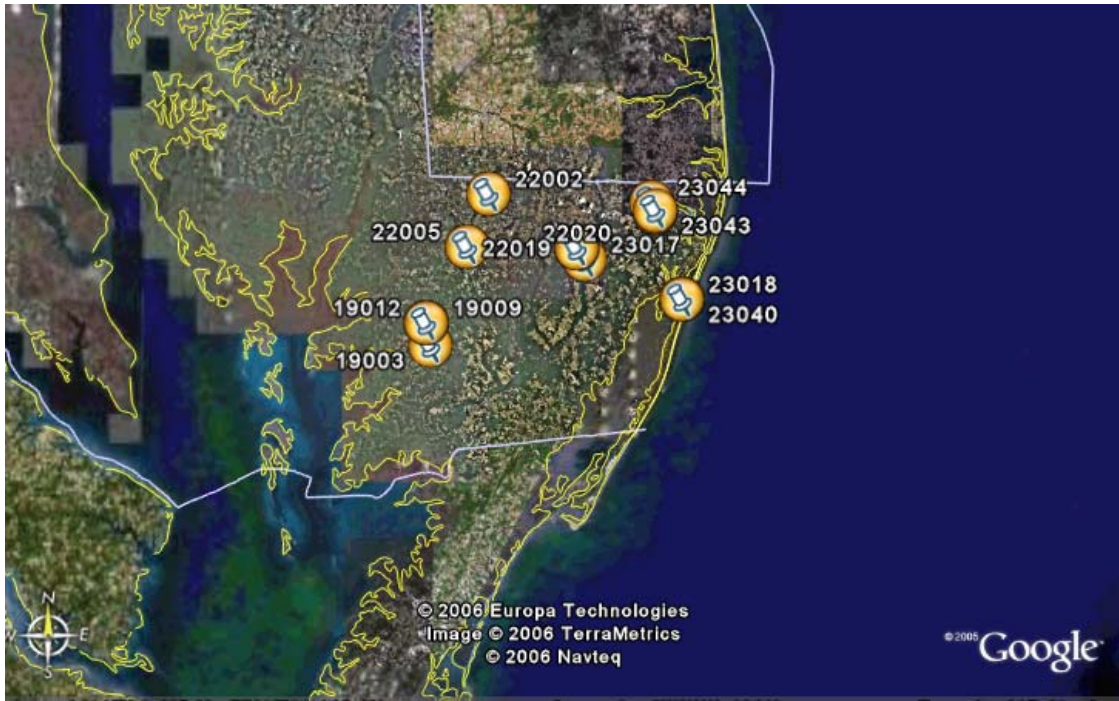


Figure C.5 - Southeast 1 Group

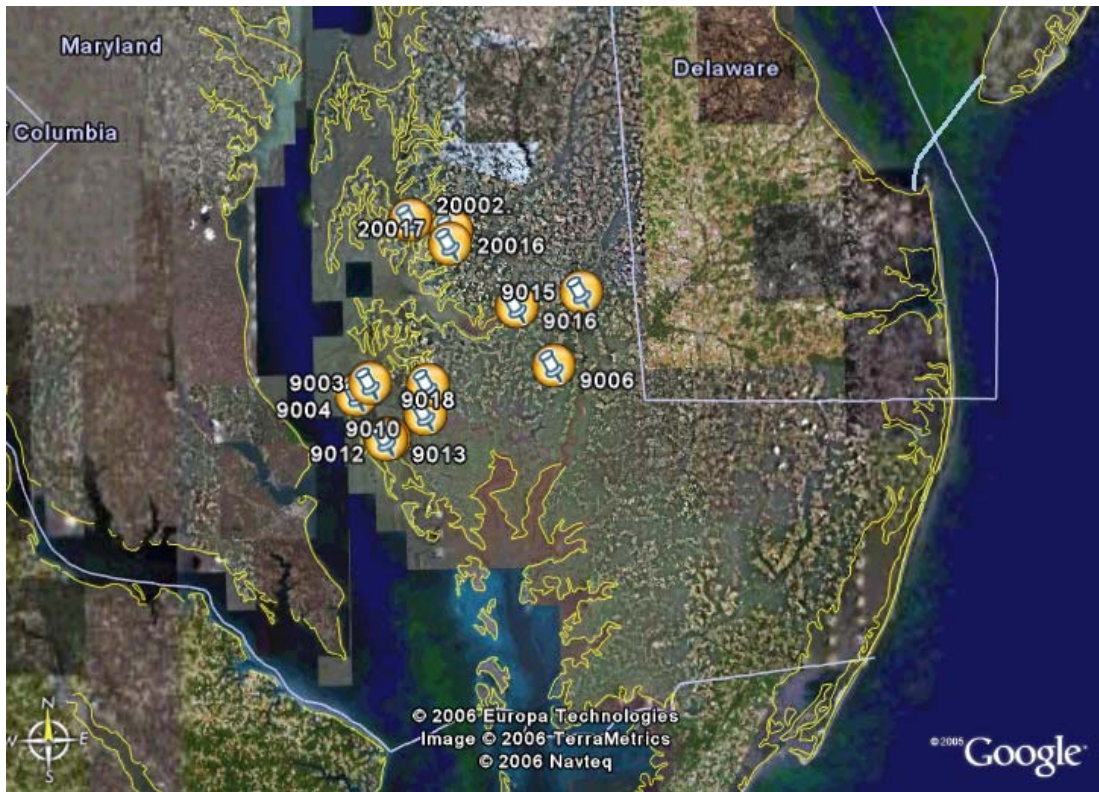


Figure C.6 - Southeast 2 Group



Figure C.7 - South Group

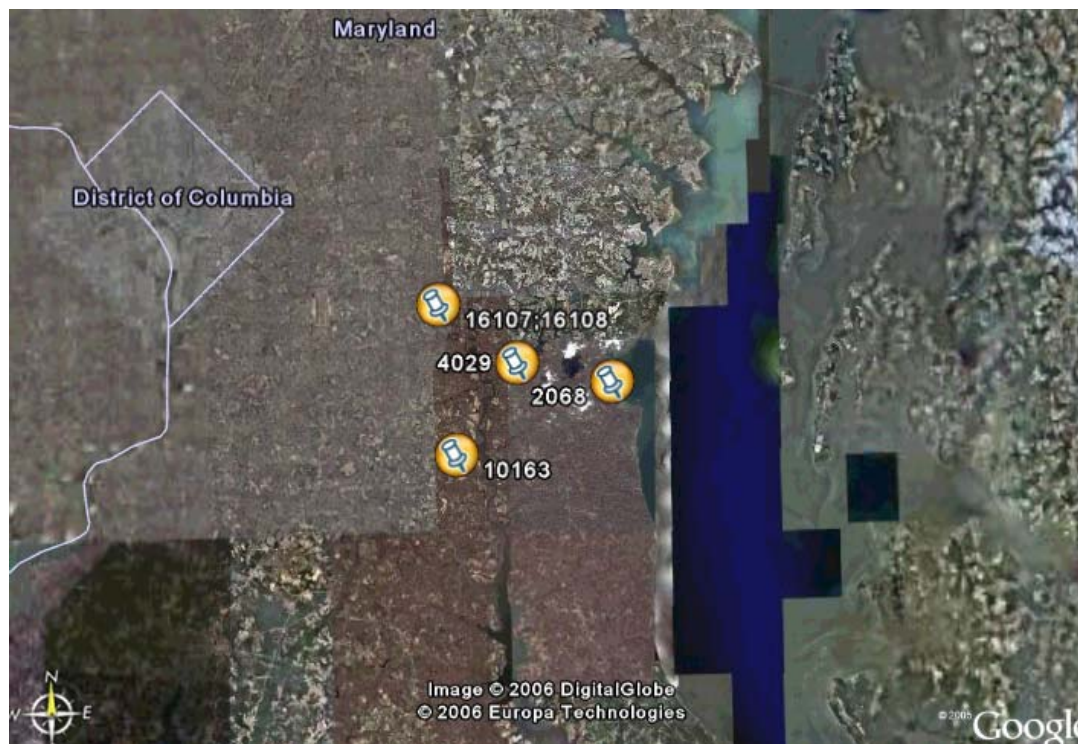


Figure C.8 - Mid South Group

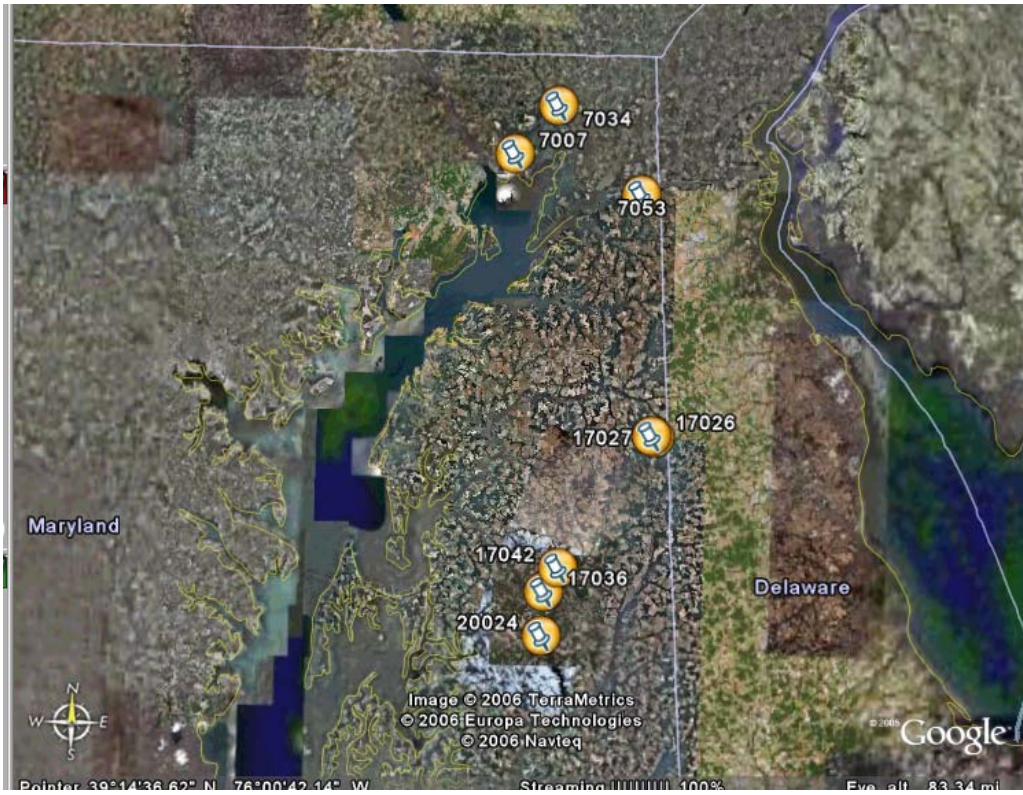


Figure C.9 - Southeast 2 Group



Figure C.10 - North 1 Group

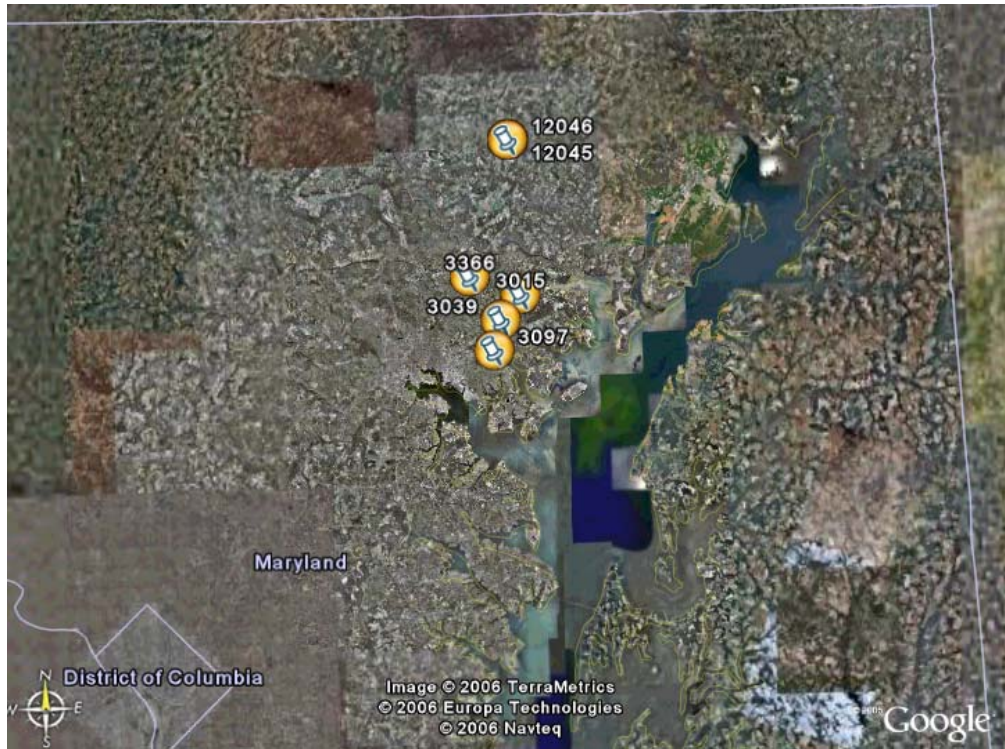


Figure C.11 - North 2 Group

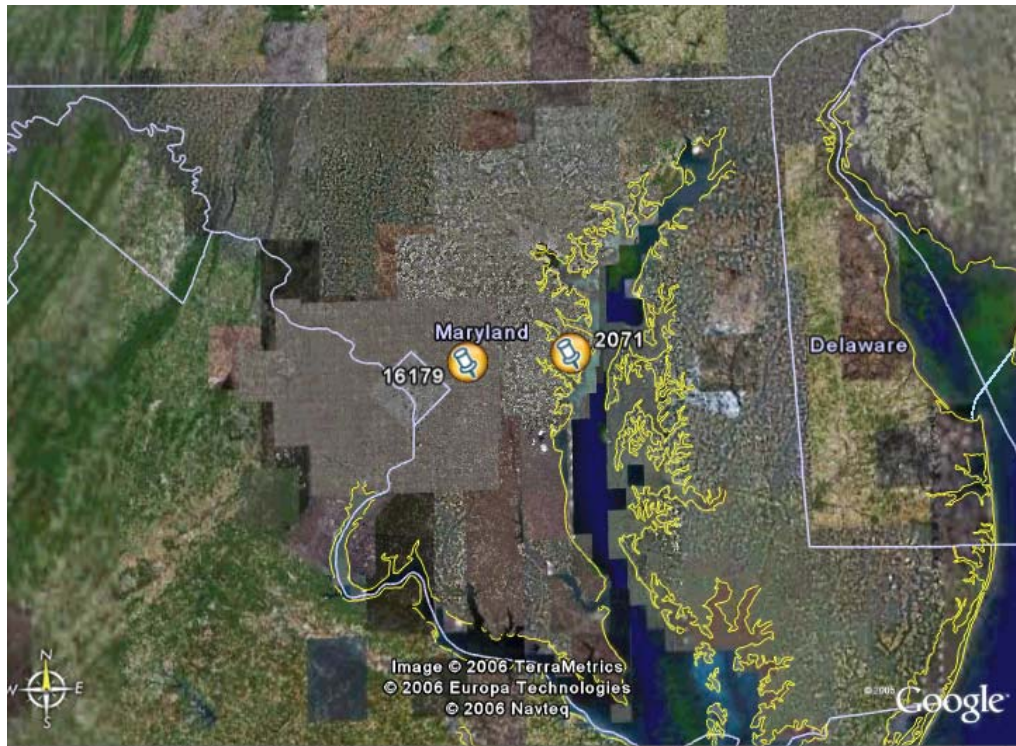


Figure C.12 - Central Group

C.2.1 Trip Planning

Planning the trips was based on two factors, the time to inspect a bearing and the travel time between bridges. One hour was allowed for each bridge inspection. The travel time between bridges was calculated by Google Earth. Each bridge grouping was given its own day. The Southeast 1 and Southeast 2 trips were combined into a two day trip as was the West and Midwest trips. The goal time to finish the trips was two weeks. Trip booklets were created to organize directions and to give approximate times. There are examples in the Appendix A.

C.2.2 Schedule

A preliminary schedule was calculated in Microsoft Project to estimate how long the project would take. A goal of two weeks was set out and used as a constraint. The GANTT can be seen in Table C.1 below.

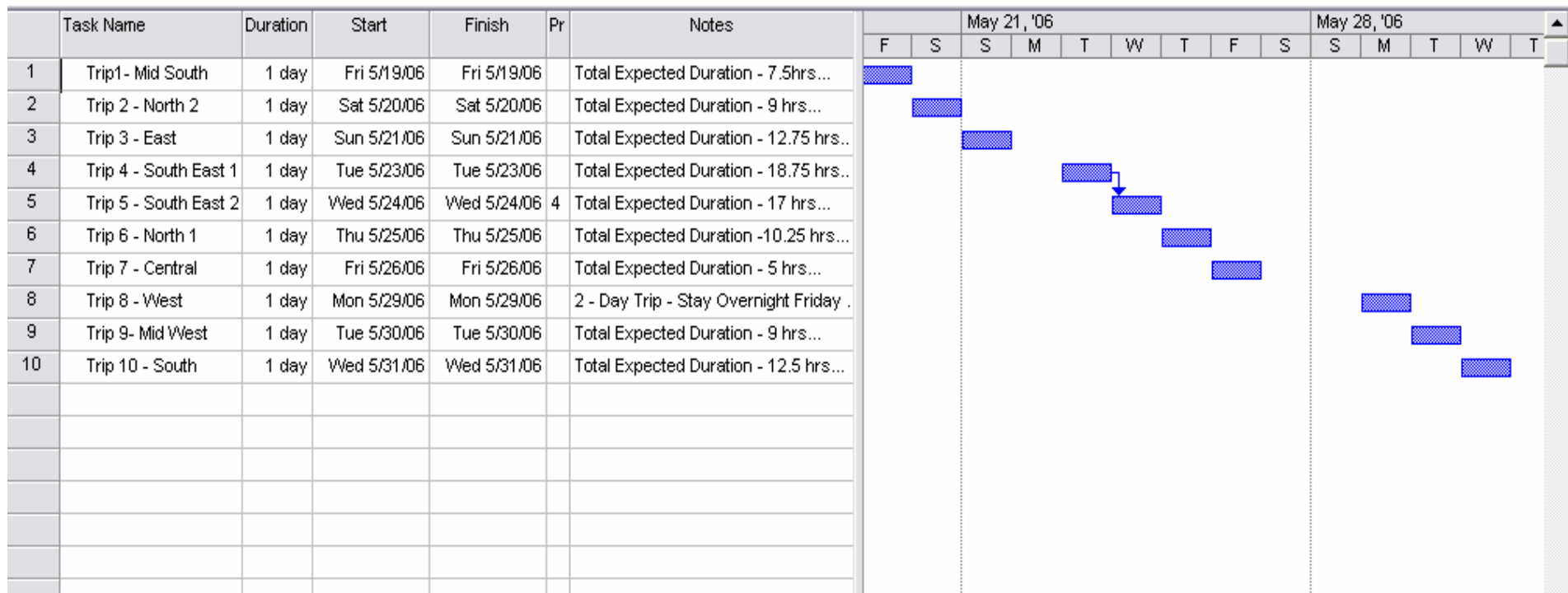


Table C.1 - GANTT Chart for Bridge Trips

C.3 Actual Trip Schedule

During the field study the original schedule was adhered to as closely as possible. The overall trend was that the time taken to inspect one bridge was less than an hour. Travel times were quicker than expected as well. This allowed a quicker completion of the project, as well as allowing extra inspections during the day. The images from Google Earth (figures C.13-21) show the actual days of inspection.



Figure C.13 - May 19th – Mid-South

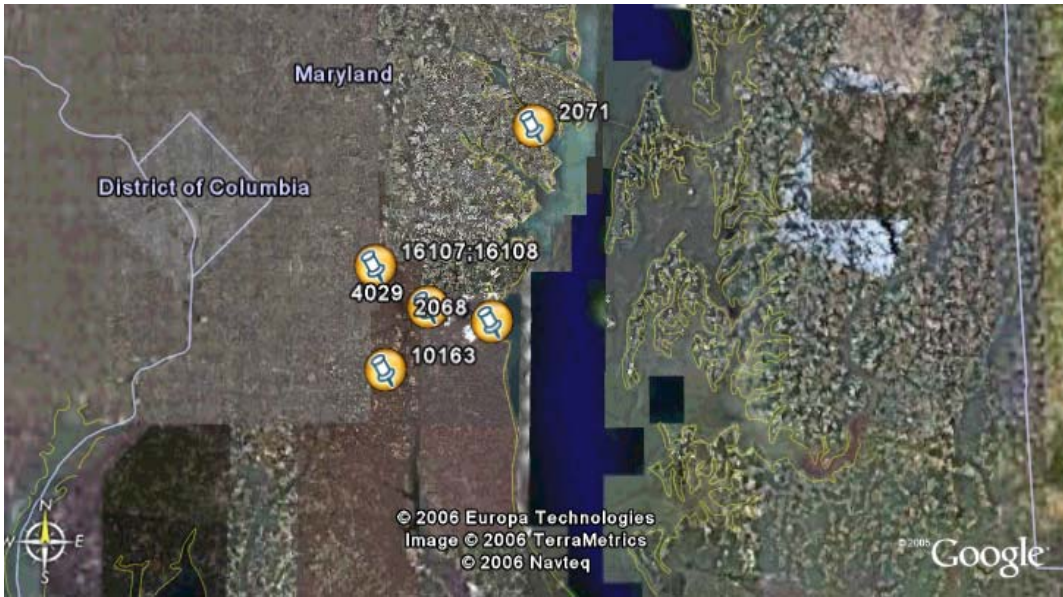


Figure C.14 - May 20th – North 2



Figure C.15 - May 21st – East



Figure C.16 - May 23rd – Southeast 1

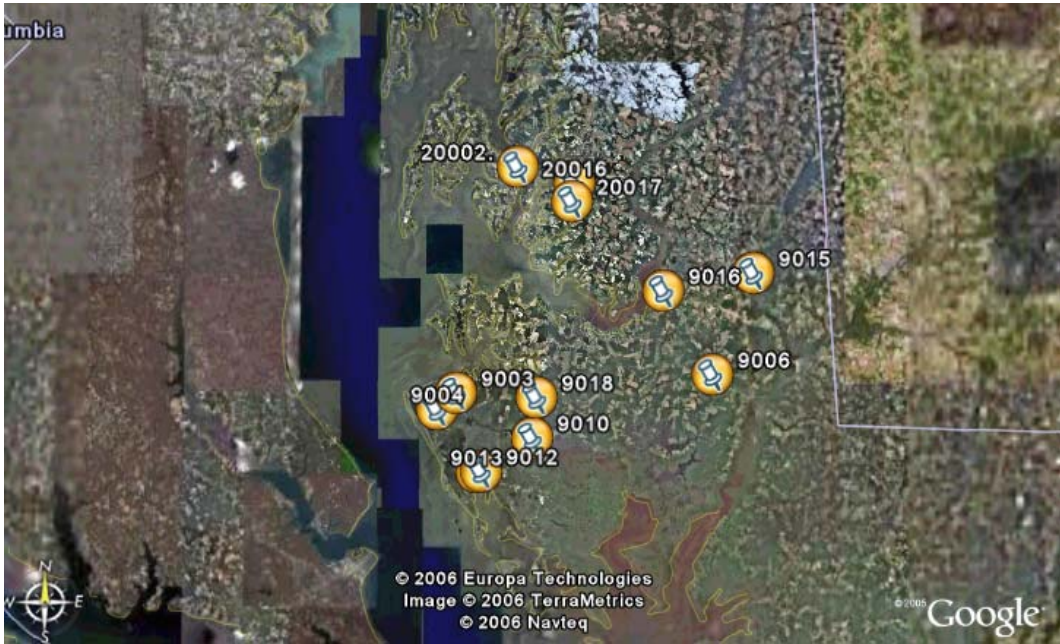


Figure C.17 - May 24th – Southeast 2



Figure C.18 - May 25th – North 1



Figure C.19 - May 30th – West

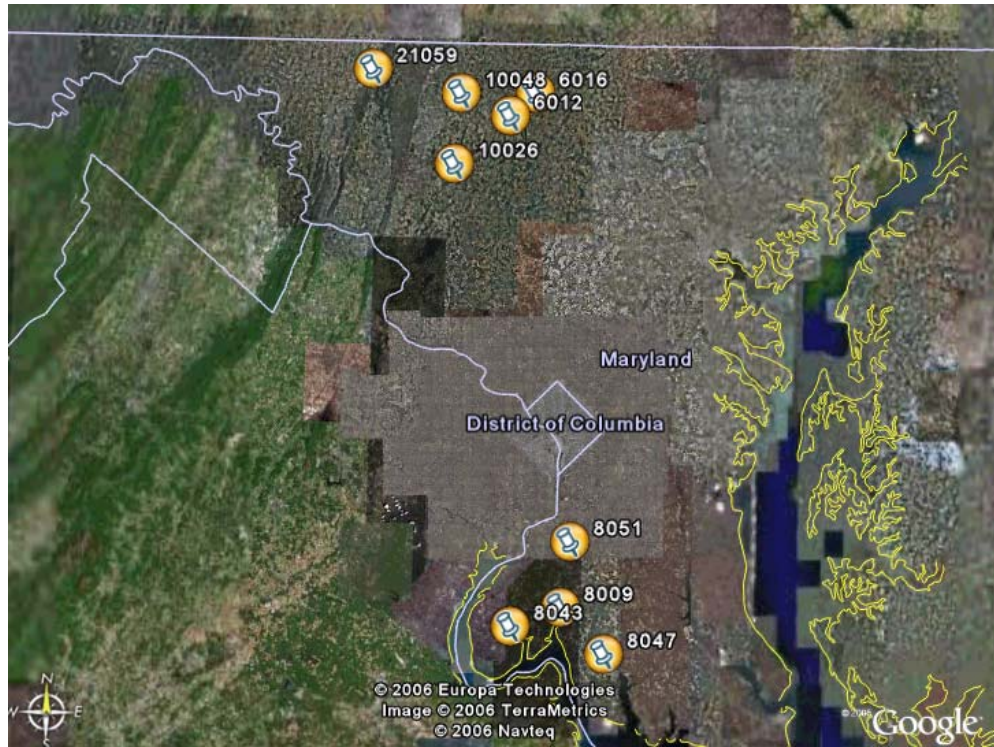


Figure C.20 - May 31st – Midwest

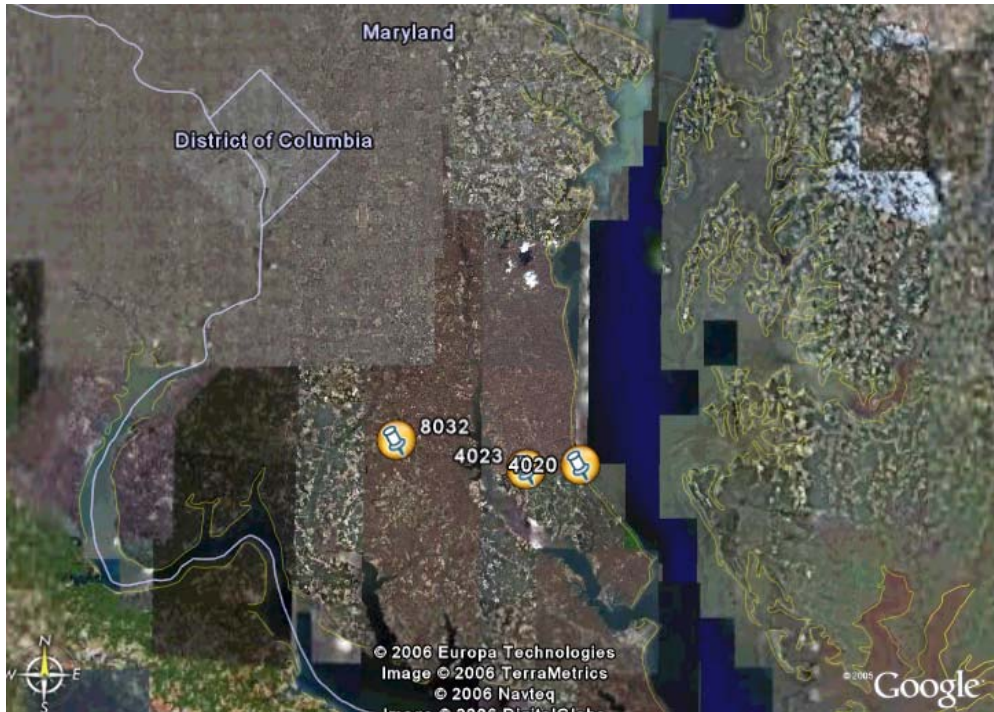


Figure C.21 - June 1st – South

References

1. AASHTO, *Standard Specifications for Highway Bridges, The American Association of State Highway Officials. Tenth Edition*, Washington D.C., Association of General Offices, 1969.
2. AASHTO, *Standard Specifications for Highway Bridges, The American Association of State Highway and Transportation Officials. Twelfth Edition*, Washington D.C., Association of General Offices, 1977.
3. AASHTO, *Standard Specifications for Highway Bridges, The American Association of State Highway and Transportation Officials. Fourteenth Edition*, Washington D.C., Association of General Offices, 1989.
4. AASHTO, *Standard Specifications for Highway Bridges, The American Association of State Highway and Transportation Officials. Fifteenth Edition*, Washington D.C., Association of General Offices, 1992.
5. AASHTO, *Standard Specifications for Highway Bridges, The American Association of State Highway and Transportation Officials. Sixteenth Edition*, Washington D.C., Association of General Offices, 1997.
6. AASHTO, *Standard Specifications for Highway Bridges, The American Association of State Highway and Transportation Officials. Seventeenth Edition*, Washington D.C., Association of General Offices, 2002.
7. AASHTO, *The American Association of State Highway and Transportation Officials Load and Resistance Factor Design Bridge Design Specifications, Fourth Edition*, Washington D.C., Association of General Offices, 2007.
8. Cohen, M., Weinrobe, M. and Miller, J., *Multivariate Analysis of Patterns of Informal and Formal Caregiving among Privately Insured and Non-Privately Insured Disabled Elders Living in the Community*. Retrieved: January 24, 2007, from <http://aspe.hhs.gov/daltcp/reports/multanal.htm> . April 2000.
9. *Logistic Regression*. Retrieved: January 24, 2007, from <http://usermmm.sfsu.edu/~efc/classes/biol710/logisticreg.htm>
10. Mackerle, J., *Rubber and Rubber-like Materials, Finite Element Analyses and Simulations: A Bibliography (1976 - 1997)*. Retrieved: October 2, 2006, 1997.

11. MDOT, *Guide for Completing Structure Inventory and Appraisal Input Forms*, Office of Bridge Development, Maryland Department of Transportation and The State Highway Administration, 2003.
12. MDOT, *Office of Bridge Development, Bridge Inventory*, Maryland Department of Transportation and The State Highway Administration, 2005.
13. Minor, J. and Egen, R., *Elastomeric Bearing Research. NCHRP Report 109*. Washington, D.C., National Academy Press, 1970.
14. MNDOT, *Minnesota Department of Transportation Bridge Inspection Field Manual*, 2004
15. Park, S.H., *Bridge Inspection and Structural Analysis (Handbook of Bridge Inspection) Second Edition*. Trenton, N.J., 2000.
16. Potter, W., Ansley, M. and Mtenga, P., *Condition of Elastomeric Bearing Pads after 40 Years of Service*. Retrieved: October 19, 2006, 2004.
17. Roeder, C., Stanton, J., and Feller, T. *Low Temperature Behavior and Acceptance Criteria for Elastomeric Bridge Bearings. NCHRP Report 325*. Washington, D.C., National Academy Press, 1989.
18. Stanton, J., Roeder, C., and Taylor, A. *Performance of Elastomeric Bearings. NCHRP Report 298*. Washington, D.C., National Academy Press, 1987.
19. Stanton, J., and Roeder, C. *Elastomeric Bearings Design, Construction, and Materials. NCHRP Report 248*. Washington, D.C., National Academy Press, 1982.
20. Yura, J., Kumar, A., Yakut, C., Topkaya, C., Becker, E., and Collingwood, J. *Elastomeric Bridge Bearings: Recommended Test Methods. NCHRP Report 449*. Washington, D.C., National Academy Press, 2001.